Supporting Information

Solution size variation of linear and dendritic bis-MPA analogs using DOSY-^{1}H NMR

*Oluwapelumi O. Kareem[a], Farzin Rahmani[b], Jason A. Hyman[a], Christopher B. Keller[a], Melissa A. Pasquinelli[b], Daniel A. Savin[c], and Scott M. Grayson[a]**

[a]Department of Chemistry, Percival Stern Hall, Tulane University, New Orleans, Louisiana 70118, United States

[b]Department of Forest Biomaterials, Biltmore Hall, North Carolina State University, Raleigh, North Carolina, 27695, United States

[c]Department of Chemistry, Leigh Hall, University of Florida, Gainesville, Florida 32611, United States

KEYWORDS: bis-MPA, PBBM, Diffusion, DOSY-NMR, Hydrodynamic Radius, Polyester, GPC, Apparent Mass, Solution Size

S1. Materials and Methods

S1.1 Materials. Reagents were used as obtained from the indicated commercial suppliers unless stated otherwise: ε-Caprolactone (Tokyo Chemical Industry), calcium hydride (CaH_2, Millipore-Sigma), benzyl alcohol (Millipore-Sigma), tin(II) ethyl hexanoate ($Sn(Oct)_2$, Millipore-Sigma),

xylenes (Millipore-Sigma), dichloromethane (DCM, Fisher), Pd/C (Millipore-Sigma), chloroform-d ($CDCl_3$, Cambridge Isotope Laboratories), methanol-d_4 (MeOD, Cambridge Isotope Laboratories), dimethyl sulfoxide-d_6 ($(CD_3)_2SO$, DMSO-d_6, Cambridge Isotope Laboratories), acetone-d_6 ($(CD_3)_2CO$, Ace-d_6, Cambridge Isotope Laboratories, dimethyl formamide-d_7 ($(CD_3)_2NCOD$, DMF-d_7, Cambridge Isotope Laboratories), tetrahydrofuran-d_8 ($(CD_2)_4O$, THF-d_8, Cambridge Isotope Laboratories), tetrahydrofuran (THF, VWR), sodium trifluoroacetate (Tokyo Chemical Industry), and *trans*-2-[3-(4-*tert*-butylphenyl)-2-methyl-2-propenylidene]malononitrile (DCTB, Tokyo Chemical Industry).

S1.2 Methods. Nuclear magnetic resonance (NMR) spectroscopy was performed on a Bruker AVANCE 300 MHz spectrometer (Figs. 1-4, S11-73). ^1H (300 MHz) experiments were performed at 298 K at a concentration of 3 mg mL^{-1} in chloroform-d ($CDCl_3$) and DMSO-d_6, purchased from Cambridge Isotope Laboratories (Andover, MA, USA). A number of scans were collected to generate sufficient signal to noise with a relaxation delay of 3-6 seconds depending on sample. Diffusion NMR (DOSY-^1H NMR) Measurements and R_h Calculation. Standard PSGE diffusion NMR experiments were performed using a Bruker AVANCE 300 MHz spectrometer with dilute solutions (5 mg mL^{-1}) of each polymer in THF-d_8, $CDCl_3$, Ace-d_6, DMF-d_7, and DMSO-d_6 (purchased from Cambridge Isotope Laboratories Andover, MA, USA) at 298 K. Each sample was dried overnight under high vacuum, dissolved in the respective solvent, and then allowed to equilibrate to 298 K as detected by the Bruker AVANCE spectrometer temperature probe. An additional ten minutes was used to ensure temperature uniformity before the experiment began. Experiments were calibrated using the HOD proton signal in D_2O (98.9%). Each diffusion experiment included 16 experiments (32 scans each) with a gradient intensity from 5% to 95%. The diffusion time, Δ, ranged from 30-150 ms, and the

gradient duration, δ, ranged from 1-3 ms such that signal intensity decreased by 90-95%. Delay times ranged from 3-6 seconds depending on molecular weight range examined (1 kDa – 3 seconds, 2 kDa – 4 seconds, 5 kDa – 5 seconds, 10 kDa – 6 seconds). The diffusion coefficient, D, was derived from peak intensities using the TopSpin Software from Bruker. The diffusion coefficients were obtained using an average of diffusion values calculated by the variable gradient fitting function (Equation S1) from TopSpin using four different ^{1}H signals for each run.

$$I = I(0)e^{-D\left(\Delta - \frac{\delta}{3}\right)(\sqrt{2\pi\gamma\delta g}) * 10^4}$$

Equation S1. Variable gradient fitting function provided by Bruker TopSpin software for the non-linear fit of selected ^{1}H NMR peaks (Figs. S71-S73).

In Equation S1, D represents the diffusion coefficient, Δ is the gradient distance, δ is the diffusion gradient length, γ is the gyromagnetic ratio of the current nucleus, and g is the gradient amplitude. DOSY experiments for each sample were collected in duplicate and their corresponding D values were averaged before being used in the Stokes-Einstein equation (Equation S2) to calculate hydrodynamic radii.

$$R_h = \frac{k_B T}{6\pi\eta D}$$

Equation S2. The Stokes-Einstein equation used for hydrodynamic radii calculations.

In Equation S2, k_B is the Boltzmann constant (1.380×10^{-23} J K^{-1}), T is the temperature (in K), and η is the viscosity of each protonated solvent at 298 K which neglects the isotope effects of their deuterated variants. Viscosity measurements for each non-deuterated solvent used are as follows, THF (0.48 centipoise (cp)) $CHCl_3$ (0.542 cp), Ace (0.316 cp), DMF (0.796 cp), DMSO (1.98 cp).[1] A Bruker Autoflex III MALDI-TOF mass spectrometer (Bruker Daltonics, Billerica,

MA) was used to collect Table 1 and Figs. 3, S5, S7, and S9**.** Mass spectra data were collected in positive reflectron ion detection mode. Stock solutions of matrix (20 mg mL^{-1}), polymer analyte (1 mg mL^{-1}), and a cation source (1 mg mL^{-1}) in tetrahydrofuran (THF) were made. The stock solutions were combined in a 5/1/1 ratio (v/v/v) (matrix/analyte/cation) and plated via the dried droplet method. Sodium trifluoroacetate was used as the cation source and *trans*-2-[3-(4-*tert*-butylphenyl)-2-methyl-2-propenylidene]malononitrile (DCTB) was used as the matrix in the first sample preparation. MALDI-TOF MS spectra were calibrated against SpheriCal® dendritic calibrants (Polymer Factory, Sweden). Gel permeation chromatography (GPC) was performed on a Waters Model 1515 isocratic pump and a Waters Model 2414 differential refractometer detector (Waters Corp., Milford, MA) with three PSS SDV analytical 500 Å (8 × 300mm) columns in series; (Polymer Laboratories Inc., Amherst, MA). Data (Table 1 and Figs. 3, S6, S8, and S10) were collected in THF at a flow rate of 1 mL min^{-1} at 30 °C. PBBM and PCL samples for this size comparison study were collected by fractionation using a Waters Model 1515 isocratic pump and a Waters Model 2414 differential refractometer detector (Waters Corp., Milford, MA) with one PSS SDV Prep 1000 Å (40 × 250 mm); (Polymer Laboratories Inc., Amherst, MA). This was done in THF at a flow rate of 8 mL min^{-1} at 30 °C.

S1.3 Molecular dynamics simulations calculation method.

The structures of polycaprolactone (PCL), poly(3-(benzoyloxy)-2-(bromomethyl)-2-methylpropanoic acid (PBBM), and fourth generation of the bis-MPA dendrimer were created in MAPS Platform in Scienomics software. Forty-five and eighty-seven monomer units were selected for each PCL and PBBM polymer chain, respectively. Then, three different configurations of PCL, PBBM, and bis-MPA dendrimer systems consisting of twenty polymer chains were created using the Amorphous builder module within MAPS. Once the systems were created, the molecular

dynamics (MD) simulation were carried out using the deriding[2] force field within the LAMMPS[3] software package. First, the conjugate gradient[4] technique was used to perform the energy minimization for system relaxation. Once the systems relaxed, the *NPT* simulation were carried out at 1,000 K and atmospheric pressure for 1 ns with a time step of 1 fs and a cut-off distance of 14 Å. Next, the systems were cooled from 1,000 K to 300 K at rate of 7 K/ps with *NPT* simulation. Finally, the systems were equilibrated at 300 K and 1 atm with *NPT* simulation for 1 ns. The above heating/cooling cycle was repeated ten times. In this work, the long range electrostatic interactions were calculated using the Particle-Particle Particle-Mesh (PPPM)[5] method while the Nose-Hover[6] thermostat and Martyna[7] barostat were used to control the temperature and pressure, respectively.

The Hansen solubility parameter (HSP)[8] of the polymers are obtained with following formula (Equation S3):

$$\delta_T^2 = \delta_D^2 + \delta_P^2 + \delta_H^2$$

Equation S3. Hansen solubility parameter equation.[8]

where, δ_T is the total HSP and δ_D, δ_P, and δ_H are the component of dispersion, polar, and hydrogen bond, respectively. Since the hydrogen bond interaction energy cannot be obtained separately in this work, the HSP can be determined by following equation (Equation S4):

$$\delta_T^2 = \delta_{vdW}^{\ 2} + \delta_{ele}^{\ 2}$$

Equation S4. Hansen solubility parameter equation using electrostatic energy in place of polar and hydrogen bonding as seen in equation S3.

where, $\delta_{vdw}$is the van der Waals (dispersion) component and δ_{ele} is the electrostatic component consisting of polar and hydrogen bond components (equation S5).

$$\delta_{ele}^{\ 2} = \delta_P^2 + \delta_H^2$$

Equation S5. Electrostatic energy equation.[9]

The δ_{vdw} and δ_{ele} components can be given by:

$$\delta_k^2 = \left(\frac{\left\langle \sum_{i=1}^{n} E_i^k - E_{total}^{\ k} \right\rangle}{N_o \langle V \rangle} \right)$$

Equation S6. Molecular dynamics equation used for calculating δ_{vdw} and δ_{ele}.[10]

where, $\langle\,\rangle$ indicates a time average over the last 500 ps of MD simulation, n is the number of polymer chain, E_i^k is the energy components of the individual molecules, $E_{total}^{\ k}$ is the potential energy components of the simulation box, $k = 1$ and 2 for the van der Waals (dispersion) and electrostatic (polar and hydrogen bonds) component, N_o is the Avogadro number, and V is the volume of the simulation box.

S1.4 Synthesis of bis-MPA analogs[11]

S1.4.1 Pentaerythritol-core (Tetra-core) [G1-G4] dendrimers

The same samples of tetra-core [G1-G4] dendrimers used for previous work[11], were also used for this study. Synthesis and characterization data including ^{1}H NMR, ^{13}C NMR, and FTIR for all these samples can be found in that previous publication. For the sake of this comparison, the MALDI-ToF MS and GPC analysis for these samples have been included here in Figs. S5-S6.

S1.4.2 1-10 kDa Poly(3-(benzoyloxy)-2-(bromomethyl)-2-methylpropanoic acid) (PBBM)

The same samples of PBBM used for previous work[11], were also used for this study. Synthesis and characterization data including ^{1}H NMR, ^{13}C NMR, and FTIR for all these samples can be found in that previous publication. Preparative GPC was used to isolate each molecular weight fraction of this polymer used in this investigation. MALDI-ToF MS and GPC analysis for each corresponding molecular weight has been included here in Figs S7-S8.

S1.5 Synthesis of 1-10 kDa poly(caprolactone) (PCL)

S1.5.1 Caprolactone distillation

ε-caprolactone monomer was added to a 100 mL 1-neck round bottom flask with a magnetic stir bar. Dry CaH_2 was added to the flask in excess to quench any dissolved water in the monomer and the flask was stirred for 24 hours. The flask was then placed in a sand bath heated to 120 °C and connected to a flame-dried distillation apparatus with a 25 mL 1-neck round bottom collection flask. The monomer and CaH_2 solution were distilled under high vacuum until roughly 10 mL of distillate was obtained. Then, the 25 mL 1-neck flask was switched out with a flame dried 100 mL 2-neck round bottom flask with a magnetic stir bar, and 65 mL (66.95 g, 0.578 mol) of distillate was obtained. The collection flask was removed from the distillation apparatus and placed under N_2 and left to stir in preparation for polymerization.

S1.5.2 Bn-PCL polymerization

To the 65 mL of distilled ε-caprolactone monomer, 0.283 mL (0.296 g, 2.73 mmol) of benzyl alcohol (BnOH) was added using a gas-tight syringe. Then 0.113 g (0.09 mL, 0.279 mmol) of tin(II) ethyl hexanoate catalyst ($Sn(Oct)_2$) was added to a scintillation vial and dispersed via

sonication in 0.5 mL of xylenes to reduce the viscosity of the catalyst. The xylenes and $Sn(Oct)_2$ were added to the reaction flask using a gas-tight syringe. The reaction flask was then placed in a 130 °C pre-heated sand bath and stirred under inert atmosphere (N_2). Two aliquots (20 mL) were removed during the polymerizations to favor different molecular weight ranges. The first aliquot was taken at 20 minutes and the second at 35 minutes. Each of these aliquots were removed from the heat, cooled to room temperature, and then quenched with excess THF solvent (~ 30 mL). The remaining ~ 25 mL of the reaction mixture was removed from heat, cooled, and quench with ~ 30 mL of THF solvent after 1 hour and 35 minutes of reaction time. Each fraction was then concentrated using a rotary evaporator. A 200 mL beaker was prepared with 70 mL of diethyl ether, 70 mL of hexanes solvent, and a large magnetic stir bar. The beaker was cooled, using dry ice, to -78.5 °C and set to stir. One of the concentrated fractions was added dropwise to the cold solvent, and a white precipitate formed. The precipitate was removed from the solvent by vacuum filtration and transferred to a tared scintillation vial. This was done two additional times for the two remaining fractions. Each fraction was dried under high vacuum before weighing. The total yield between of all three fractions was 10.39 g.

S1.5.3 General deprotection of Bn-PCL

1.00 g of each benzyl-initiated PCL fraction was added to a round bottom flask dendrimer along with magnetic stir bar. 20 mL of Dichloromethane (DCM) was added to the flask to dissolve the Bn-PCL. To this, a catalytic amount of Pd/C (~10%) was added and the flask was vigorously stirred under reducing atmosphere (H_2). The reaction was stirred for three hours then filtered through diatomaceous earth to remove Pd/C. The solvent was removed *in vacuo* to afford a viscous liquid. This was placed under high vacuum at 50 °C overnight forming a white solid.

S1.5.4 Isolation of 1-10 kDa PCL

400 mg of each sample of PCL were separated using preparative GPC using a concentration of 100 mg mL^{-1}. One-minute fractions were collected and then analyzed by MALDI-ToF MS and GPC to identify fractions within 10% of the mass of a corresponding bis-MPA dendrimer (1 kDa, 2.2 kDa, 4.8 kDa, 10 kDa). This was repeated for each aliquot from the Bn-PCL polymerization.

S1.6 Characterization of selected PCL samples

S1.6.1 1 kDa PCL

(0.034 g, 8.5% yield, M_n 1150). ^{1}H NMR (Fig. S1) (300 MHz, $(CD_3)_2SO$) δ 1.31 (m, $CH_{2\ \gamma\ position}$), 1.54 (m, $CH_{2\ \beta\ and\ \delta\ positions}$), 2.29 (t, $CH_{2\ \alpha\ position}$), 4.00 (t, $CH_{2\ \varepsilon\ position}$). MALDI-ToF MS (Fig. S9) calcd. m/z + 2 Na^+ [1089.60 m/z] obs. m/z + 2 Na^+ [1089.98 m/z]. GPC (Fig. S10) (THF, RI): M_n ($Đ$) = 1500 g mol^{-1} (1.25).

S1.6.2 2.2 kDa PCL

(0.047 g, 11.8% yield, M_n 2110). ^{1}H NMR (Fig. S2) (300 MHz, $(CD_3)_2SO$) δ 1.29 (m, $CH_{2\ \gamma\ position}$), 1.53 (m, $CH_{2\ \beta\ and\ \delta\ positions}$), 2.27 (t, $CH_{2\ \alpha\ position}$), 3.98 (t, $CH_{2\ \varepsilon\ position}$). MALDI-ToF MS (Fig. S9) calcd. m/z + 2 Na^+ [2231.72 m/z] obs. m/z + 2 Na^+ [2231.70 m/z]. GPC (Fig. S10) (THF, RI): M_n ($Đ$) = 4400 g mol^{-1} (1.08).

S1.6.3 4.8 kDa PCL

(0.031 g, 7.8% yield, M_n 4420). ^{1}H NMR (Fig. S3) (300 MHz, $(CD_3)_2SO$) δ 1.29 (m, $CH_{2\ \gamma\ position}$), 1.53 (m, $CH_{2\ \beta\ and\ \delta\ positions}$), 2.27 (t, $CH_{2\ \alpha\ position}$), 3.98 (t, $CH_{2\ \varepsilon\ position}$). MALDI-ToF MS

(Fig. S9) calcd. m/z + Na^+ [4489.67 m/z] obs. m/z + Na^+ [4490.82 m/z]. GPC (Fig. S10) (THF, RI): M_n ($Đ$) = 10600 g mol^{-1} (1.04).

S1.6.4 10 kDa PCL

(0.026 g, 6.5% yield, M_n 10430). ^1H NMR (Fig. S4) (300 MHz, $(CD_3)_2SO$) δ 1.29 (m, $CH_{2\ \gamma\ position}$), 1.53 (m, $CH_{2\ \beta\ and\ \delta\ positions}$), 2.27 (t, $CH_{2\ \alpha\ position}$), 3.98 (t, $CH_{2\ \varepsilon\ position}$). MALDI-ToF MS (Fig. S9) calcd. m/z + Na^+ [10542.26 m/z] obs. m/z + Na^+ [10540.11 m/z]. GPC (Fig. S10) (THF, RI): M_n ($Đ$) = 23400 g mol^{-1} (1.12).

2. Figures

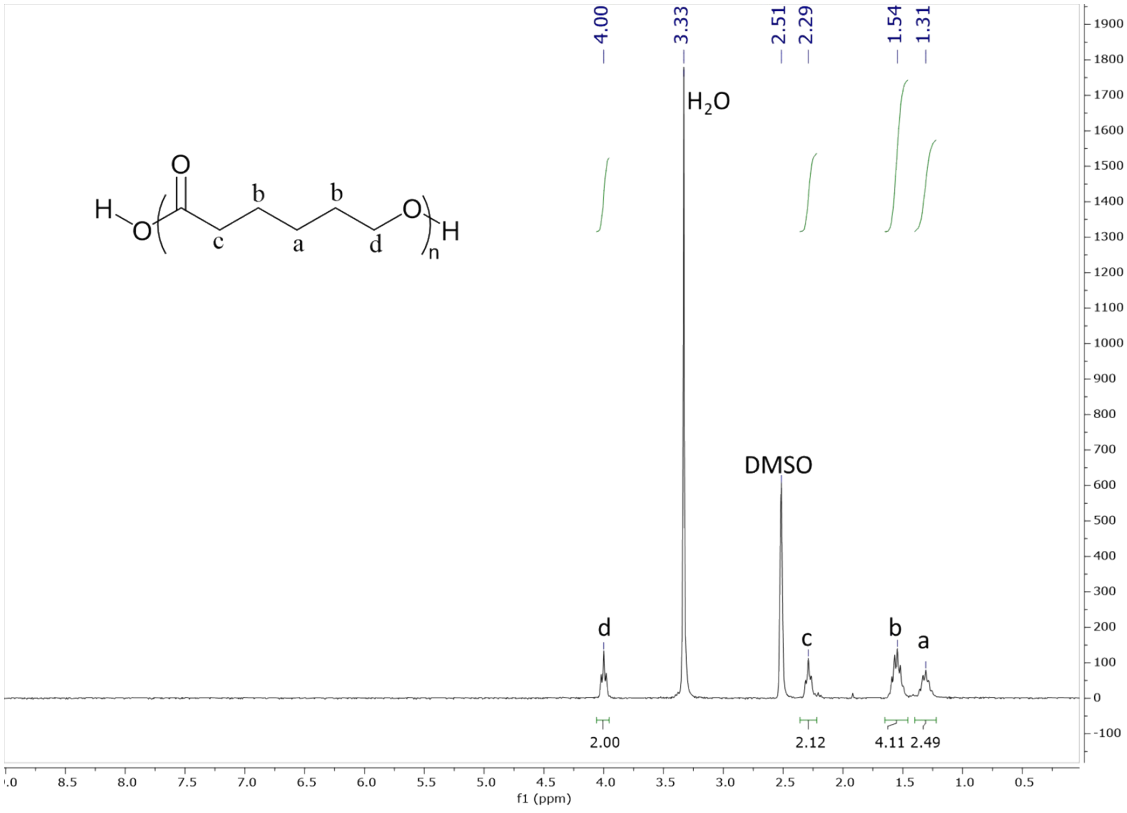

Fig. S1 ^1H NMR of 1 kDa PCL in DMSO-d_6.

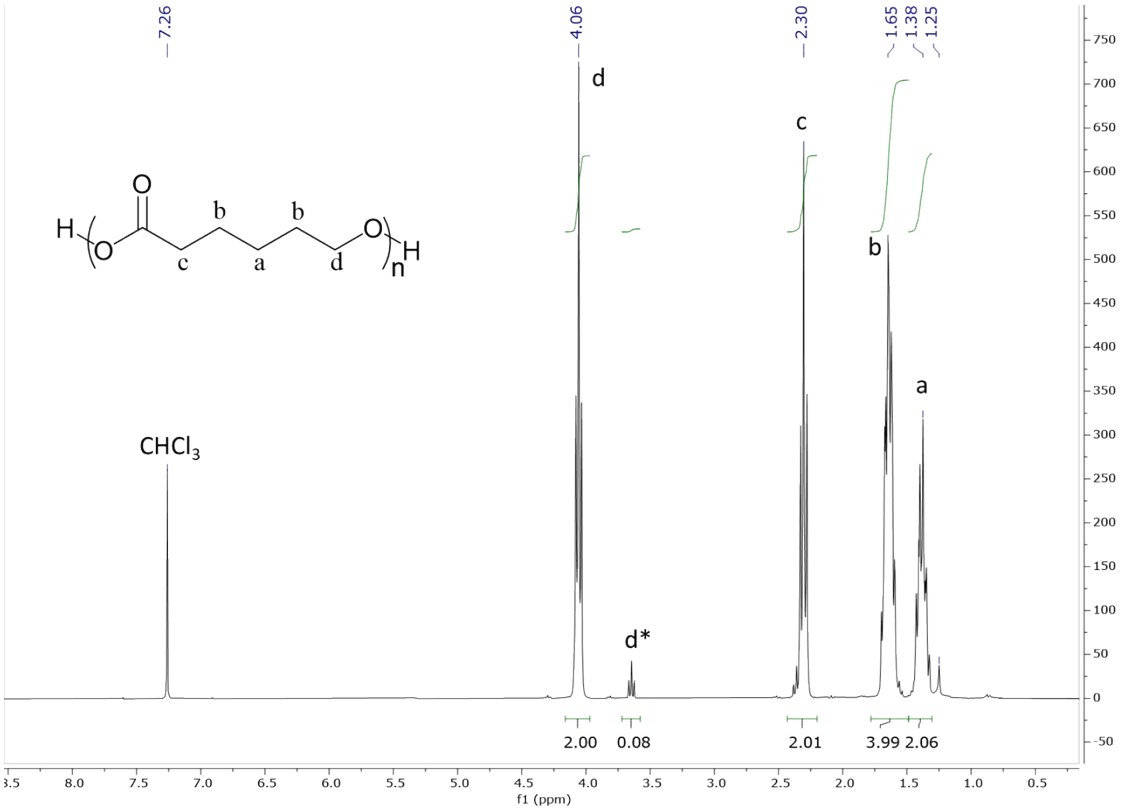

Fig. S2 ^{1}H NMR of 2.2 kDa PCL in $CDCl_3$.

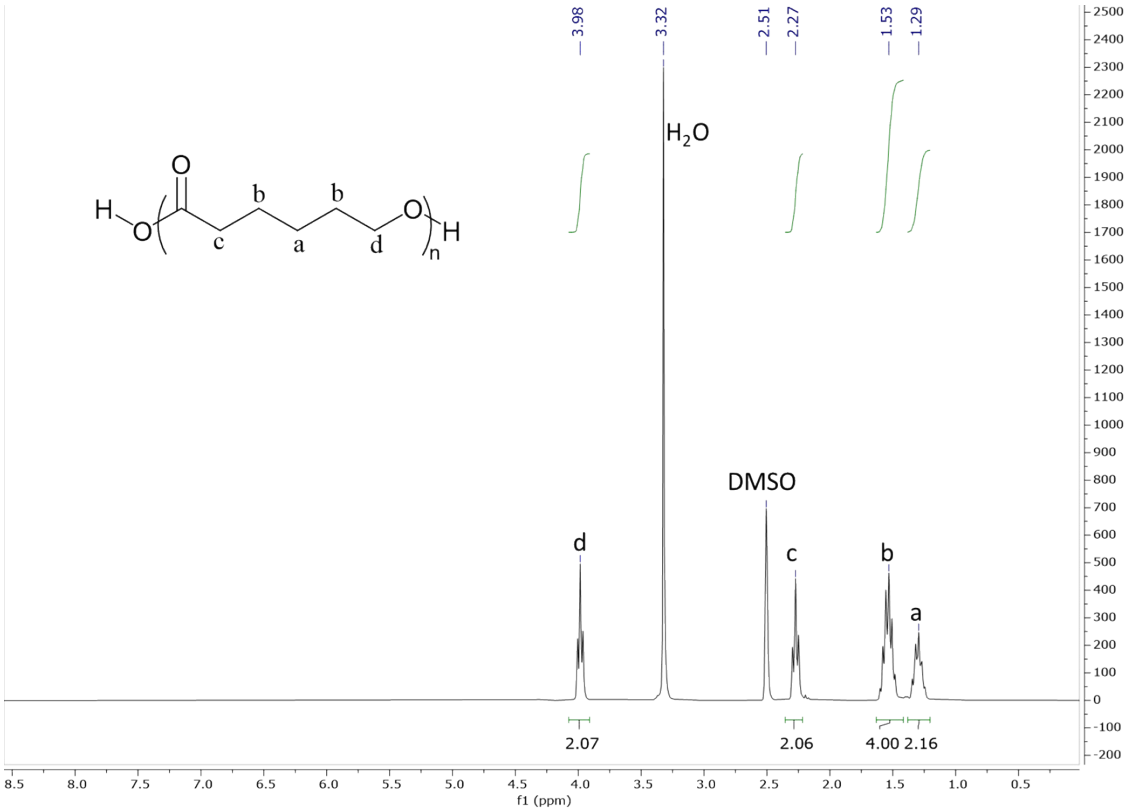

Fig. S3 ^{1}H NMR of 4.8 kDa PCL in DMSO-d_6.

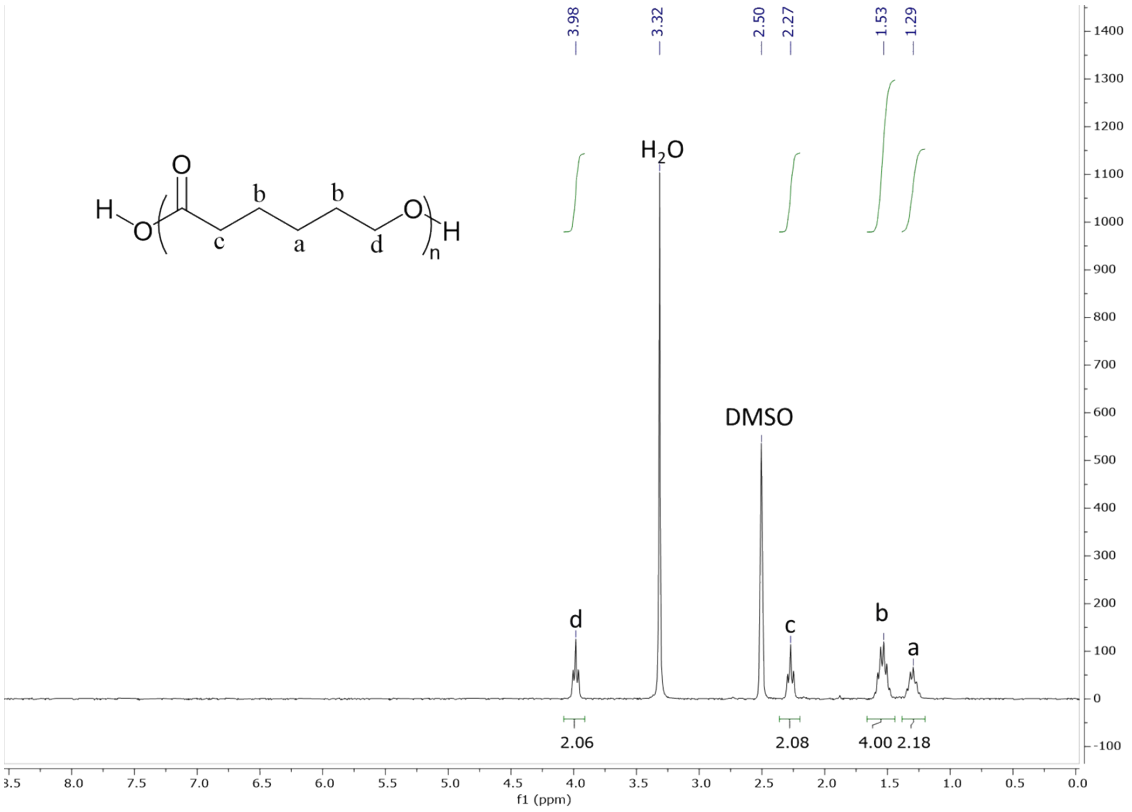

Fig. S4 ^{1}H NMR of 10 kDa PCL in DMSO-d_6.

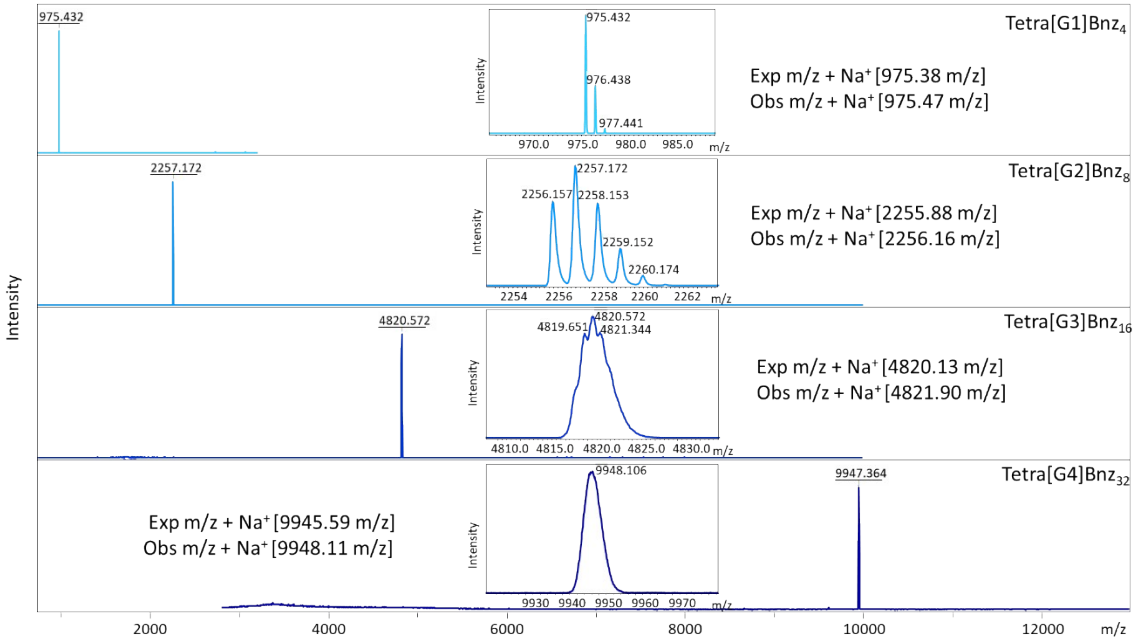

Fig. S5 MALDI-ToF MS of Tetra[G1-G4] benzylidene-protected bis-MPA.[11]

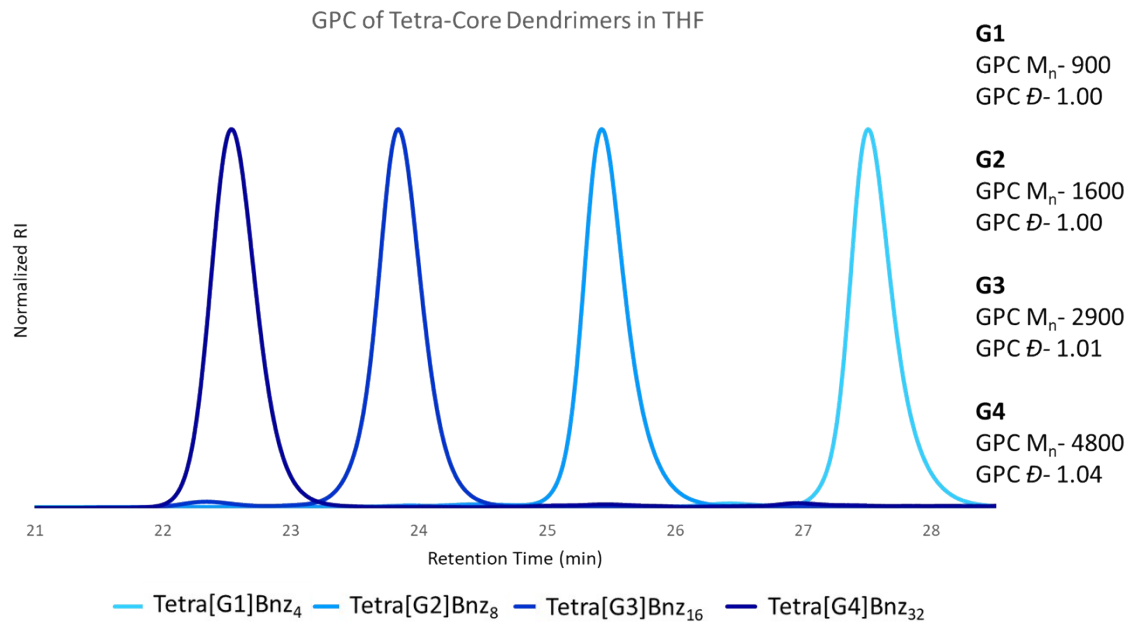

Fig. S6 GPC traces of Tetra[G1-G4] benzylidene protected bis-MPA dendrimers in THF.[11]

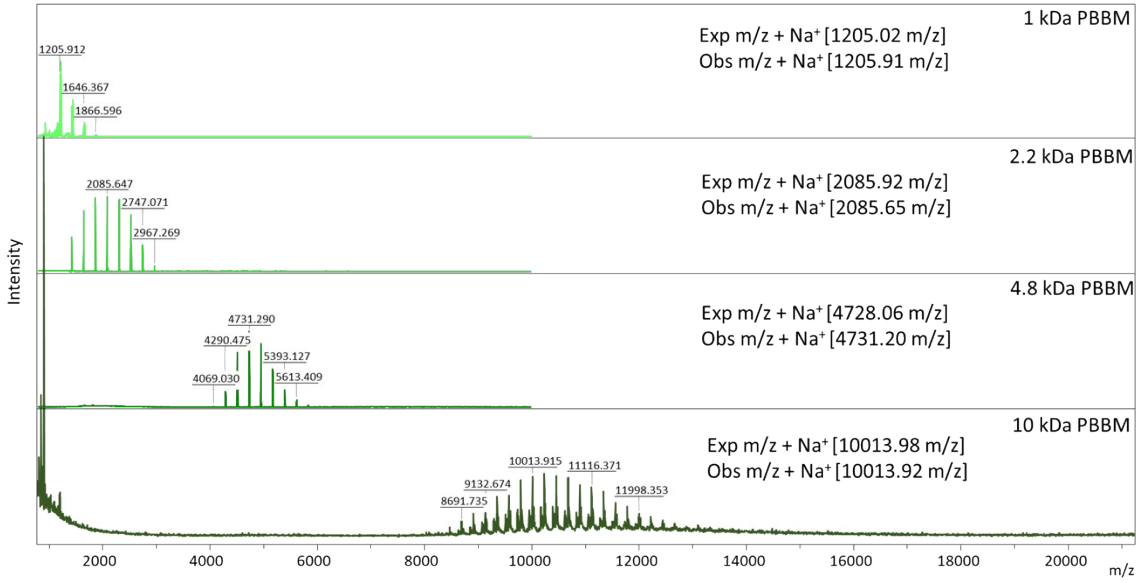

Fig. S7 MALDI-ToF MS of 1-10 kDa PBBM.[11]

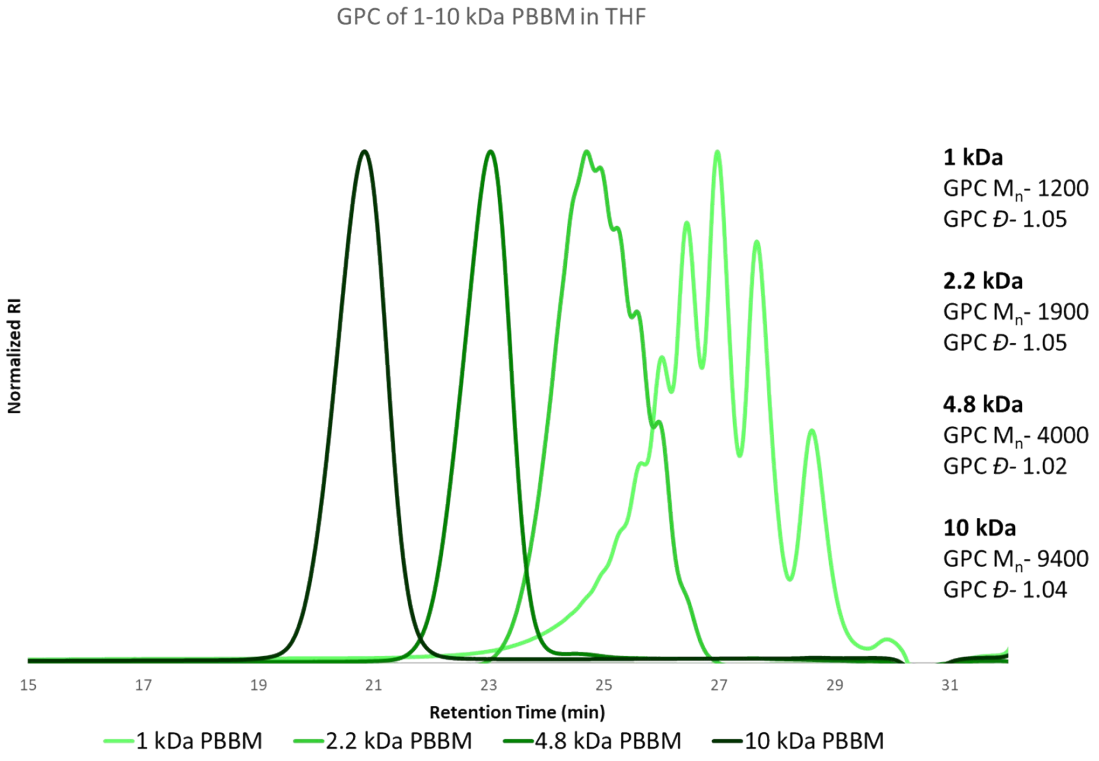

Fig. S8 GPC traces of 1-10 kDa PBBM in THF.[11]

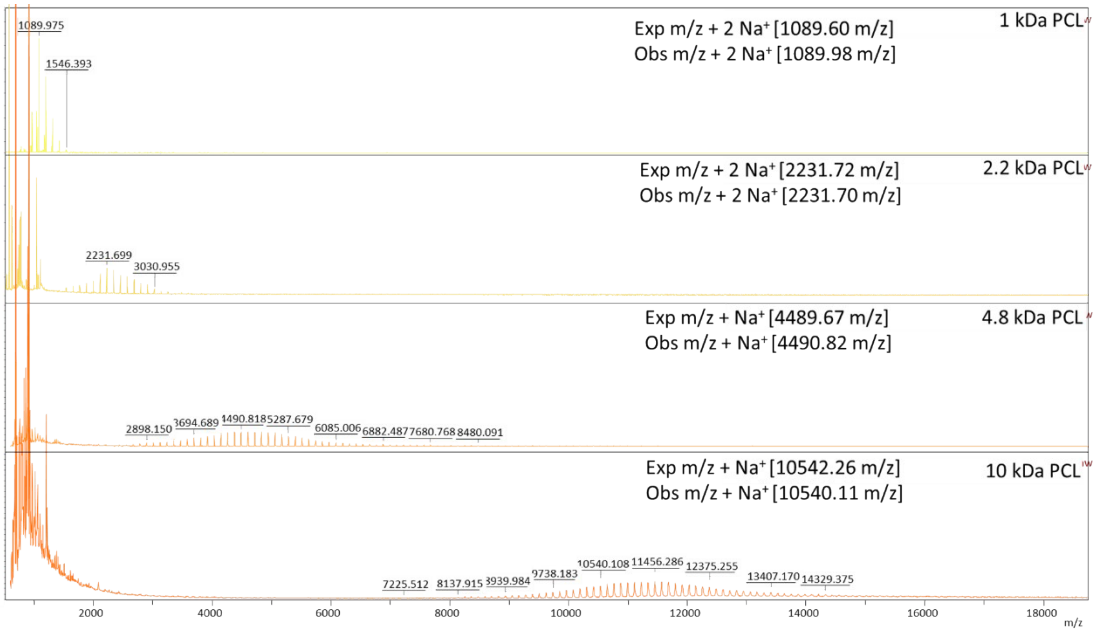

Fig. S9 MALDI-ToF MS of 1-10 kDa PCL.

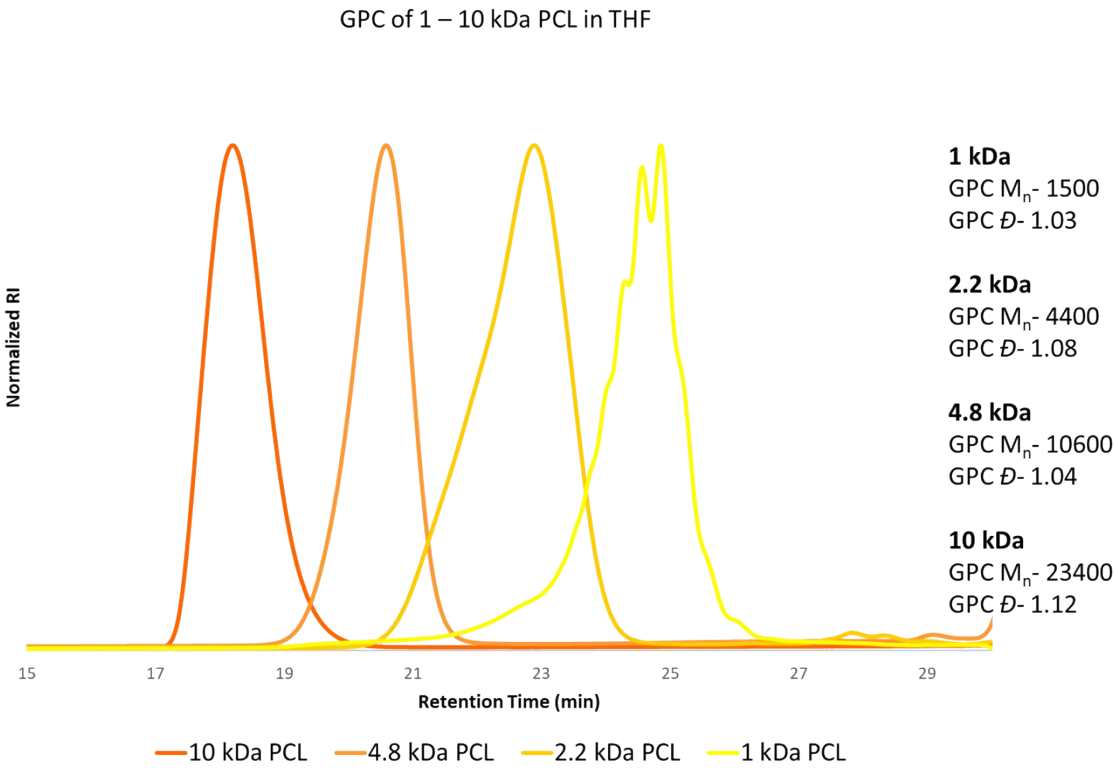

Fig. S10 GPC traces of 1-10 kDa PCL in THF.

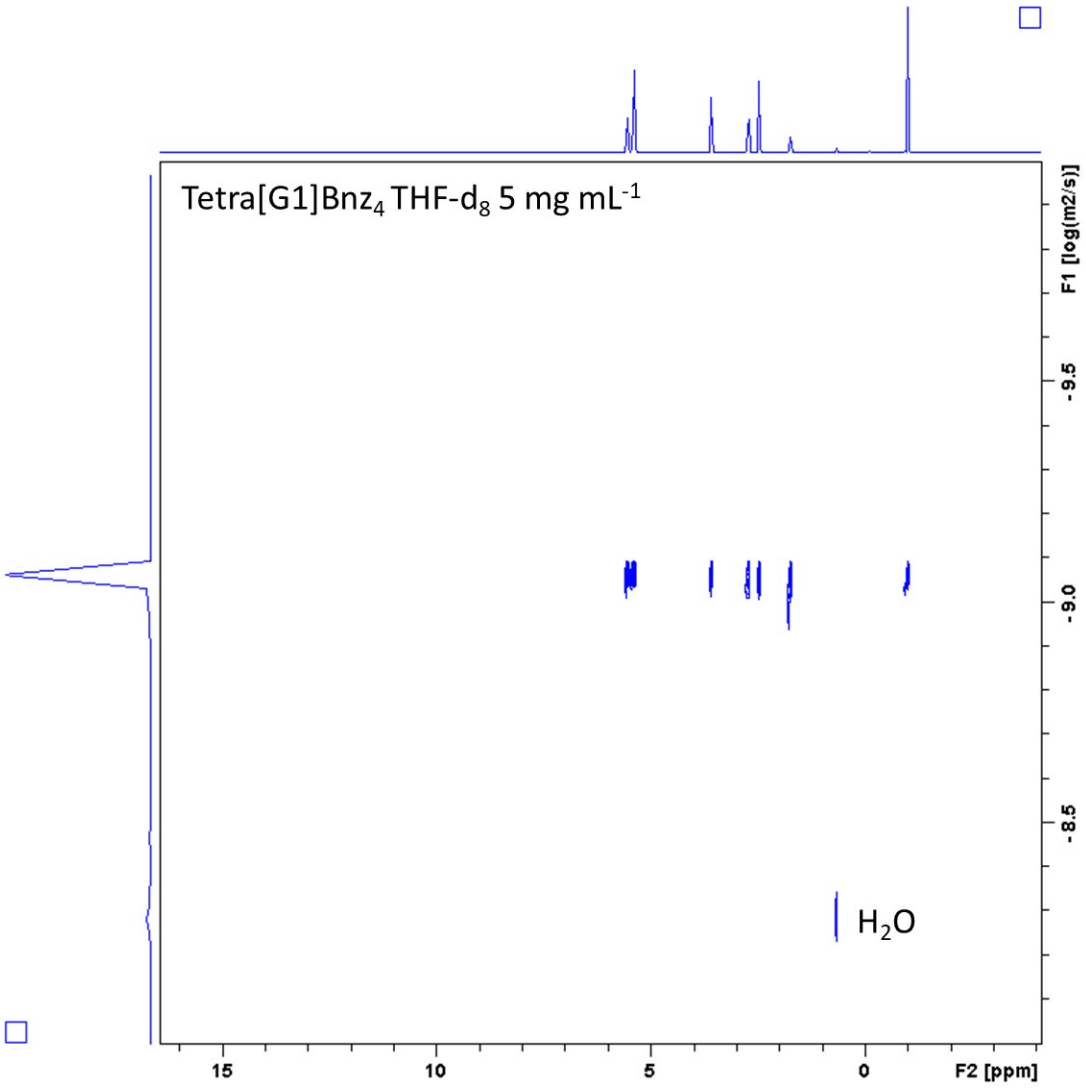

Fig. S11 DOSY-^{1}H NMR spectrum of Tetra[G1]Bnz$_4$ in THF-d$_8$.

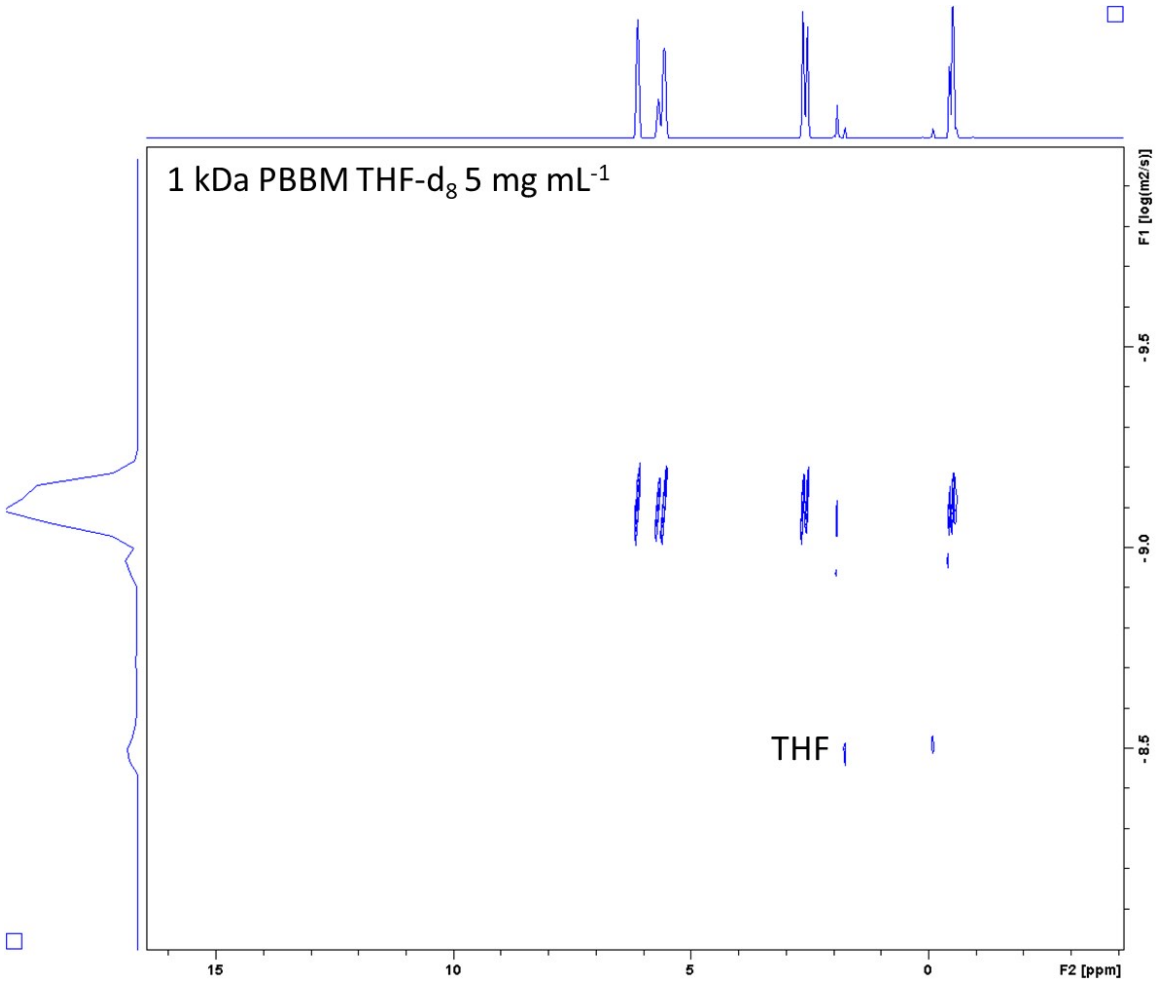

Fig. S12 DOSY-^{1}H NMR spectrum of 1 kDa PBBM in THF-d_8.

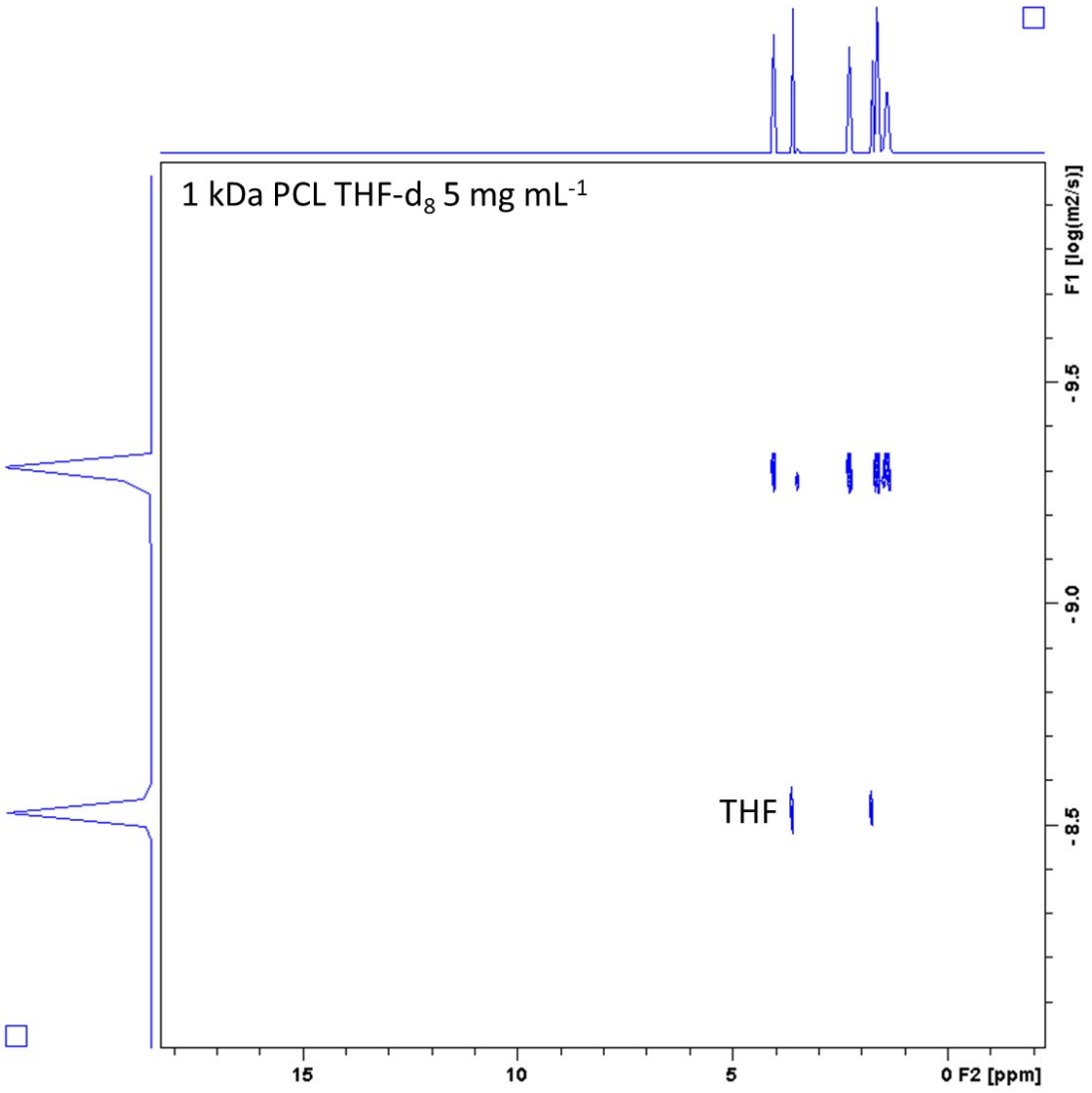

Fig. S13 DOSY-^{1}H NMR spectrum of **1 kDa PCL** in THF-d_8.

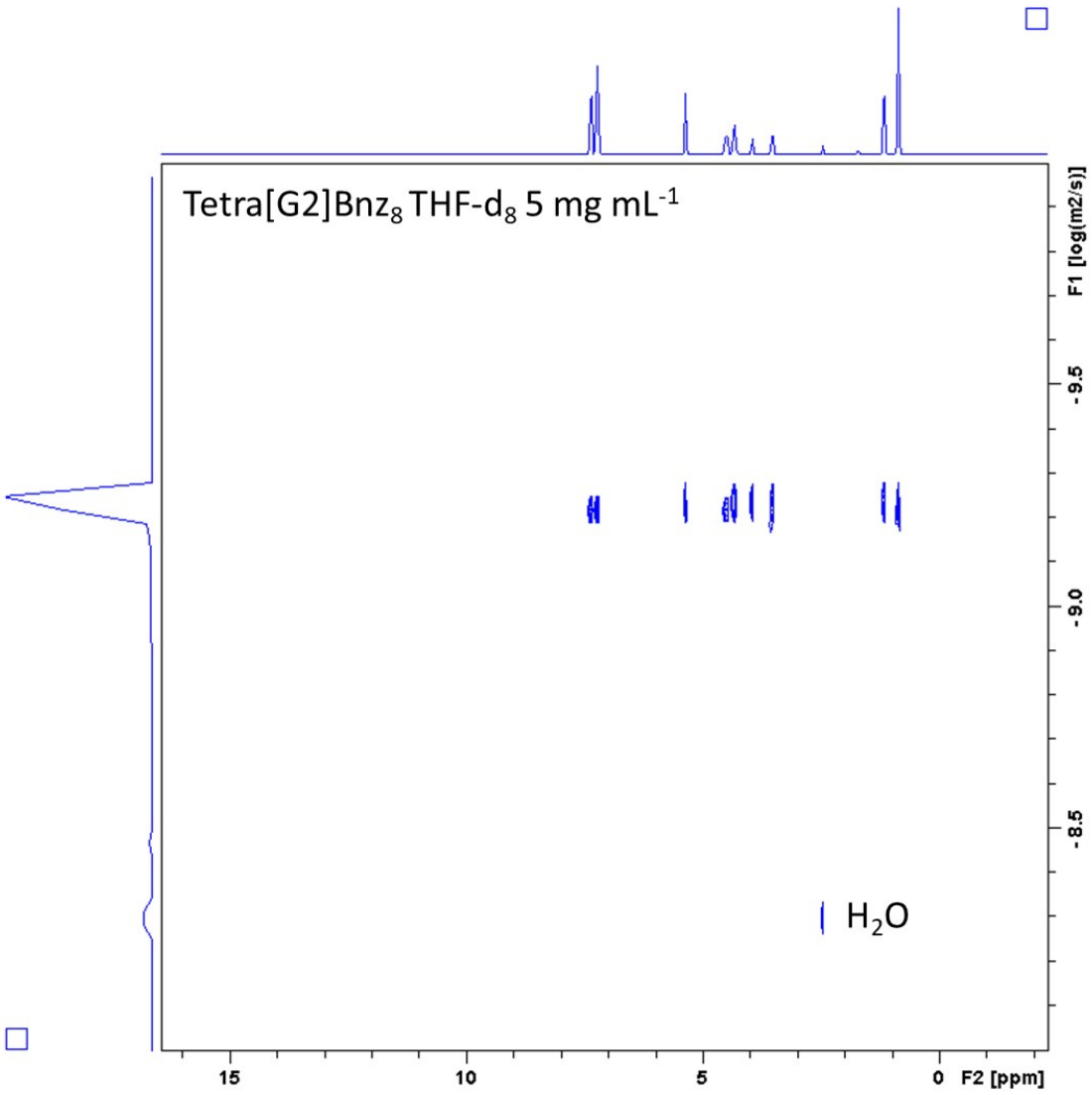

Fig. S14 DOSY-^{1}H NMR spectrum of Tetra[G2]Bnz$_8$ in THF-d$_8$.

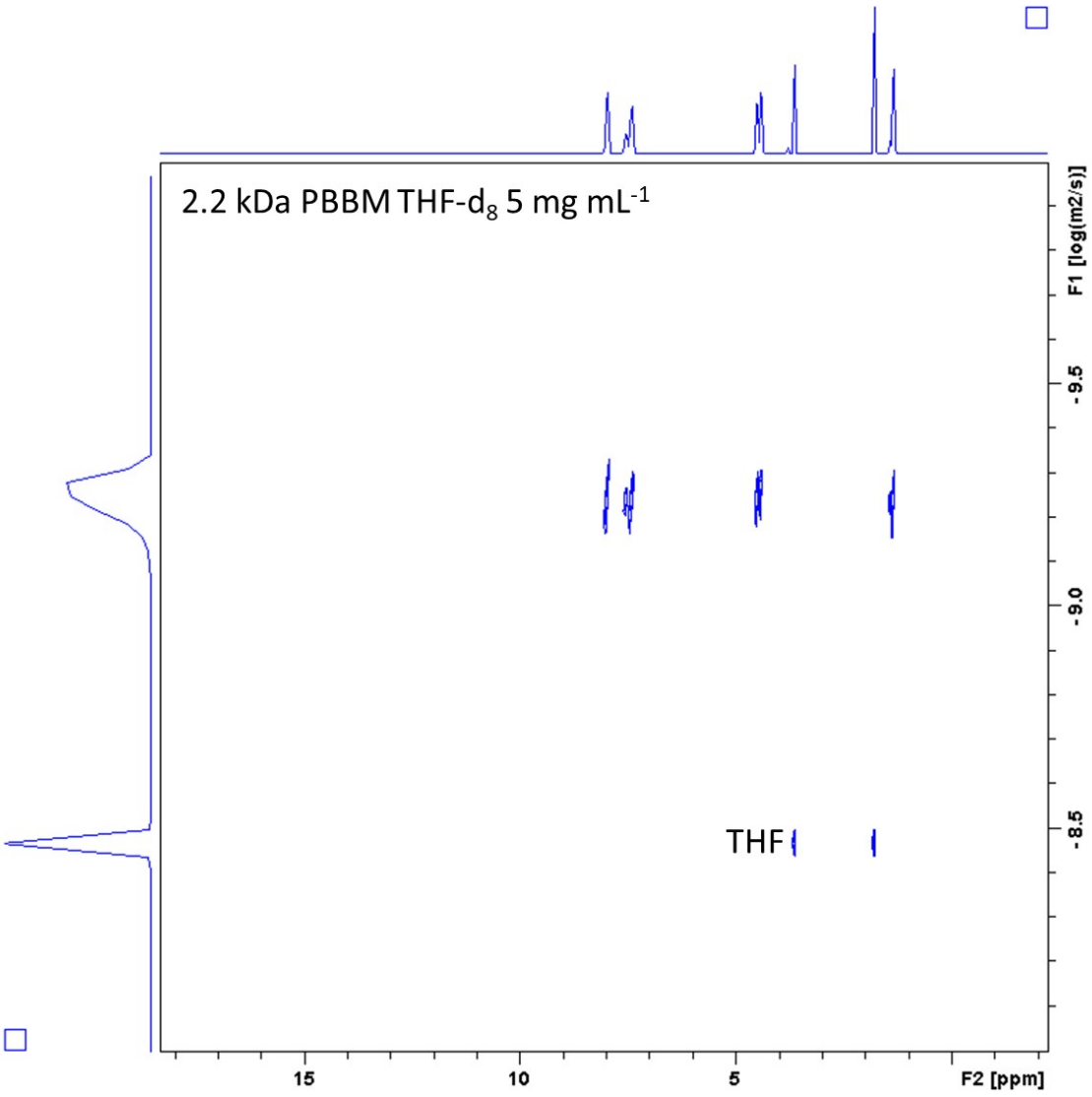

Fig. S15 DOSY-^{1}H NMR spectrum of 2.2 kDa PBBM in THF-d_8.

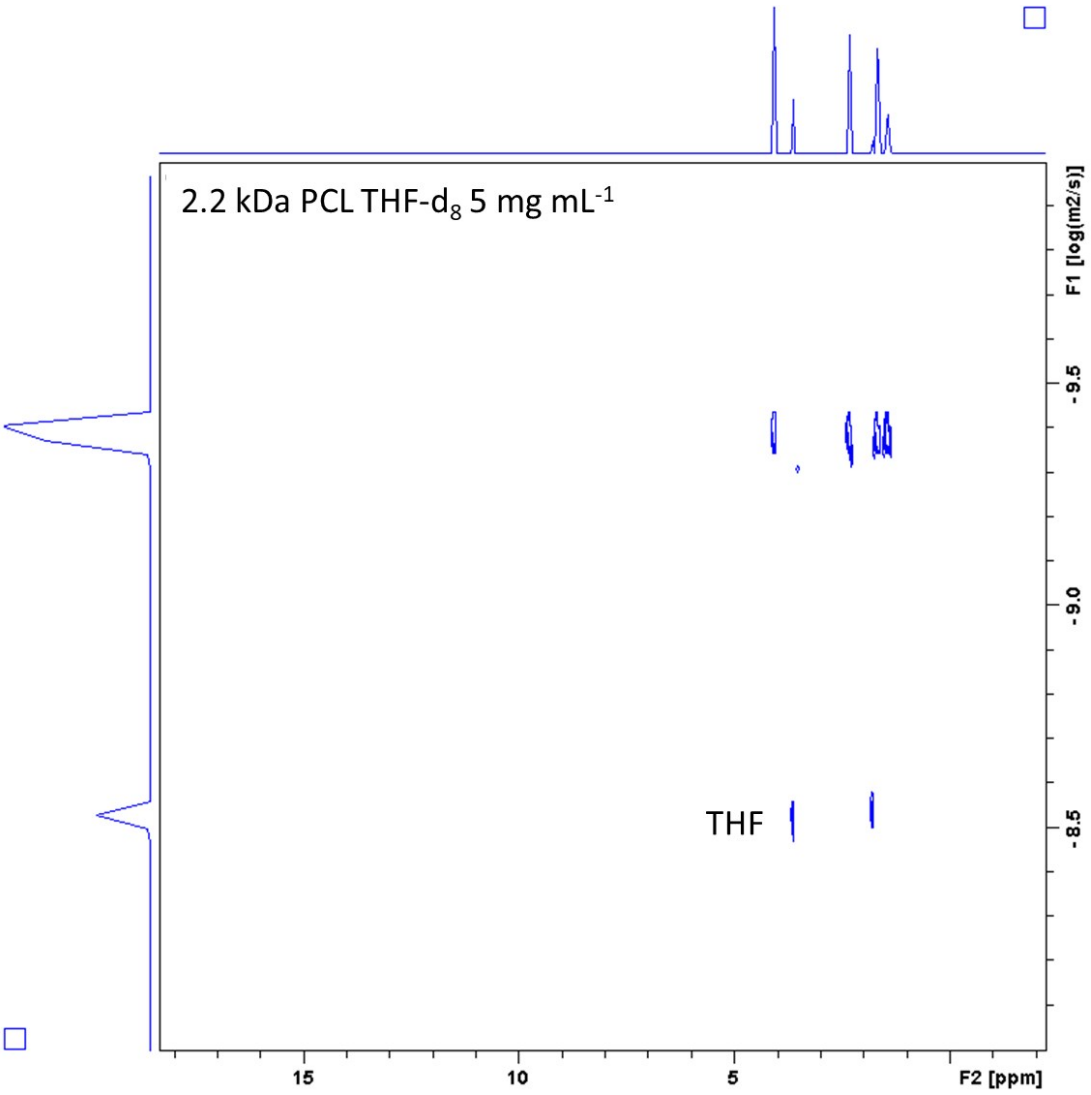

Fig. S16 DOSY-^{1}H NMR spectrum of 2.2 kDa PCL in THF-d_8.

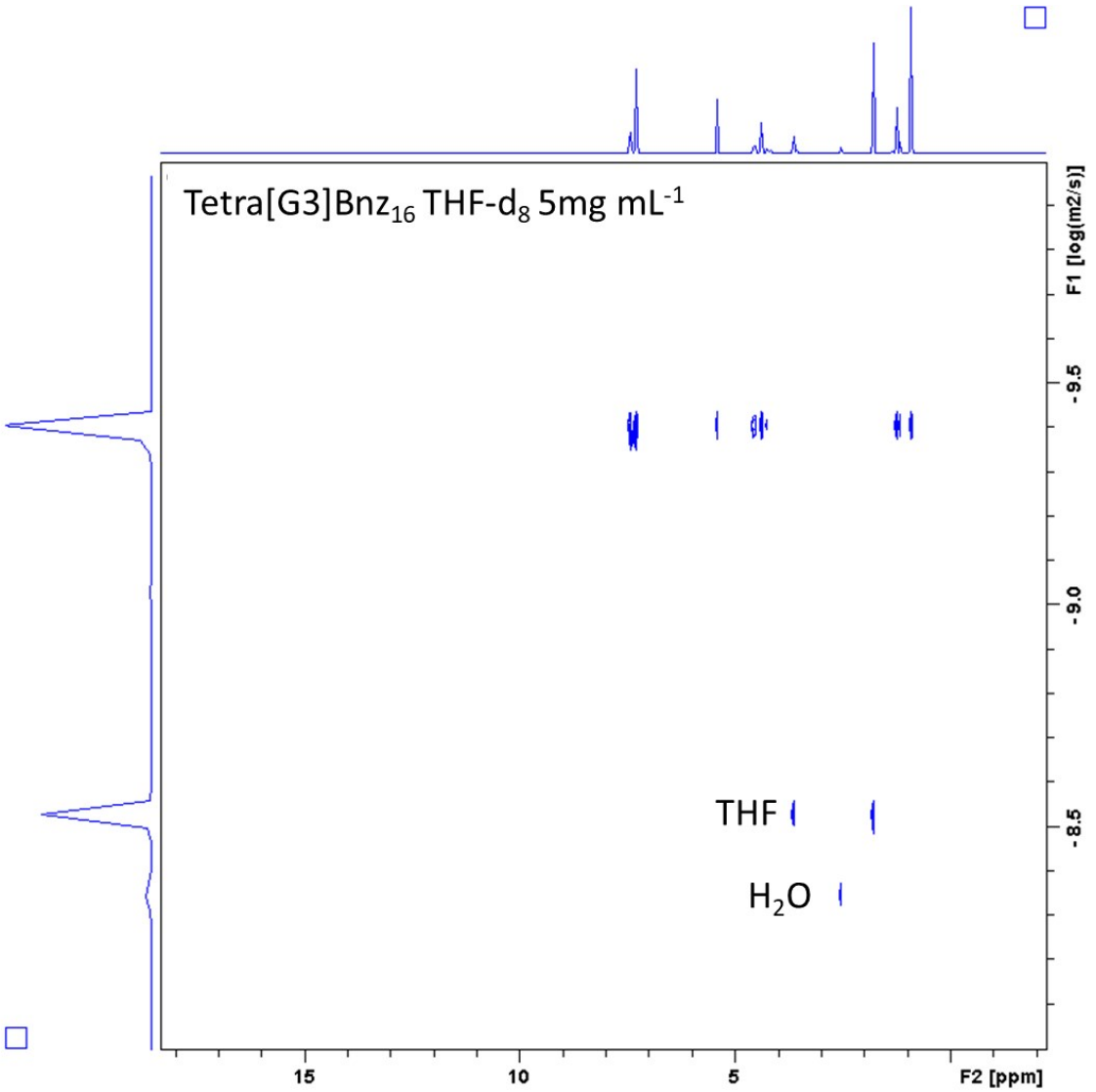

Fig. S17 DOSY-^{1}H NMR spectrum of Tetra[G3]Bnz$_{16}$ in THF-d$_{8}$.

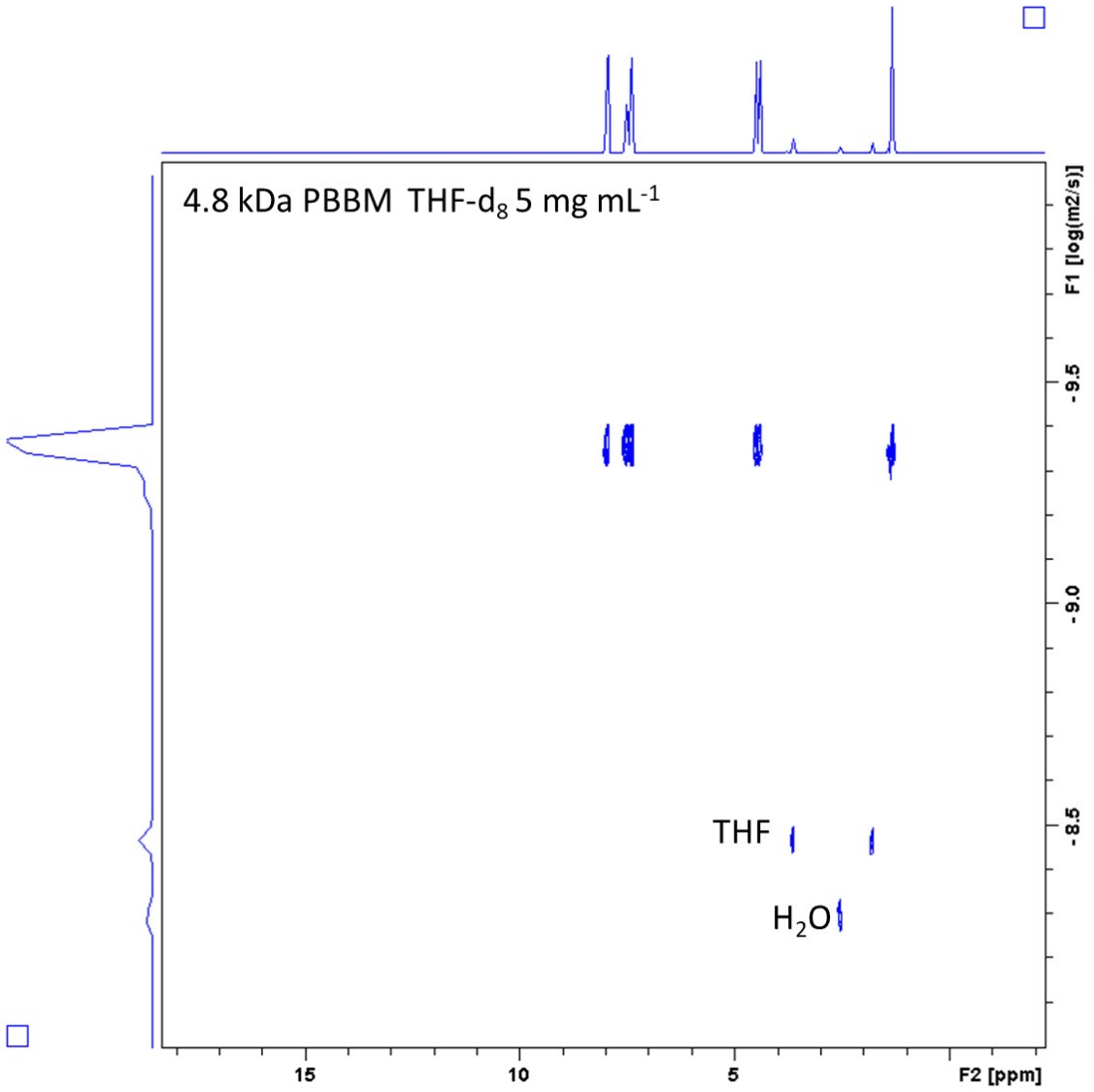

Fig. S18 DOSY-^{1}H NMR spectrum of 4.8 kDa PBBM in THF-d_8.

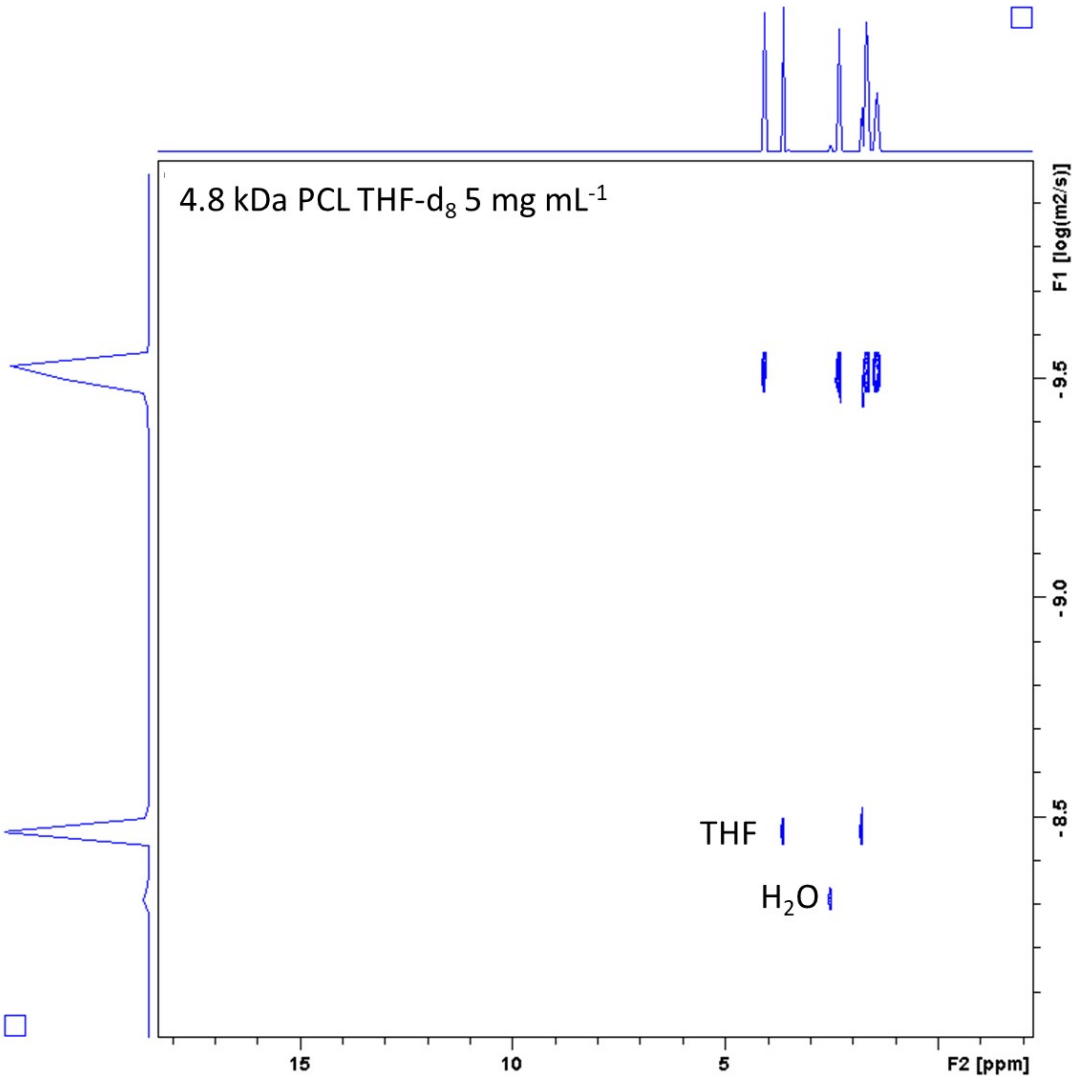

Fig. S19 DOSY-^{1}H NMR spectrum of 4.8 kDa PCL in THF-d_8.

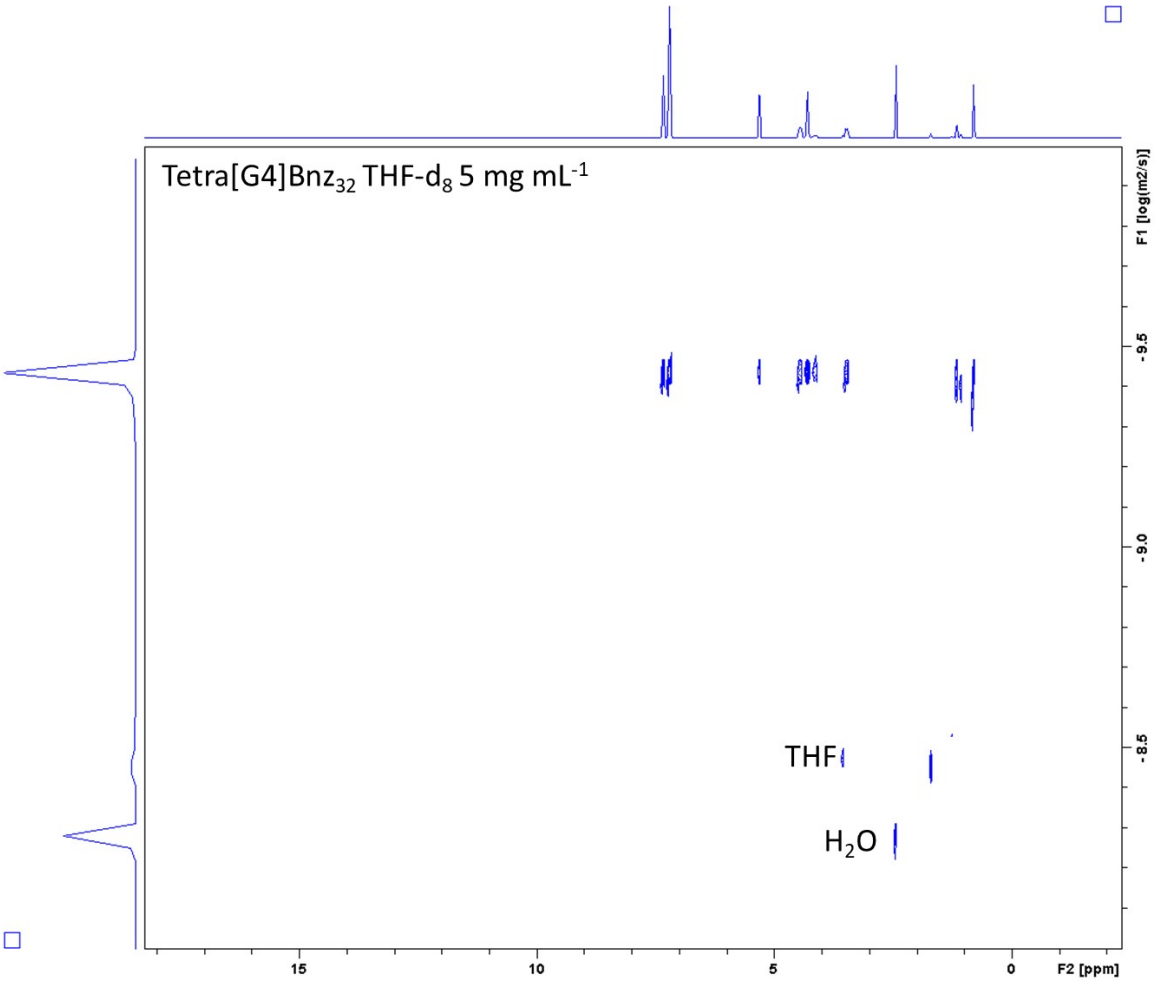

Fig. S20 DOSY-^{1}H NMR spectrum of Tetra[G4]Bnz$_{32}$ in THF-d$_{8}$.

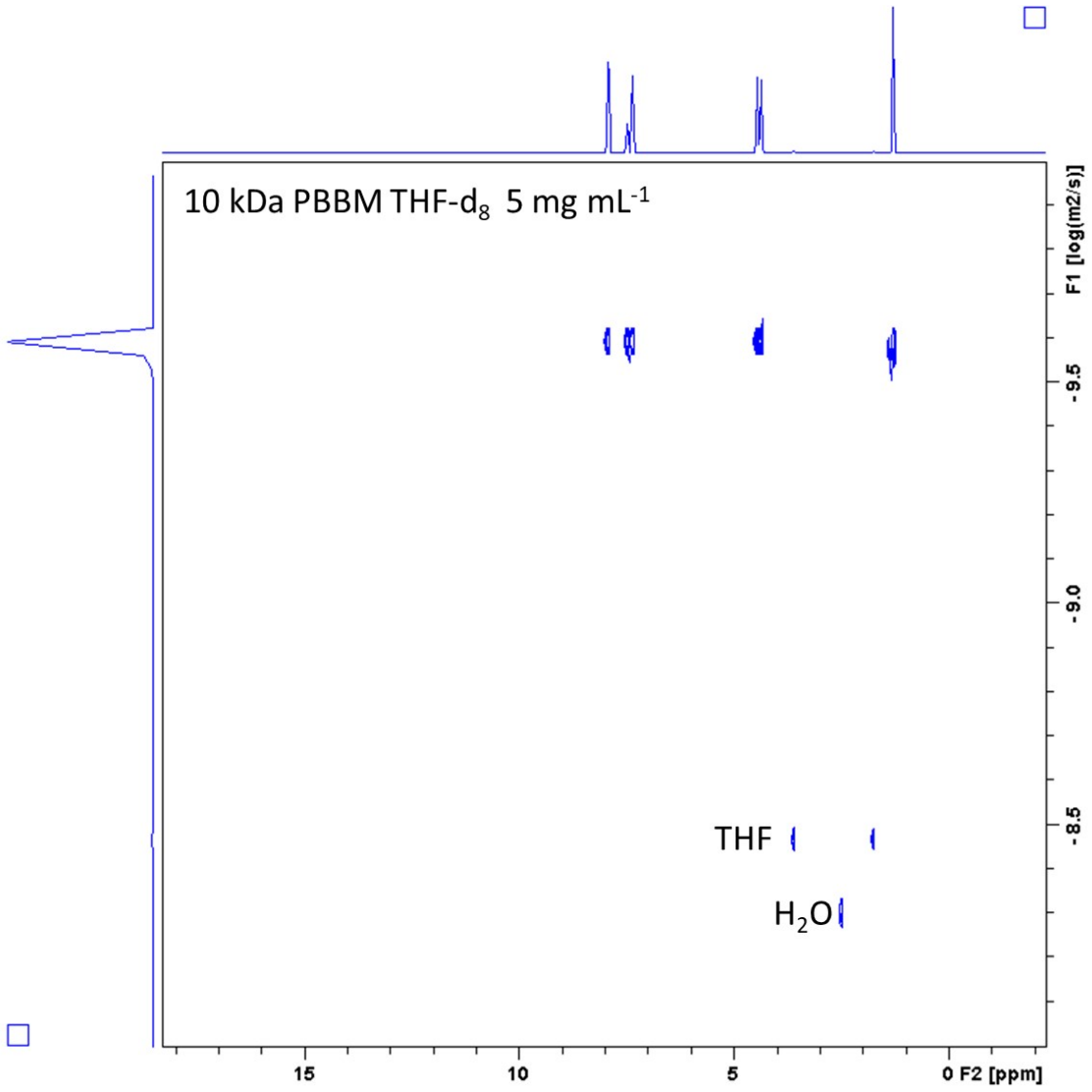

Fig. S21 DOSY-^{1}H NMR spectrum of 10 kDa PBBM in THF-d_8.

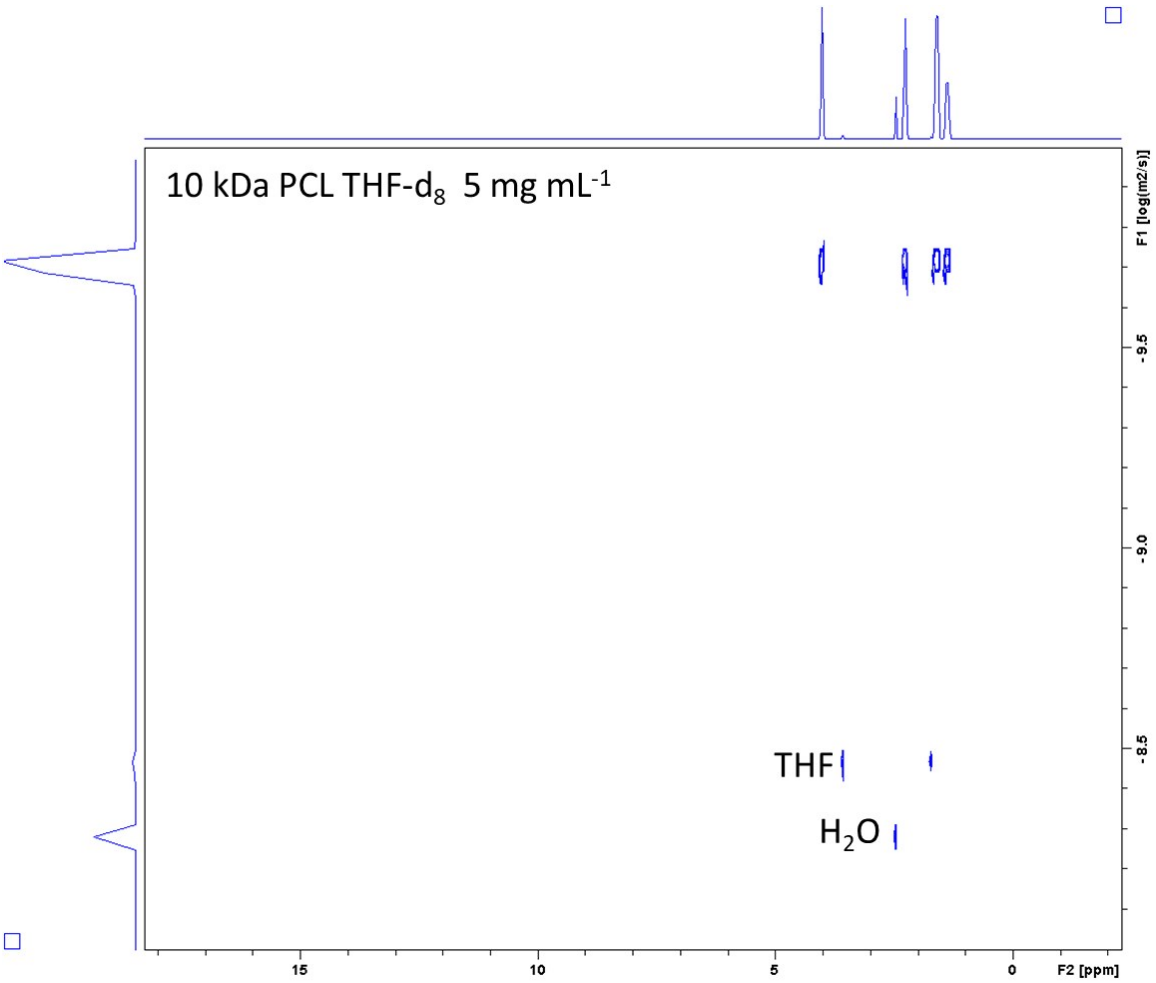

Fig. S22 DOSY-^{1}H NMR spectrum of 10 kDa PCL in THF-d_8.

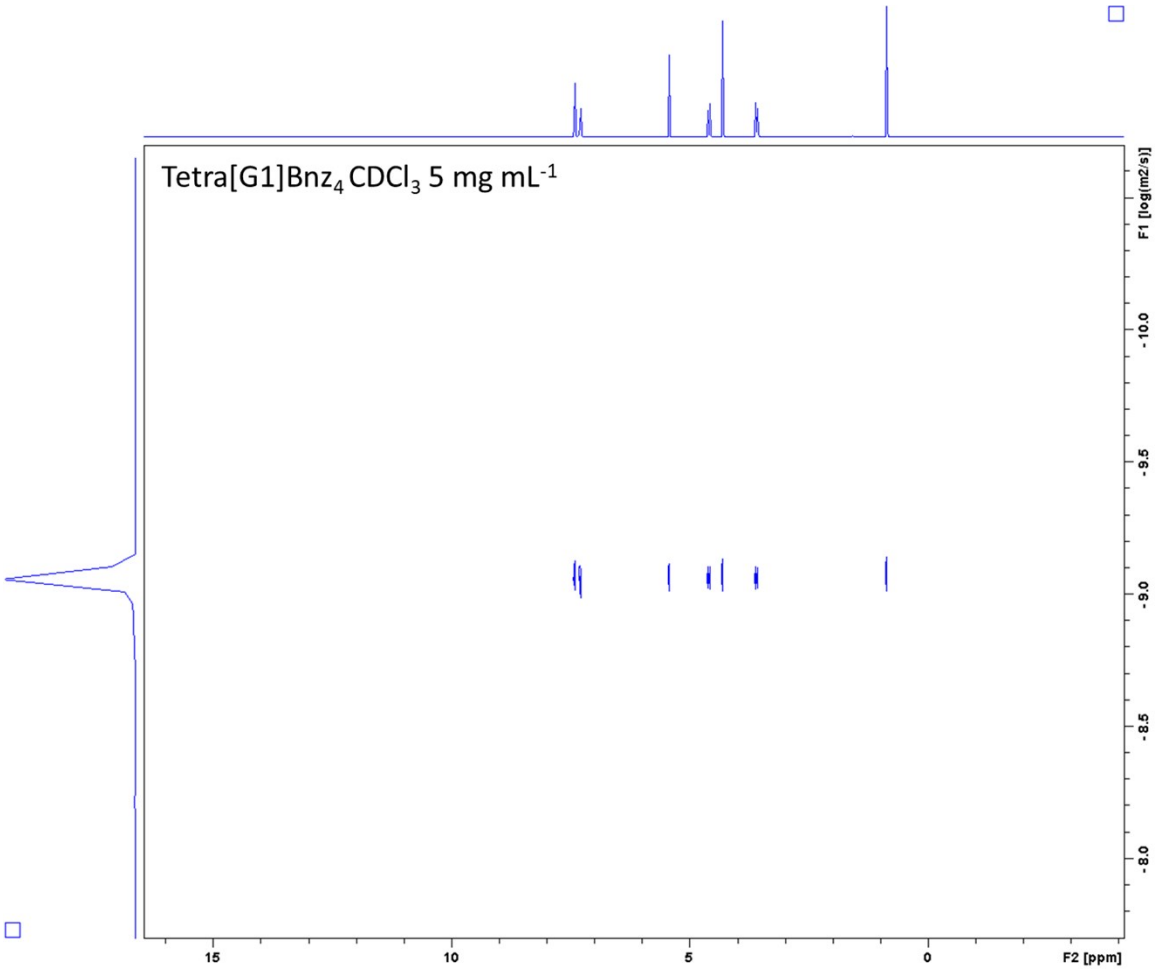

Fig. S23 DOSY-^{1}H NMR spectrum of Tetra[G1]Bnz$_4$ in $CDCl_3$.

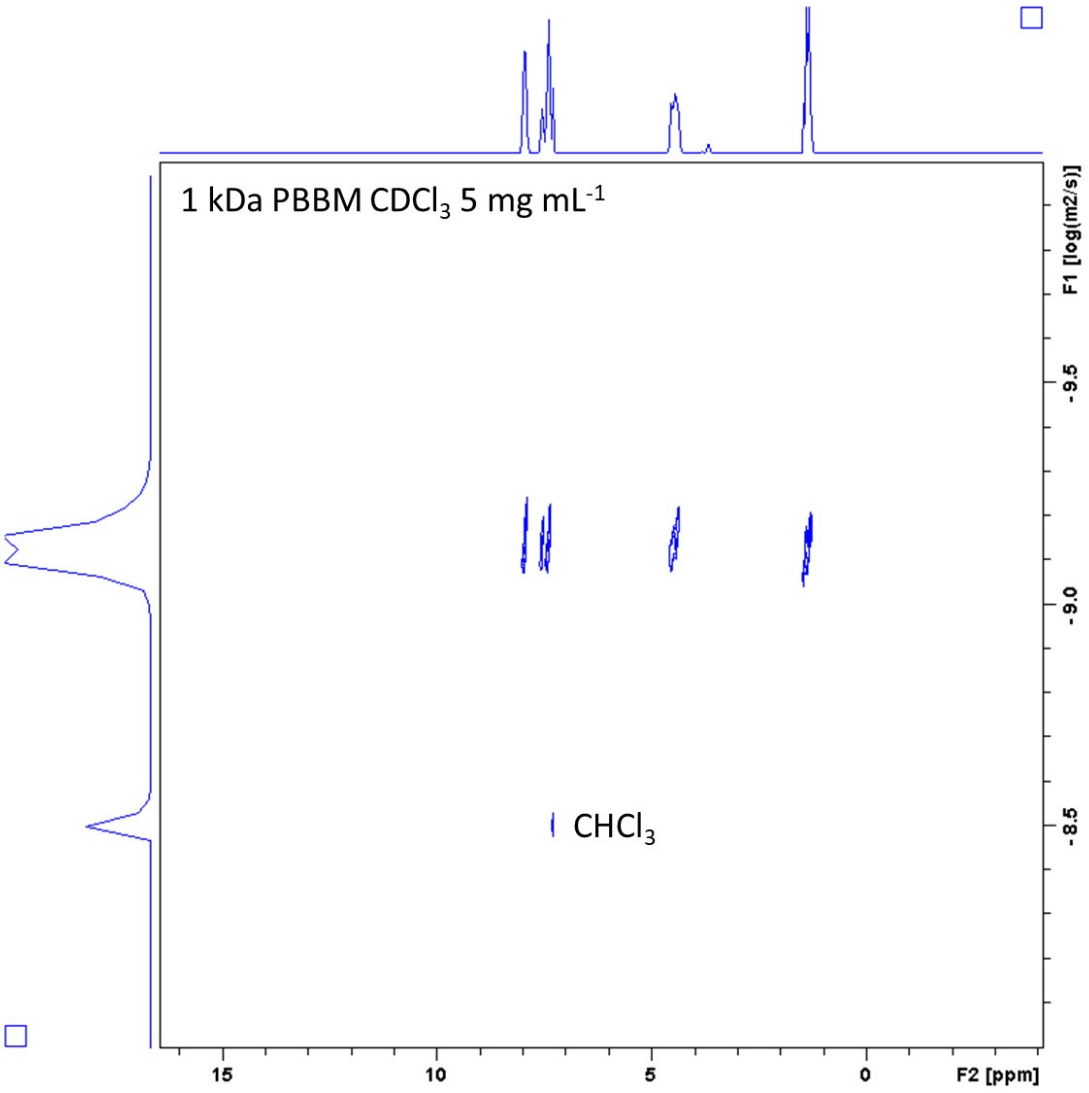

Fig. S24 DOSY-^{1}H NMR spectrum of 1 kDa PBBM in $CDCl_3$.

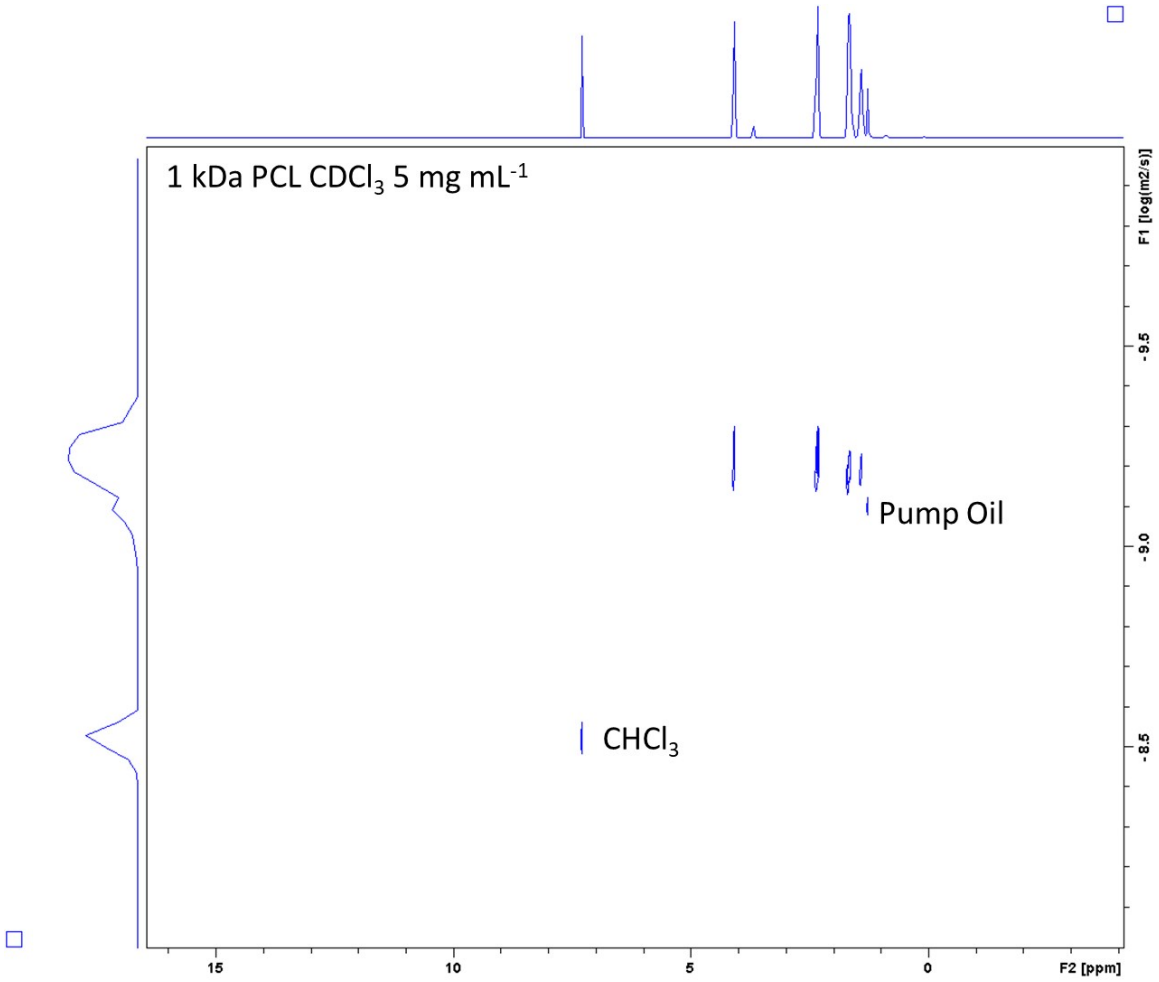

Fig. S25 DOSY-^{1}H NMR spectrum of 1 kDa PCL in $CDCl_3$.

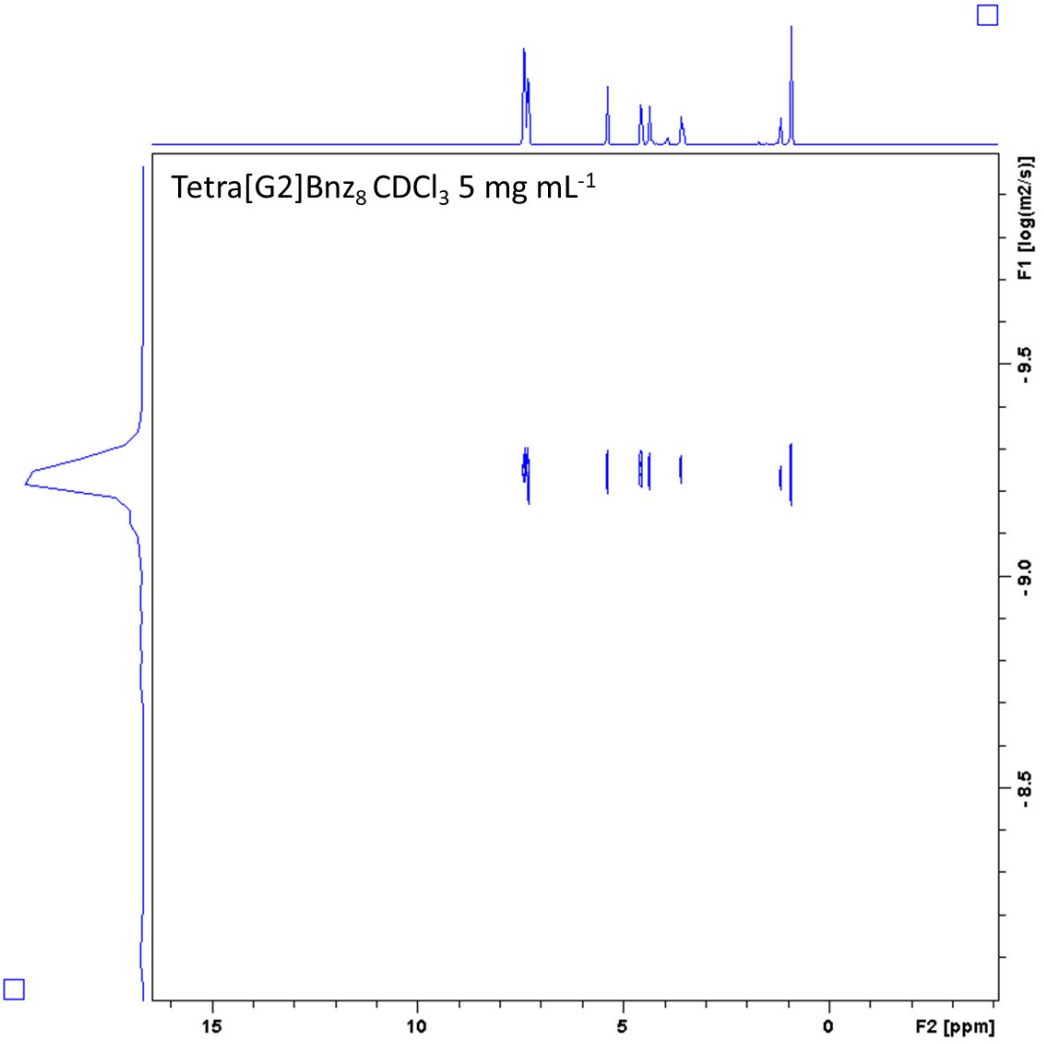

Fig. S26 DOSY-^{1}H NMR spectrum of Tetra[G2]Bnz$_8$ in $CDCl_3$.

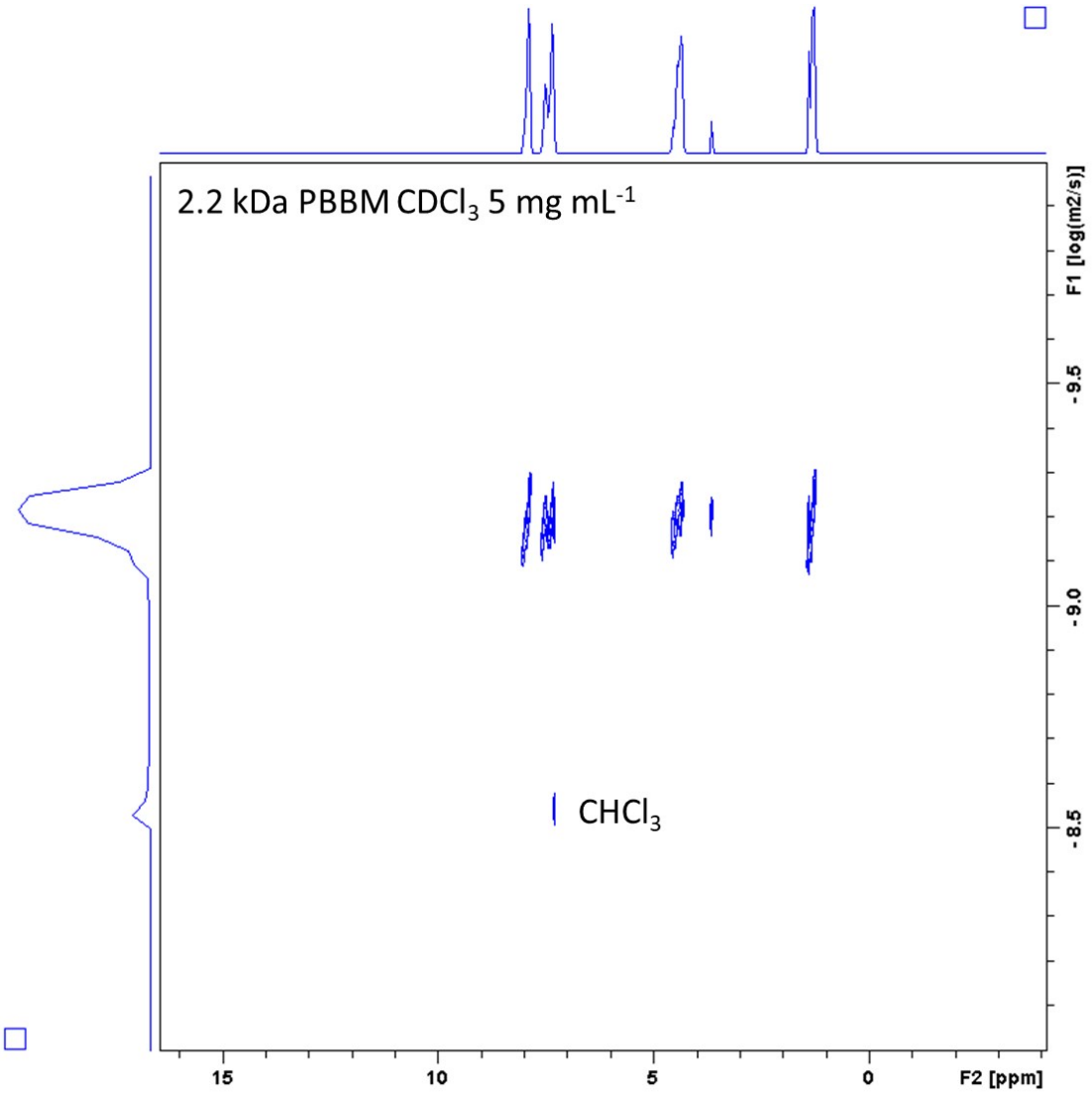

Fig. S27 DOSY-^{1}H NMR spectrum of 2.2 kDa PBBM in $CDCl_3$.

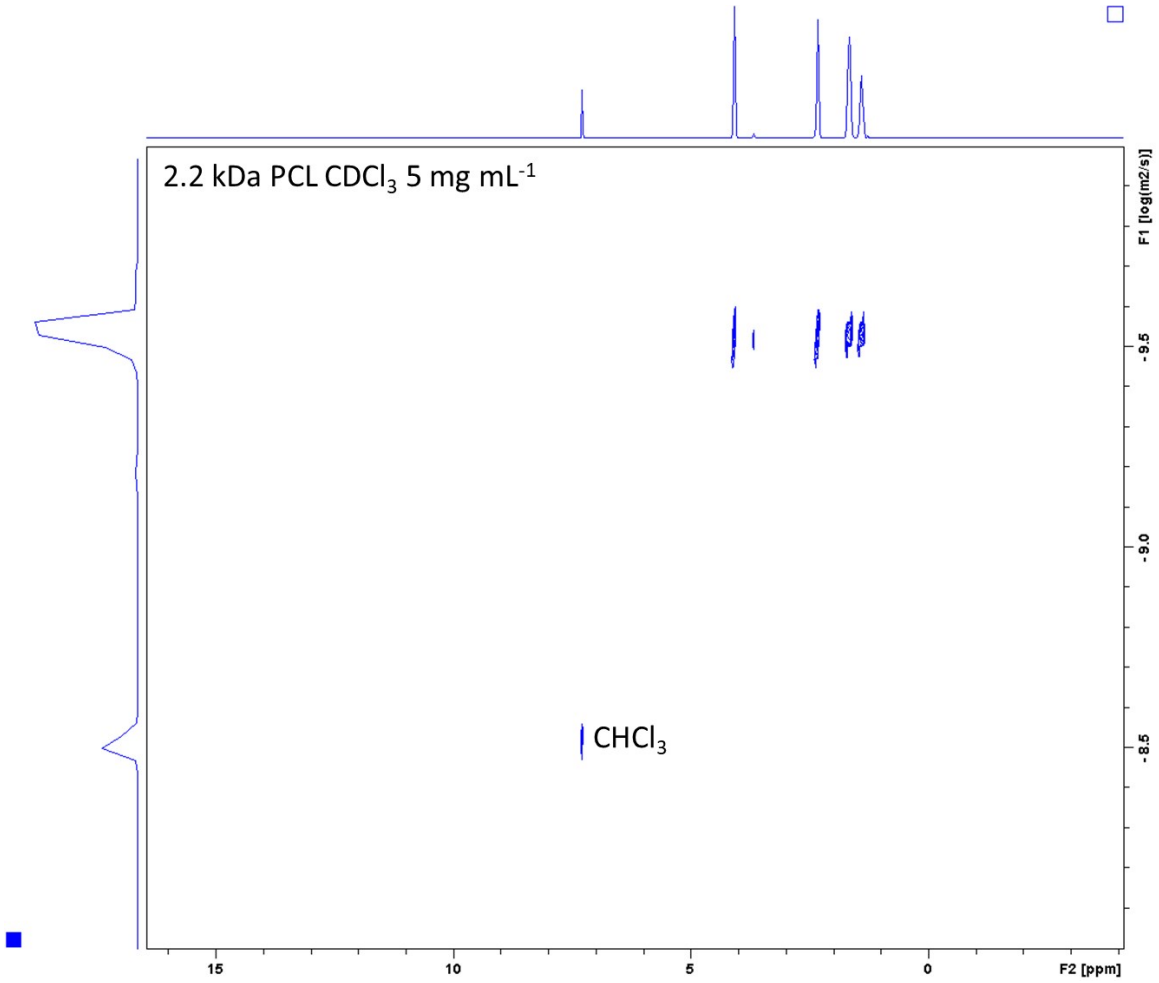

Fig. S28 DOSY-^{1}H NMR spectrum of 2.2 kDa PCL in $CDCl_3$.

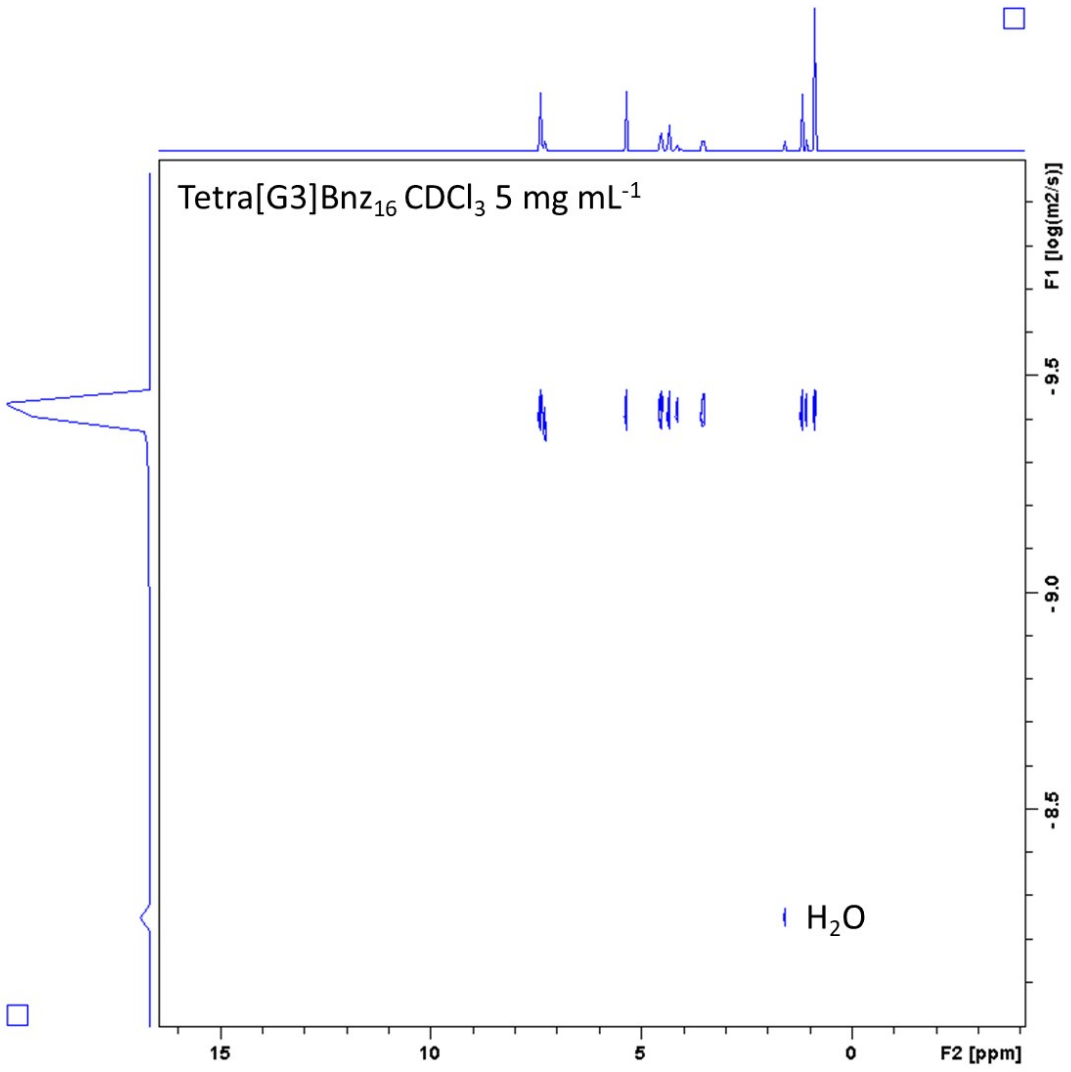

Fig. S29 DOSY-^{1}H NMR spectrum of Tetra[G3]Bnz$_{16}$ in $CDCl_3$.

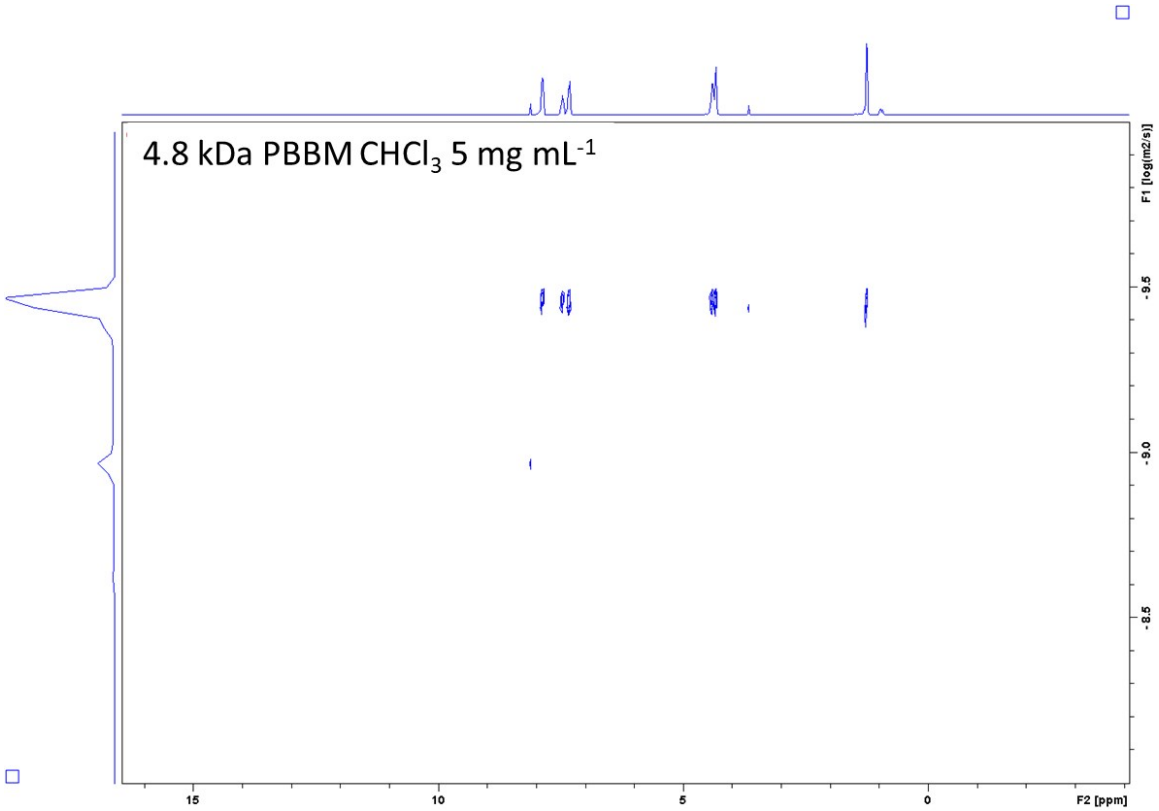

Fig. S30 DOSY-^{1}H NMR spectrum of 4.8 kDa PBBM in $CDCl_3$.

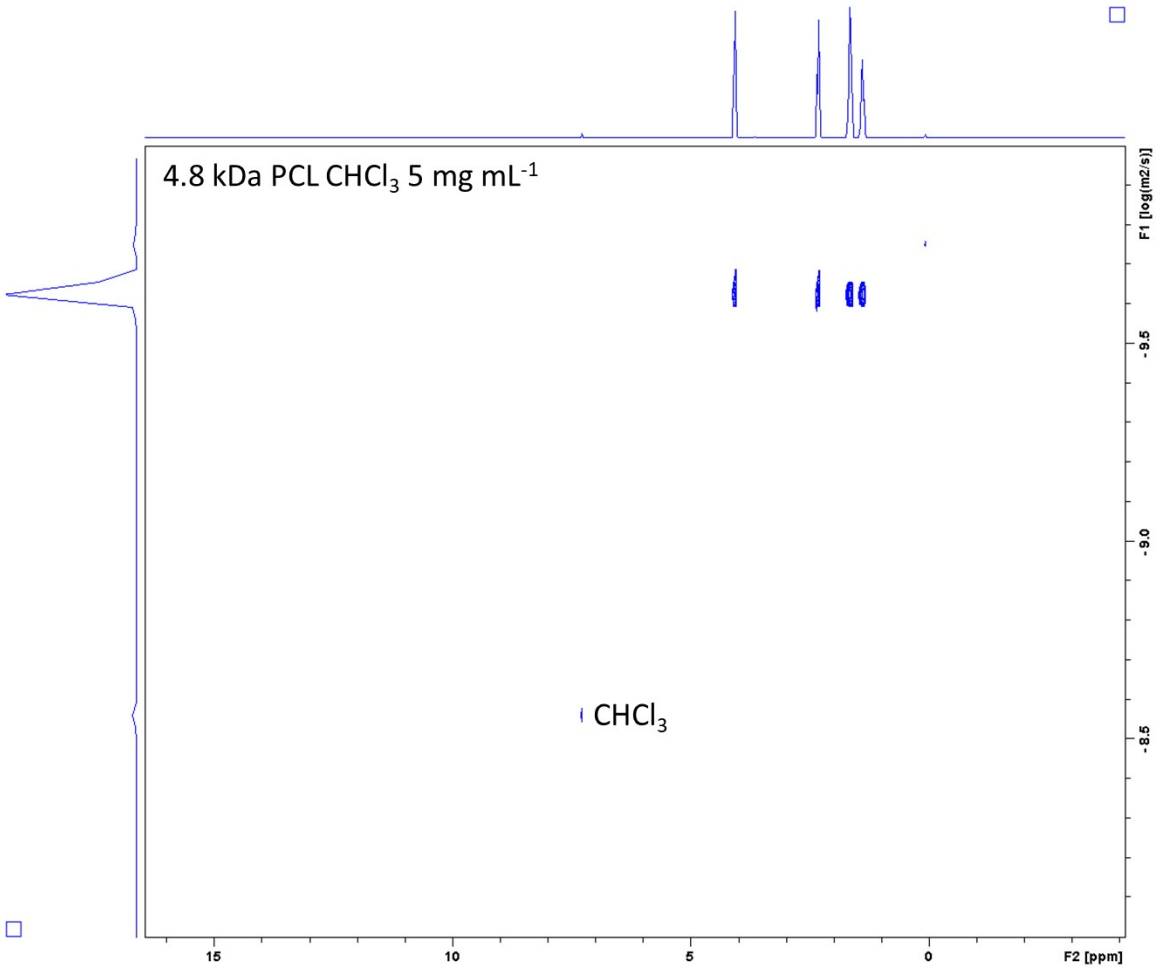

Fig. S31 DOSY-^{1}H NMR spectrum of 4.8 kDa PCL in $CDCl_3$.

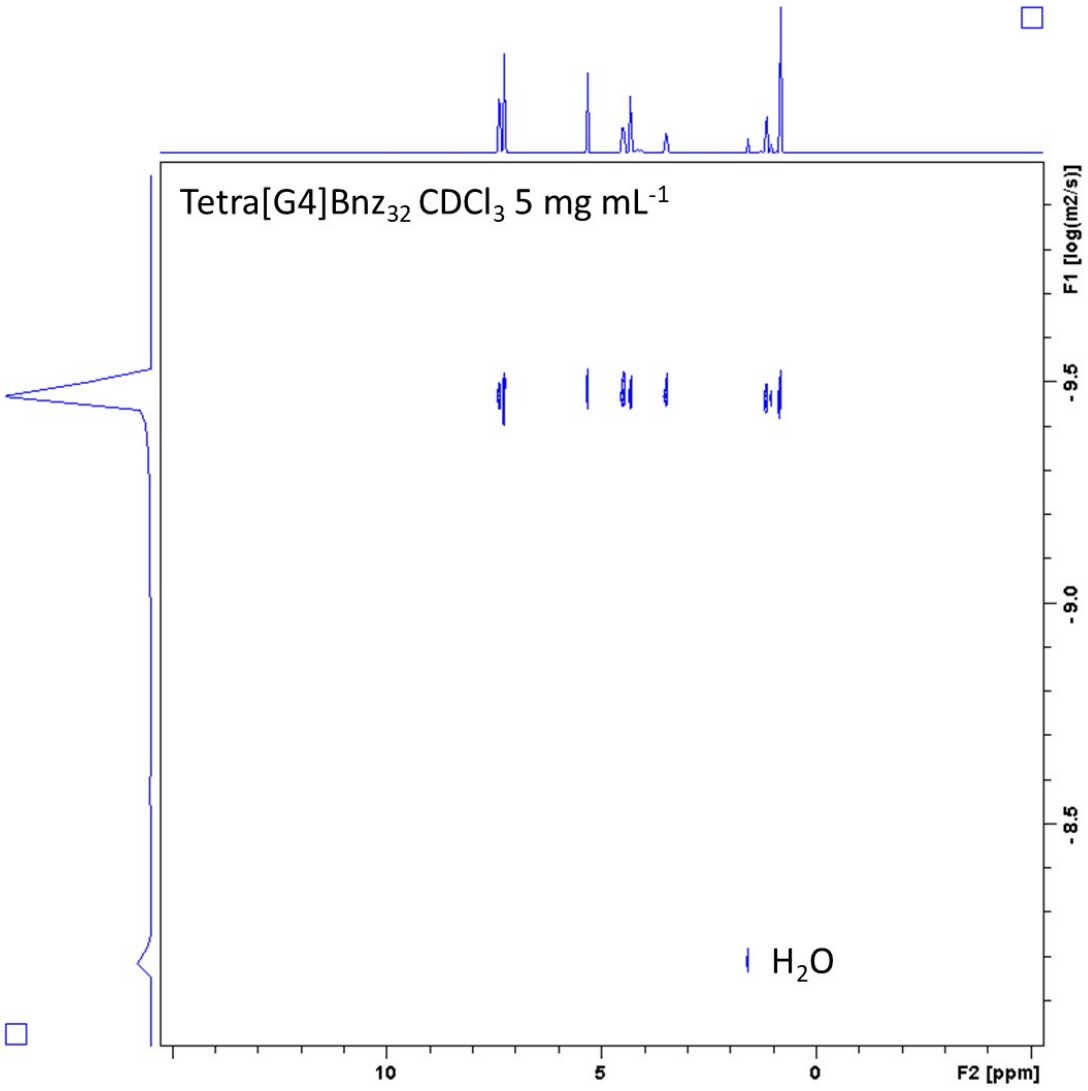

Fig. S32 DOSY-^{1}H NMR spectrum of Tetra[G4]Bnz_{32} in $CDCl_3$.

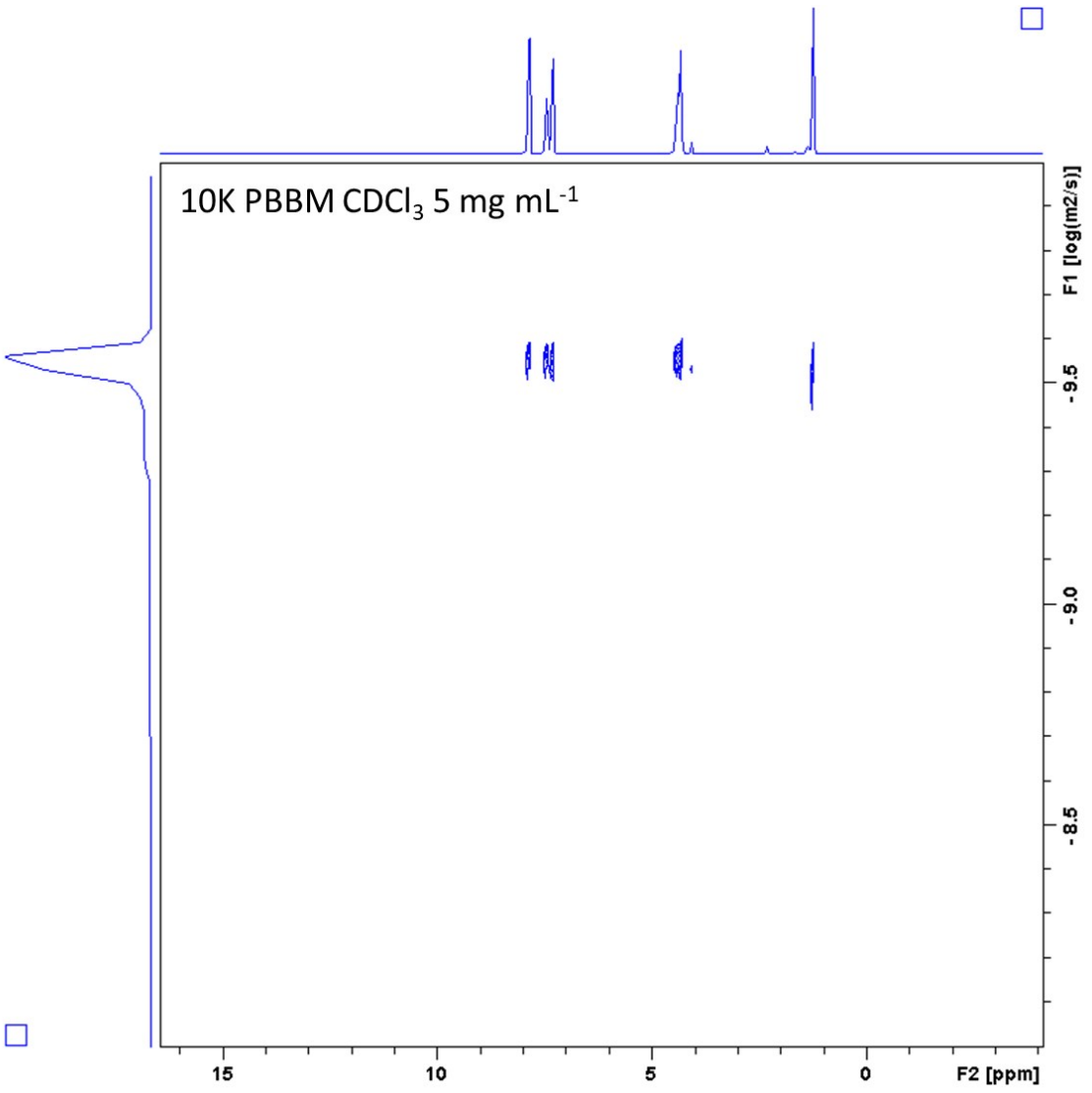

Fig. S33 DOSY-^{1}H NMR spectrum of 10 kDa PBBM in $CDCl_3$.

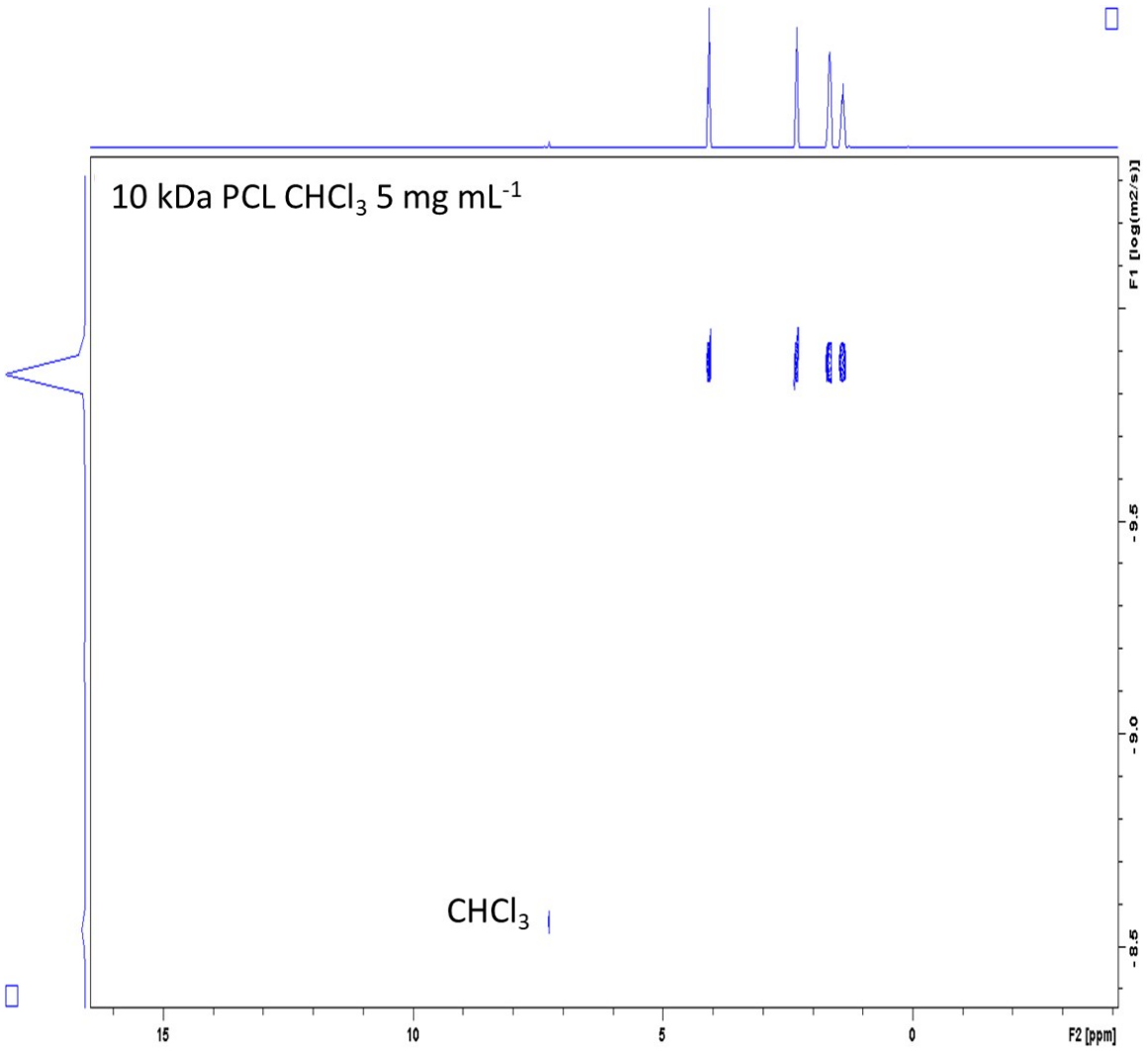

Fig. S34 DOSY-^{1}H NMR spectrum of 10 kDa PCL in $CDCl_3$.

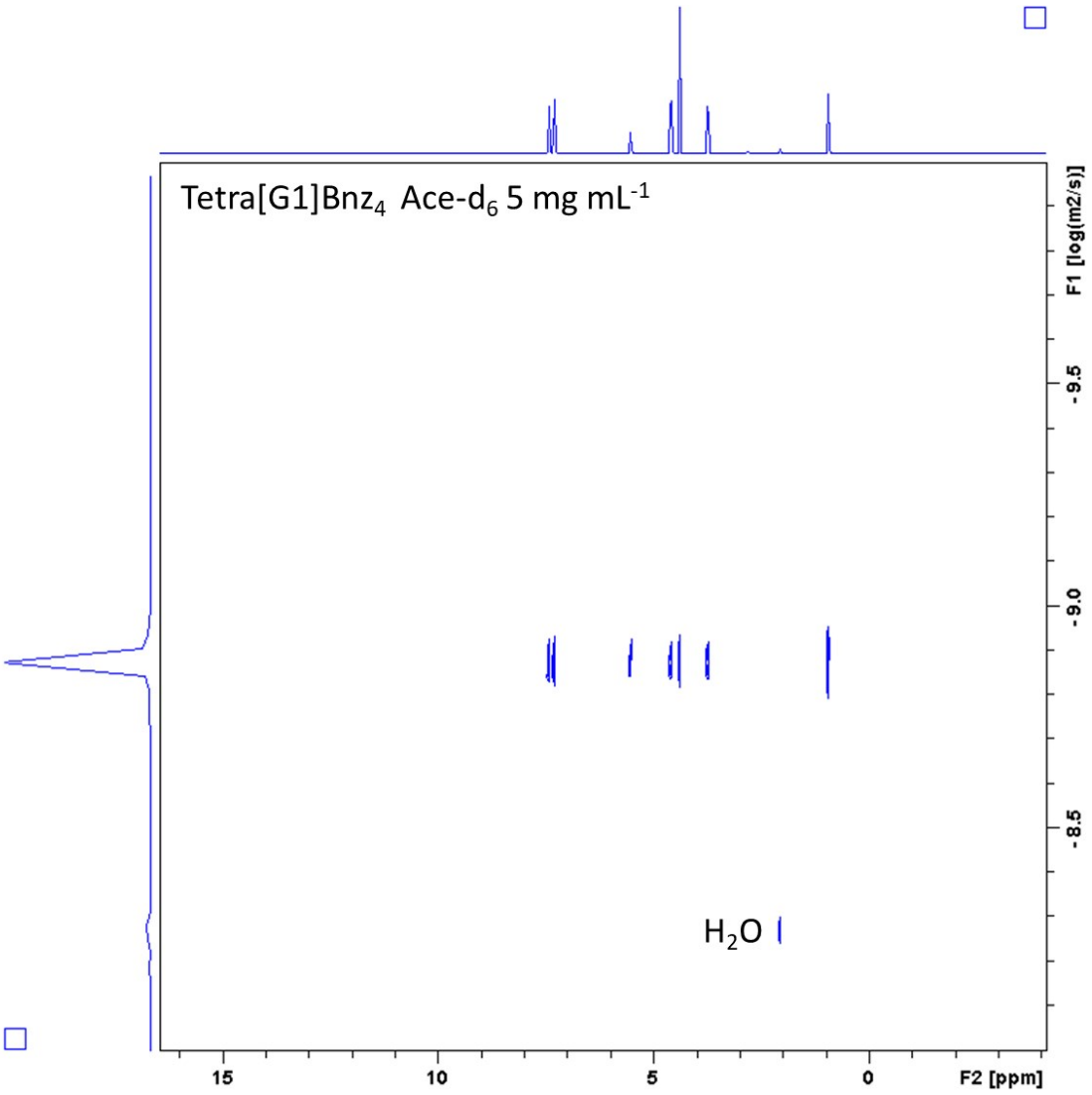

Fig. S35 DOSY-^{1}H NMR spectrum of Tetra[G1]Bnz$_4$ in Ace-d$_6$.

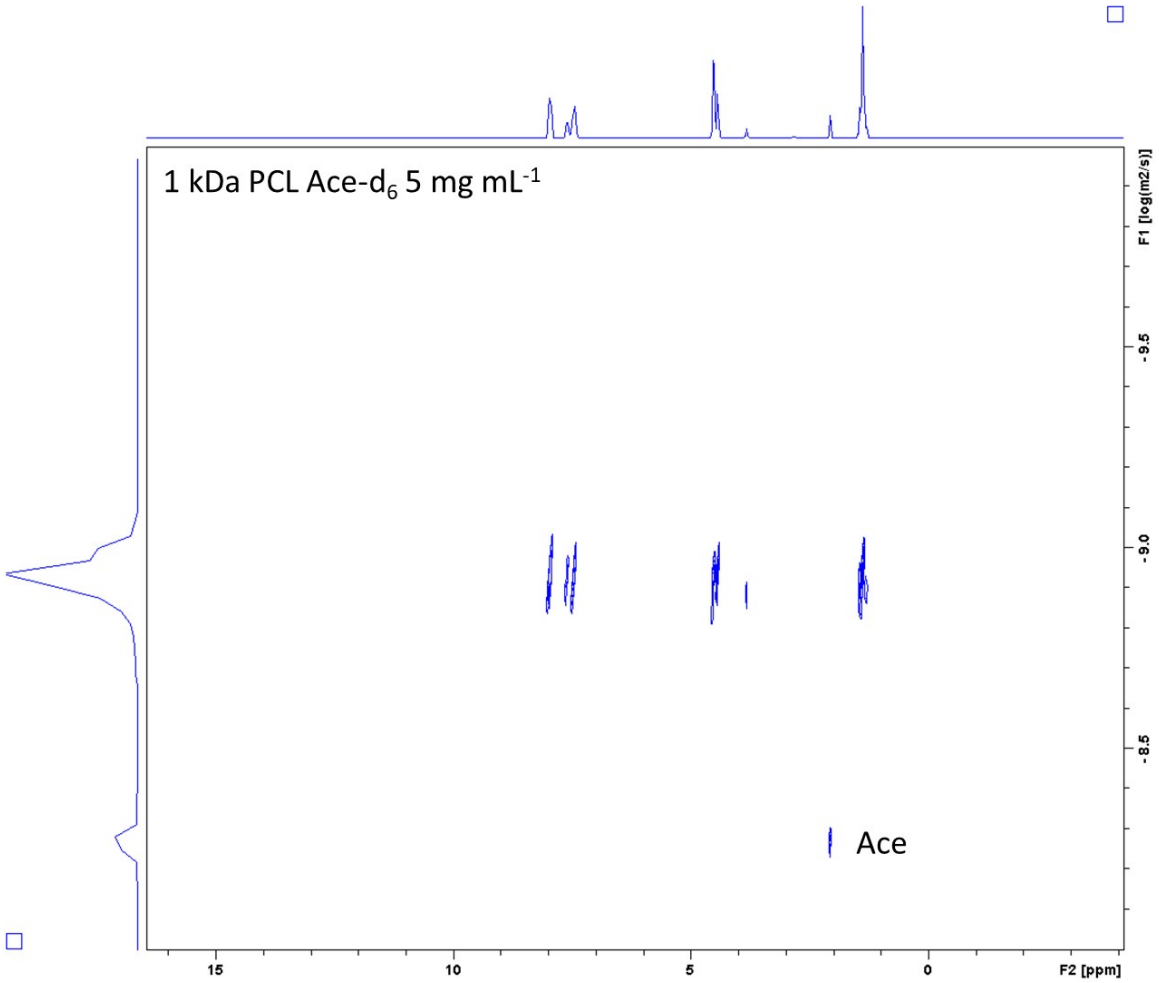

Fig. S36 DOSY-^{1}H NMR spectrum of 1 kDa PBBM in Ace-d_6.

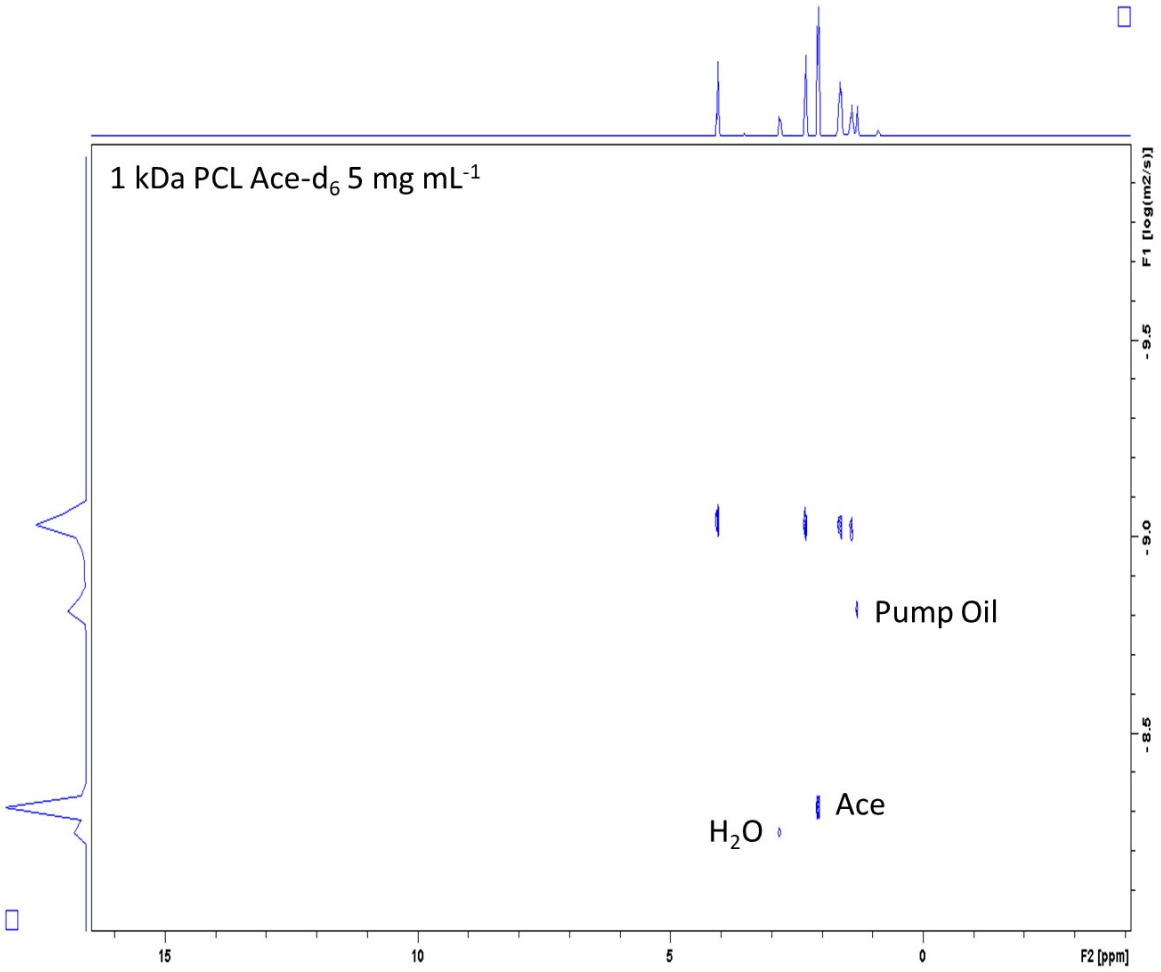

Fig. S37 DOSY-^{1}H NMR spectrum of 1 kDa PCL in Ace-d_6.

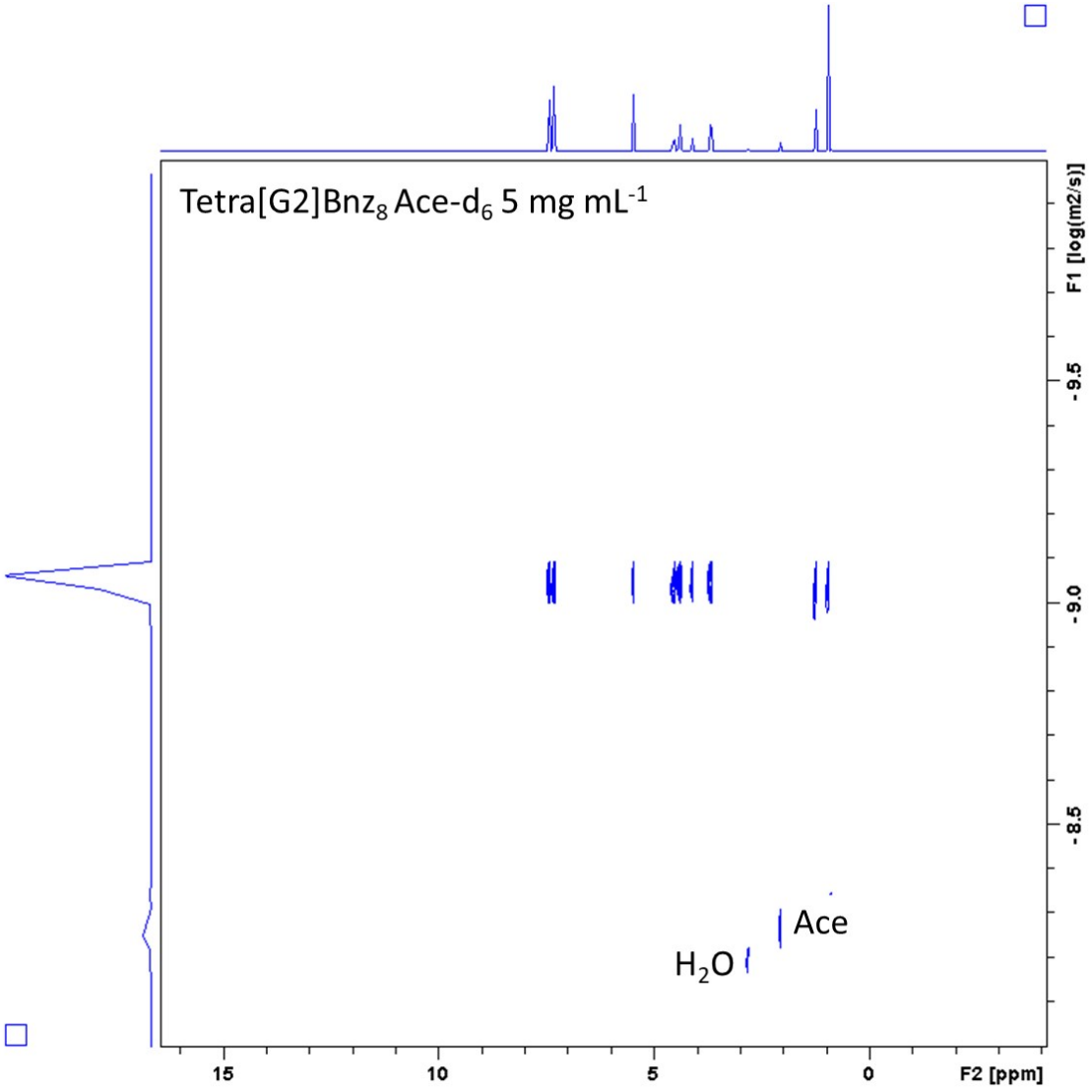

Fig. S38 DOSY-^{1}H NMR spectrum of Tetra[G2]Bnz$_8$ in Ace-d$_6$.

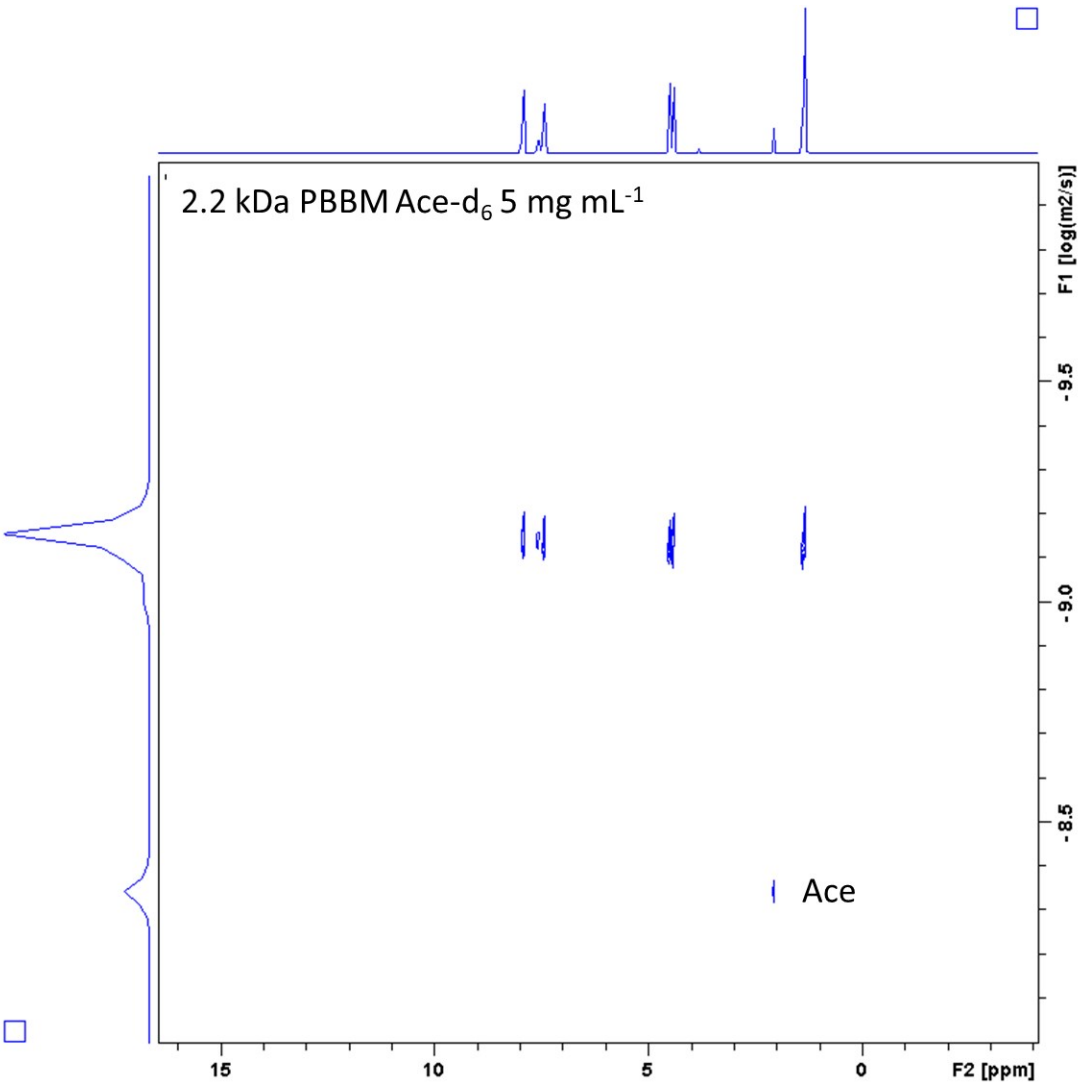

Fig. S39 DOSY-^{1}H NMR spectrum of 2.2 kDa PBBM in Ace-d_6.

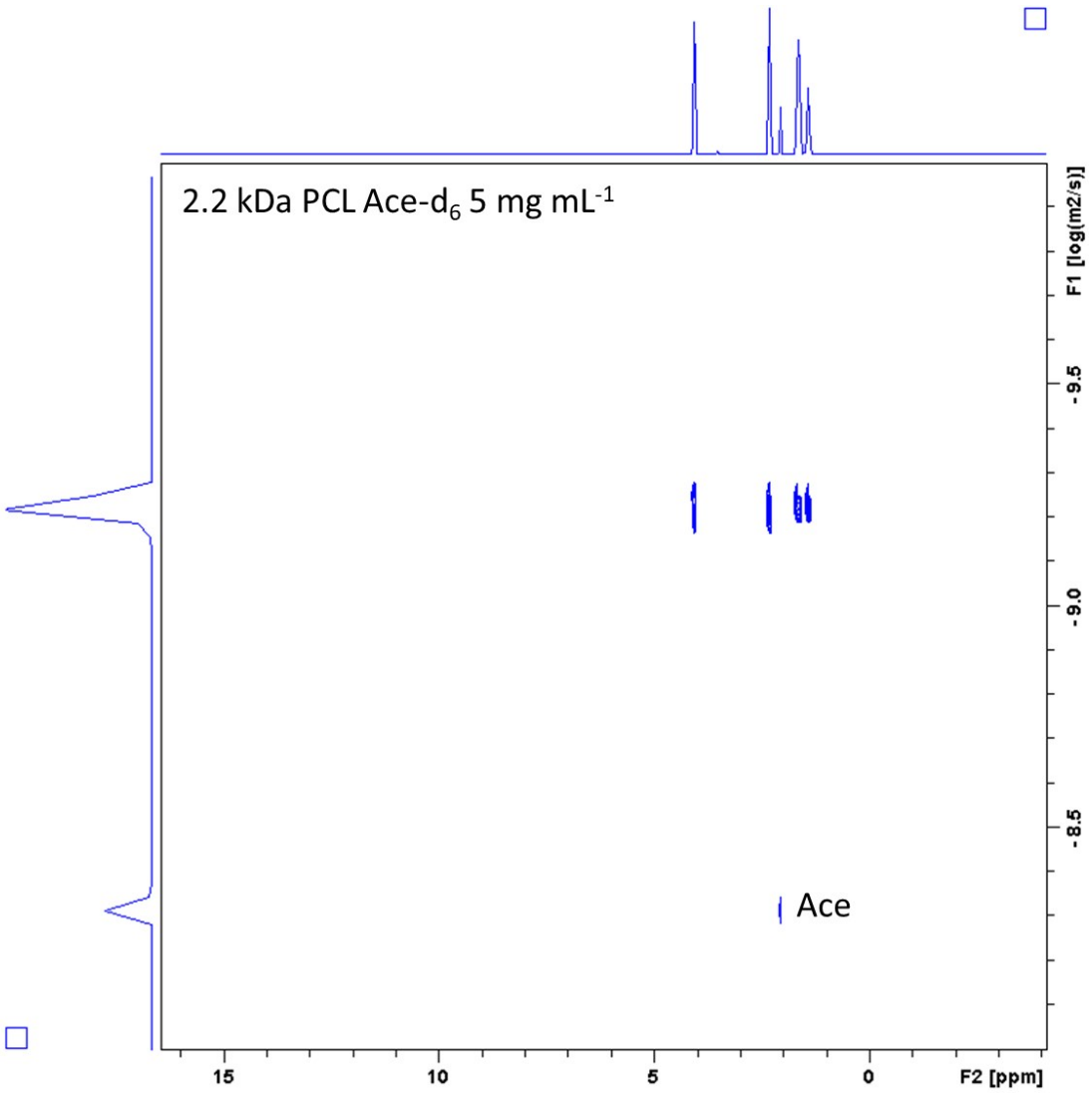

Fig. S40 DOSY-^{1}H NMR spectrum of 2.2 kDa PCL in Ace-d_6.

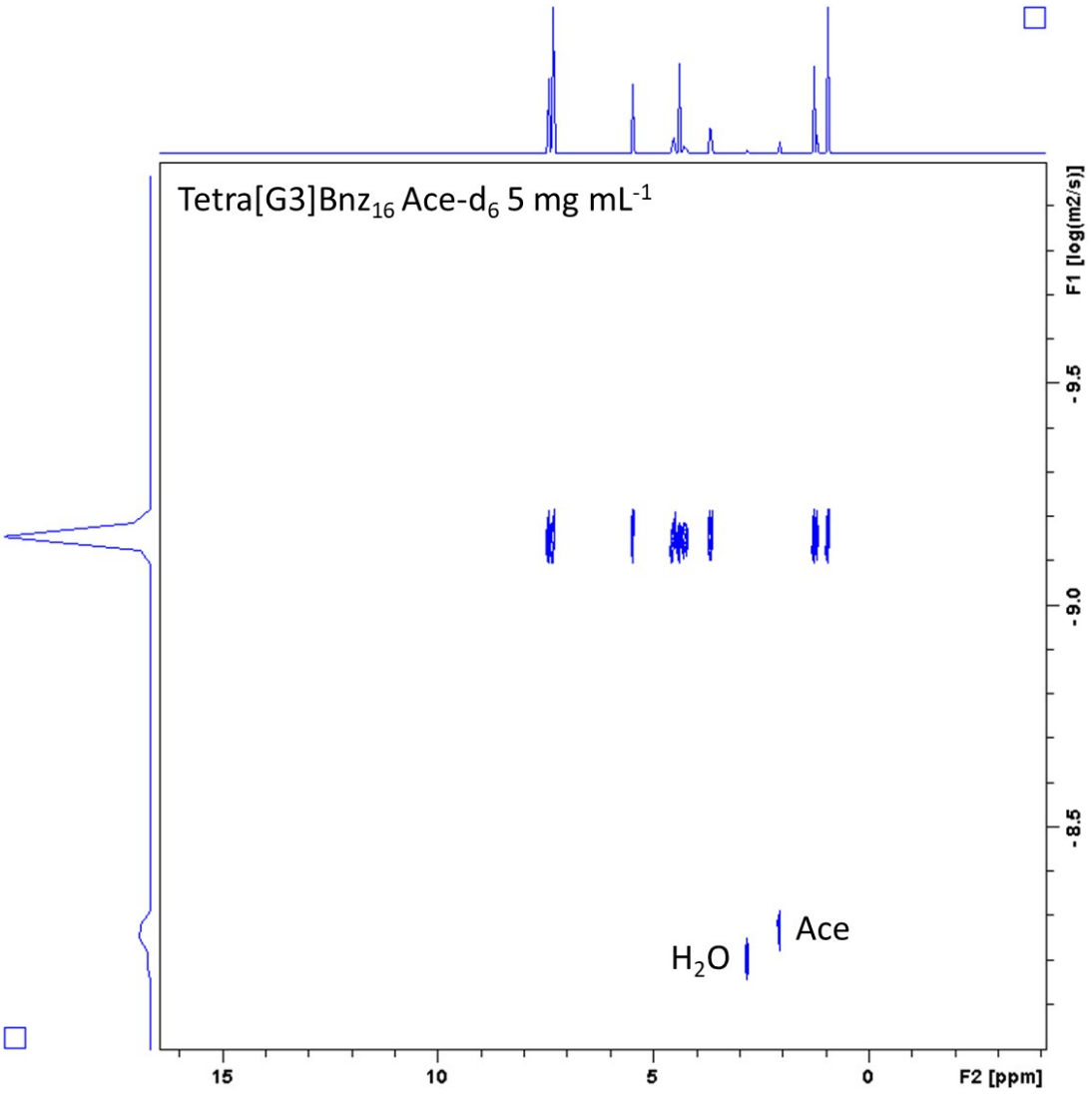

Fig. S41 DOSY-^{1}H NMR spectrum of Tetra[G3]Bnz_{16} in Ace-d_6.

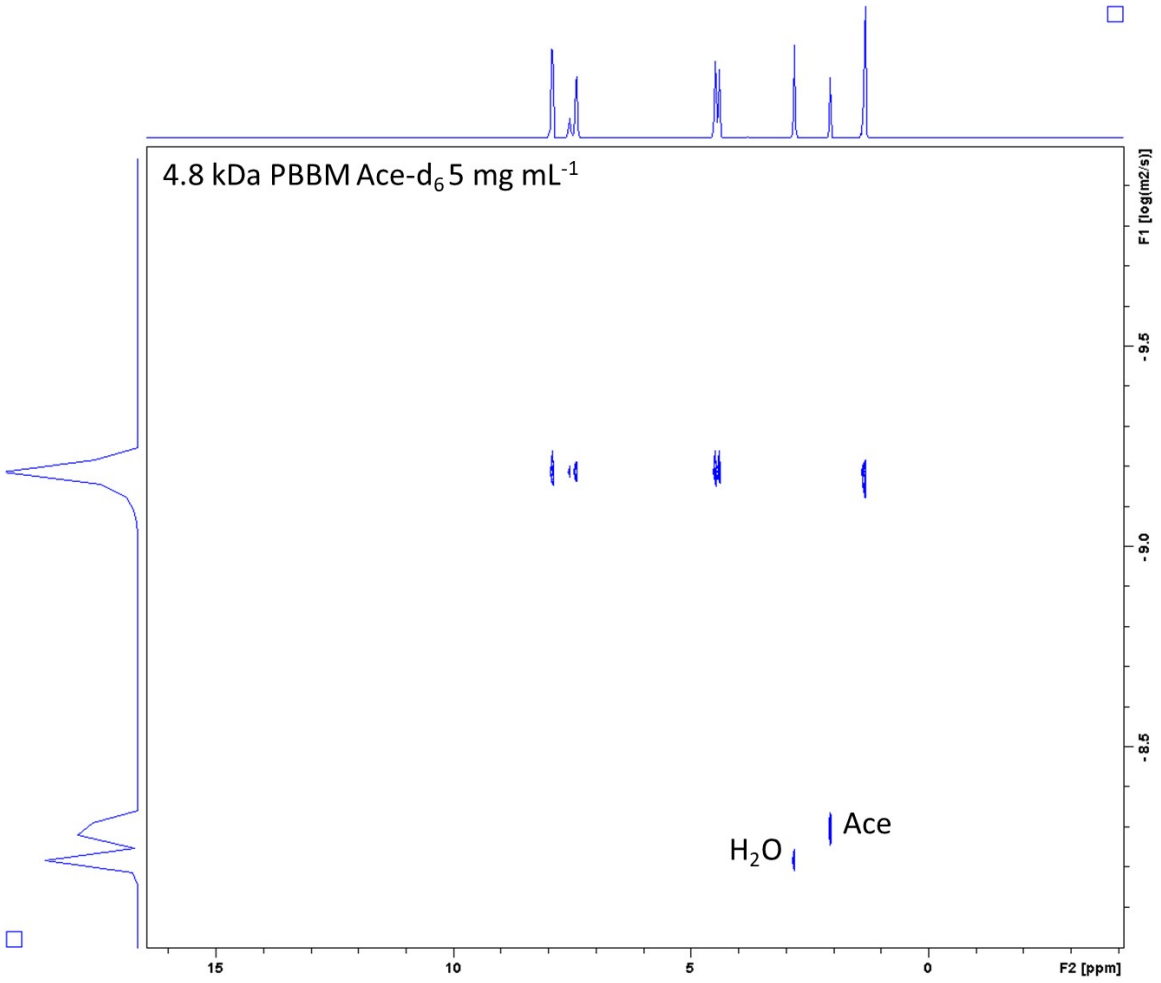

Fig. S42 DOSY-^{1}H NMR spectrum of 4.8 kDa PBBM in Ace-d_6.

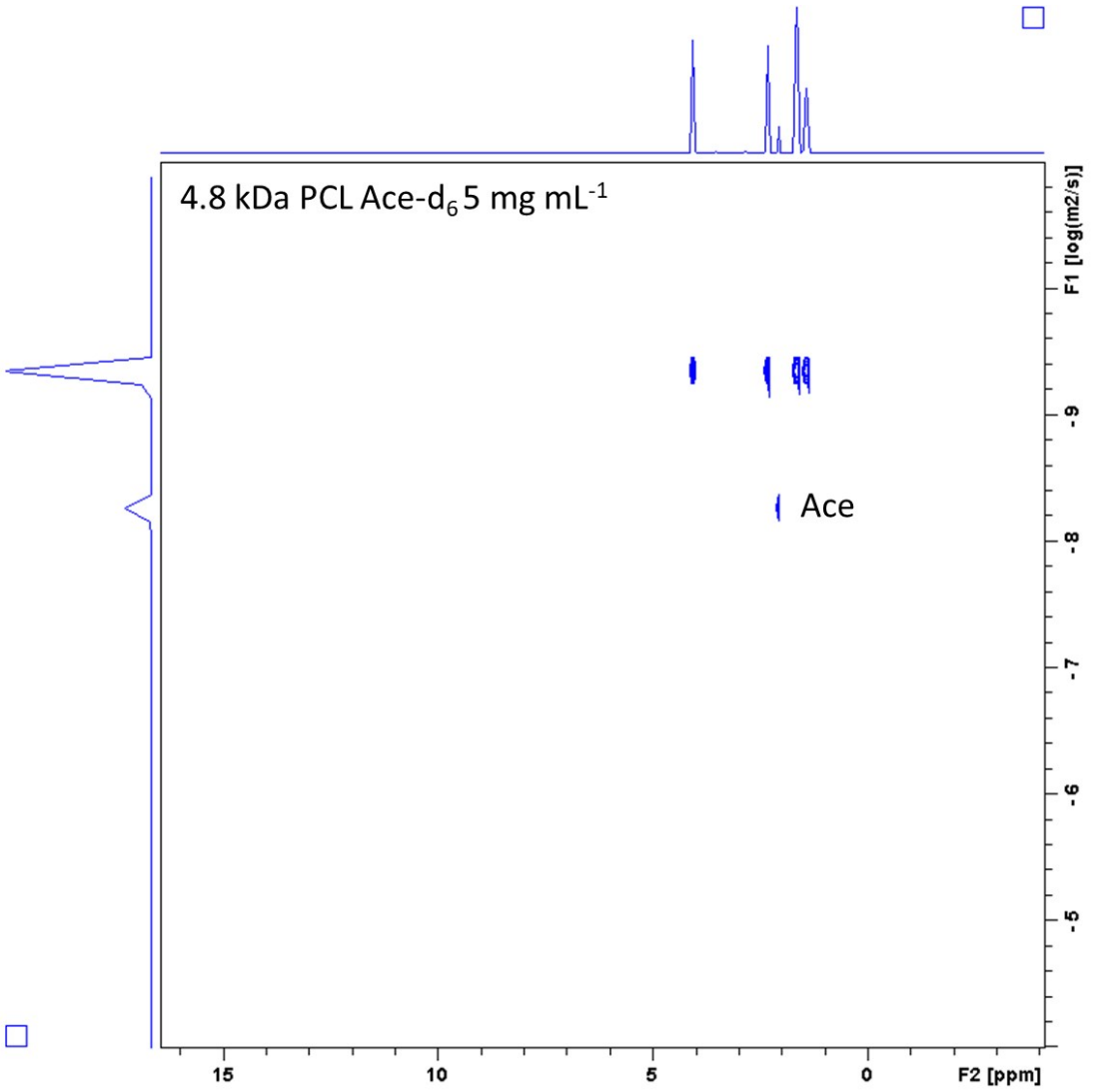

Fig. S43 DOSY-^{1}H NMR spectrum of 4.8 kDa PCL in Ace-d_6.

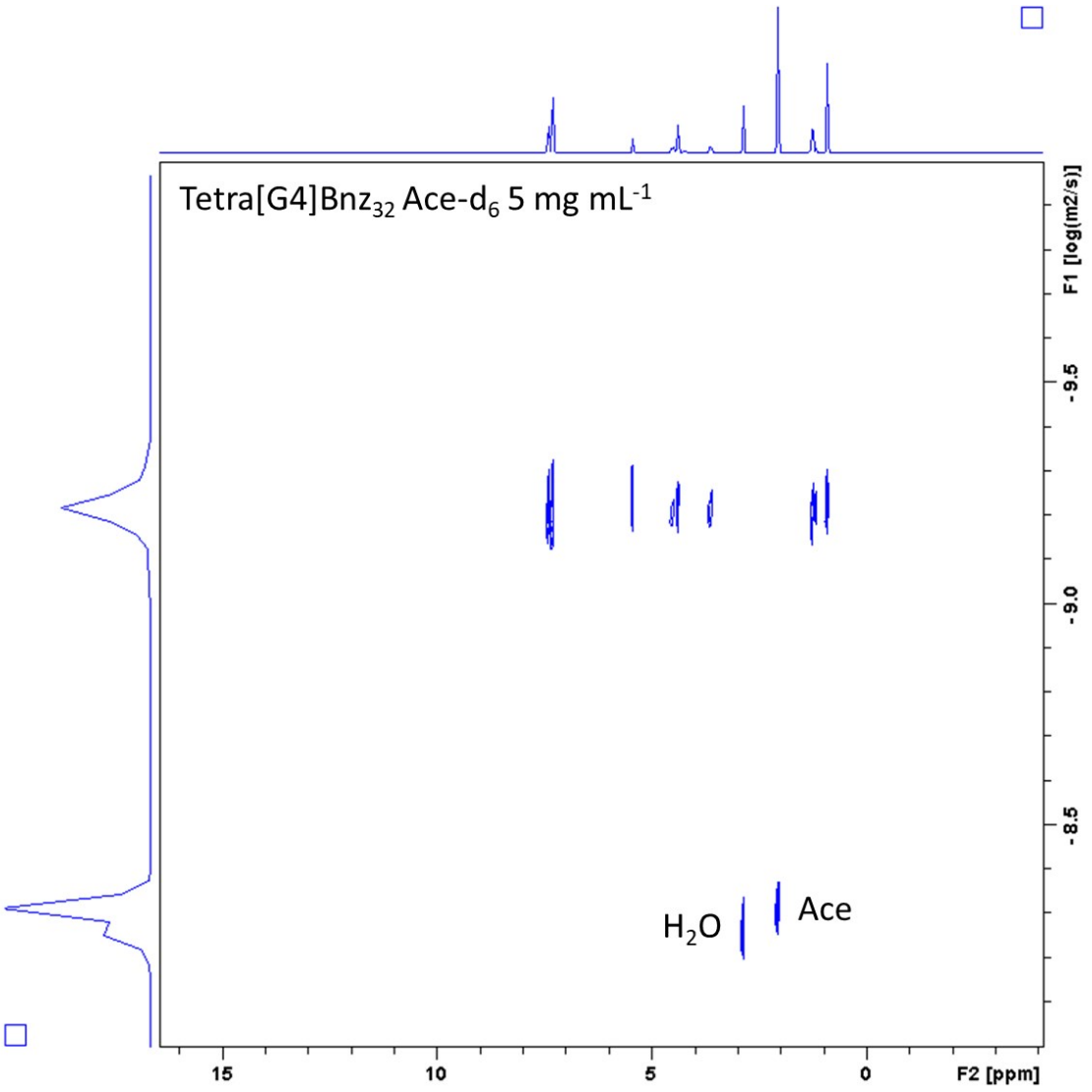

Fig. S44 DOSY-^{1}H NMR spectrum of Tetra[G4]Bnz$_{32}$ in Ace-d$_6$.

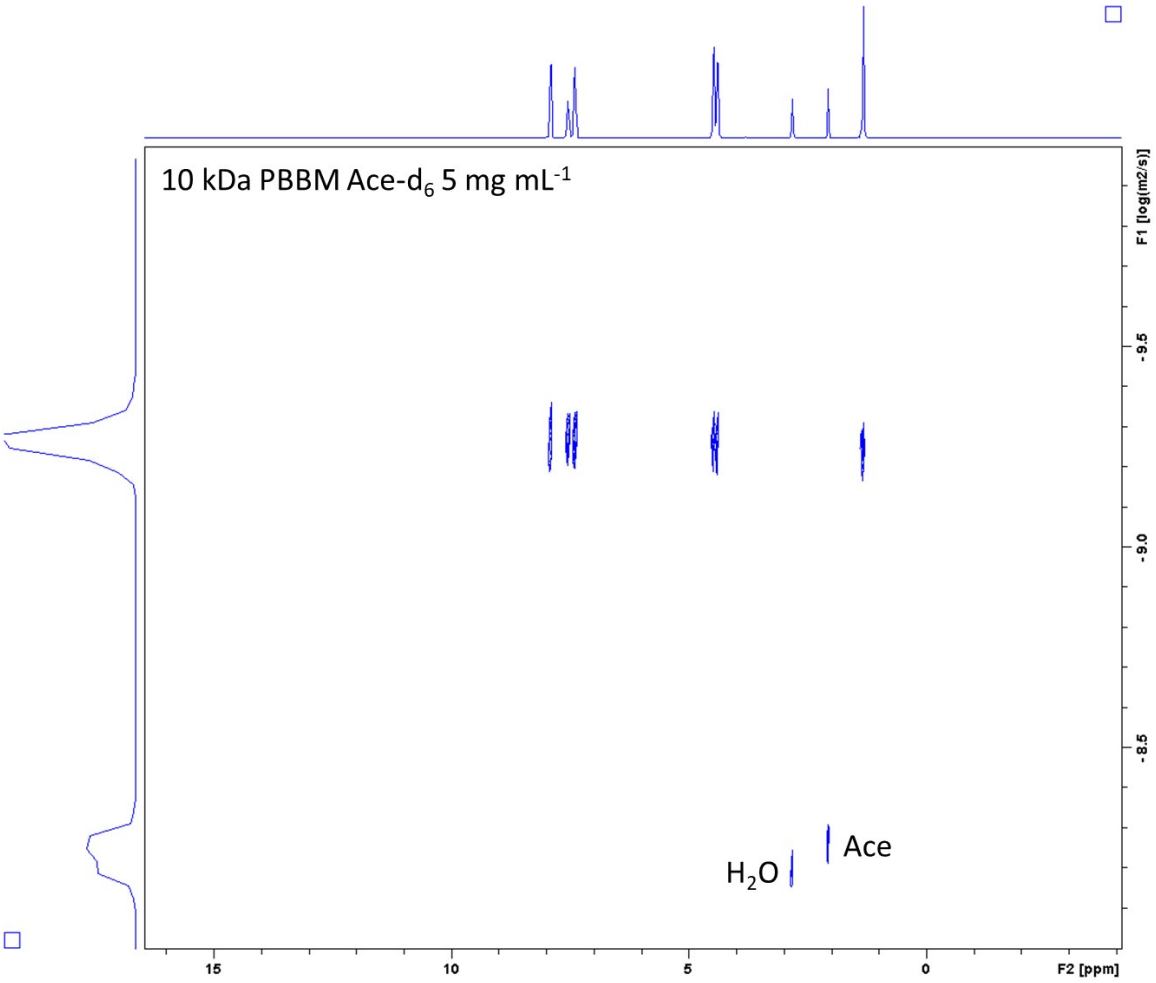

Fig. S45 DOSY-^{1}H NMR spectrum of 10 kDa PBBM in Ace-d_6.

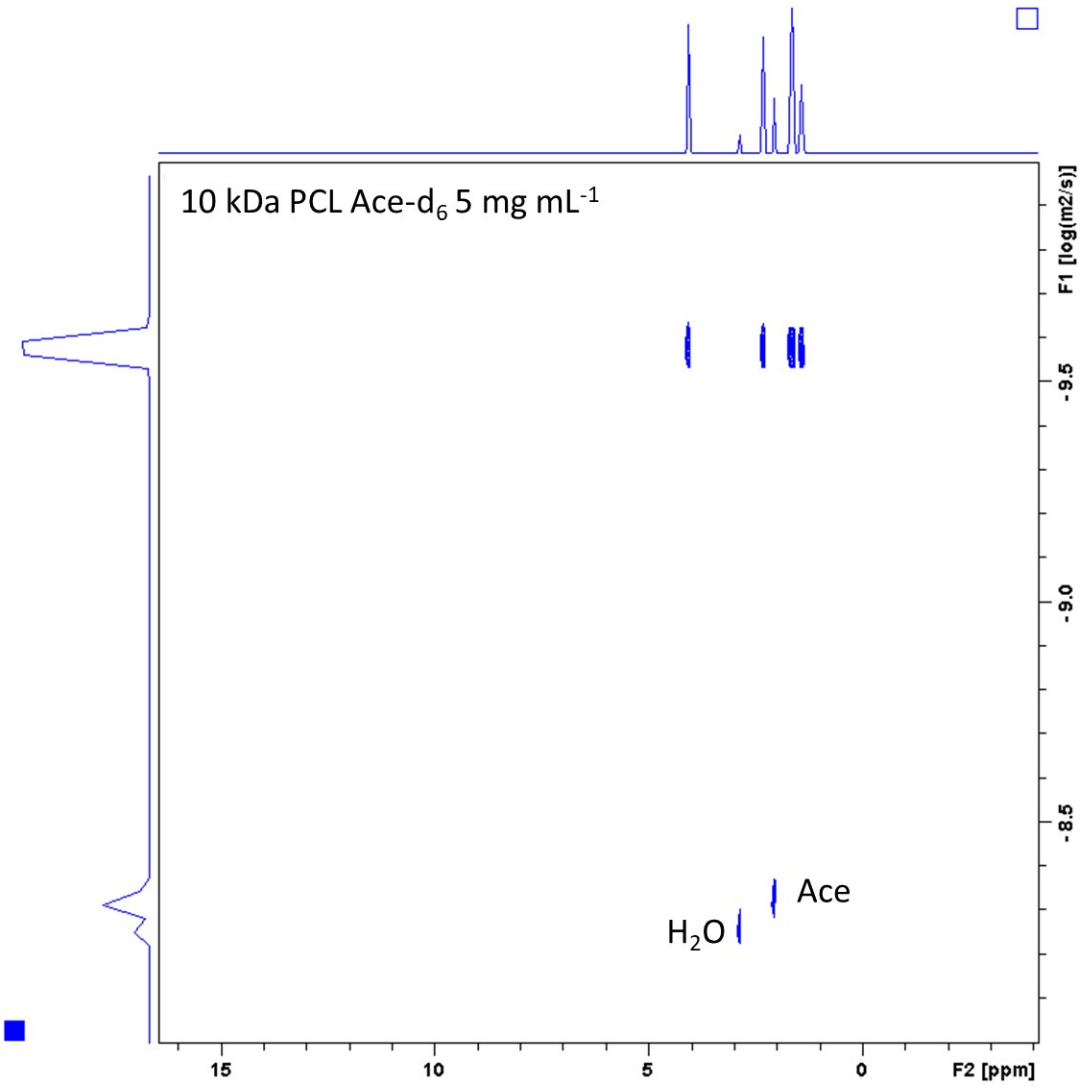

Fig. S46 DOSY-^{1}H NMR spectrum of 10 kDa PCL in Ace-d_6.

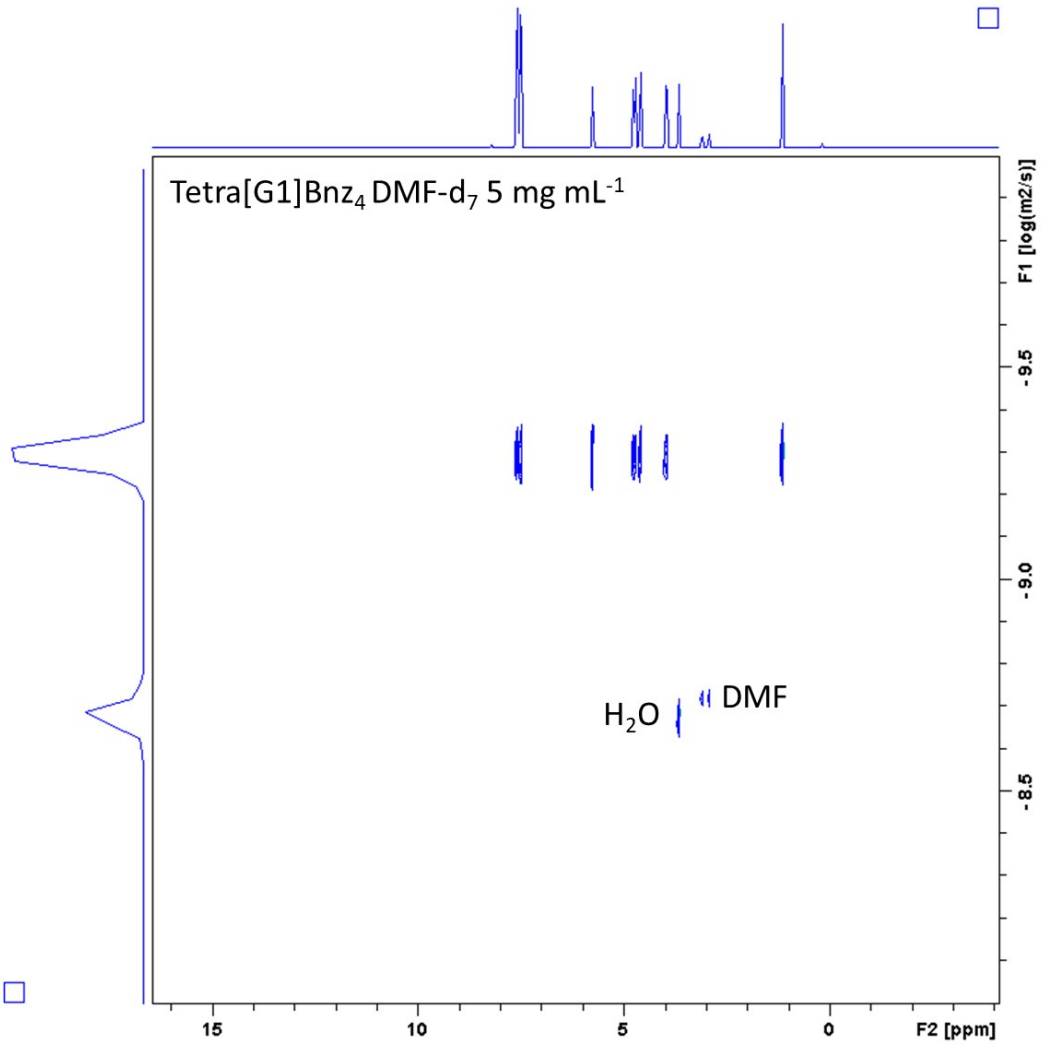

Fig. S47 DOSY-^{1}H NMR spectrum of Tetra[G1]Bnz$_4$ in DMF-d$_7$.

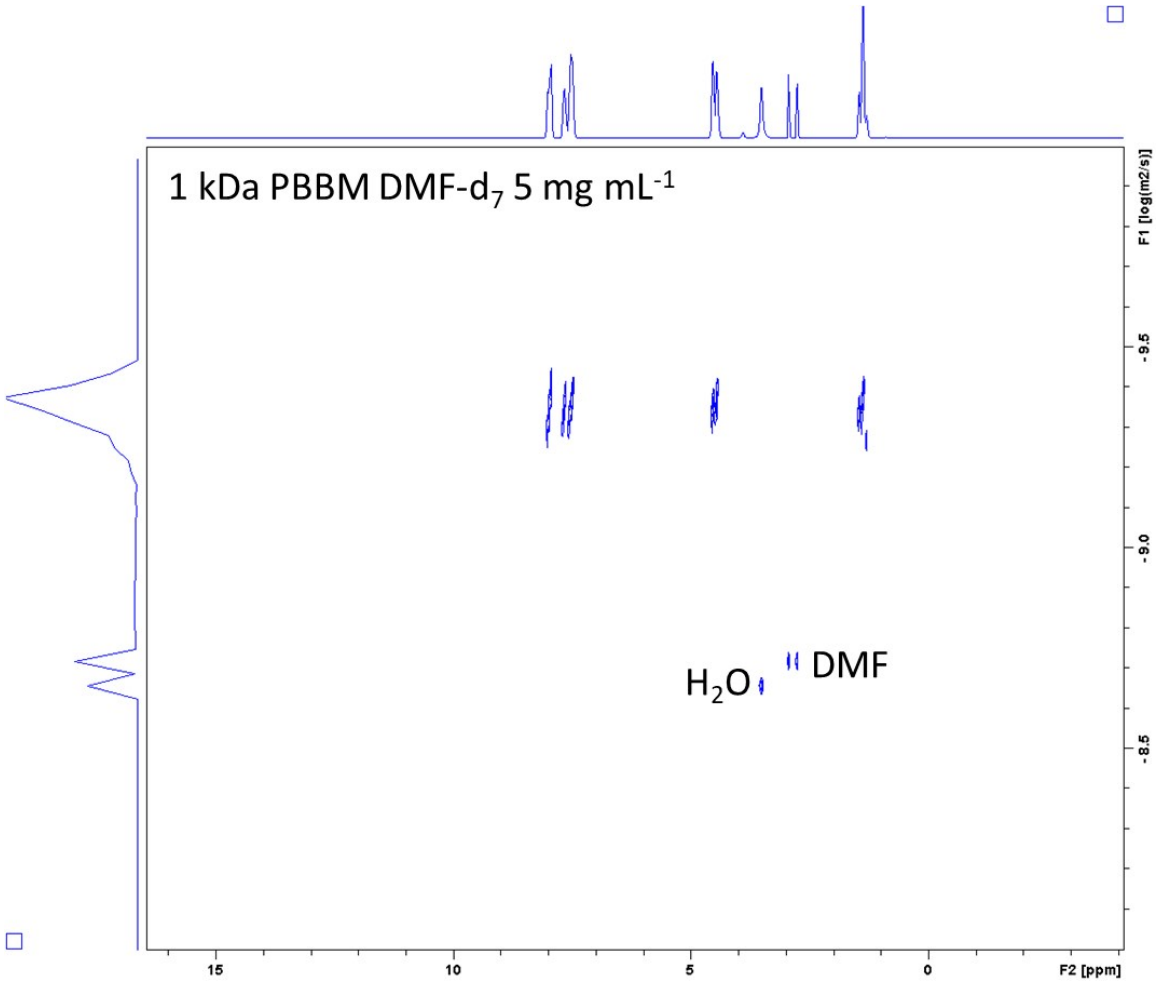

Fig. S48 DOSY-^{1}H NMR spectrum of 1 kDa PBBM in DMF-d_7.

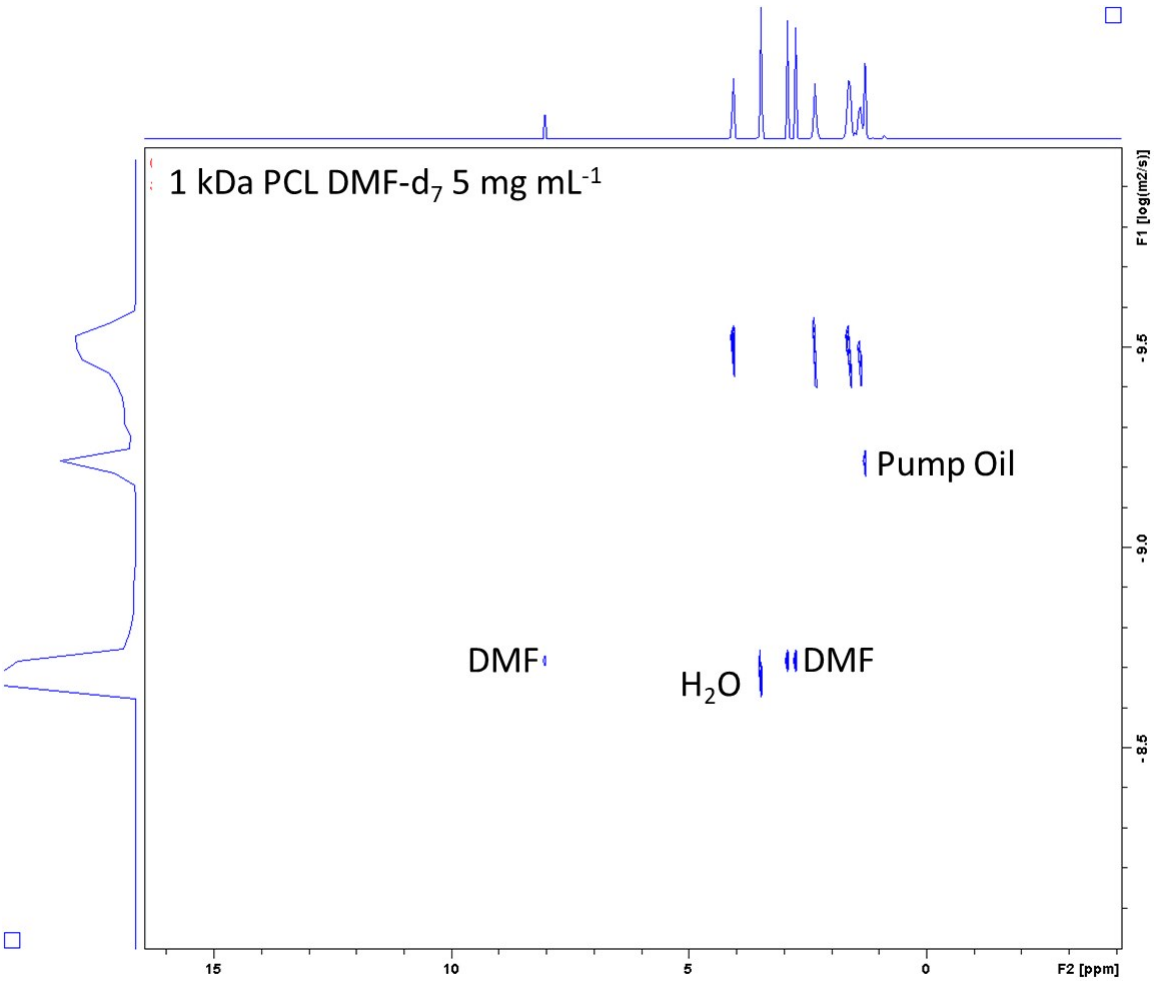

Fig. S49 DOSY-^{1}H NMR spectrum of 1 kDa PCL in DMF-d_7.

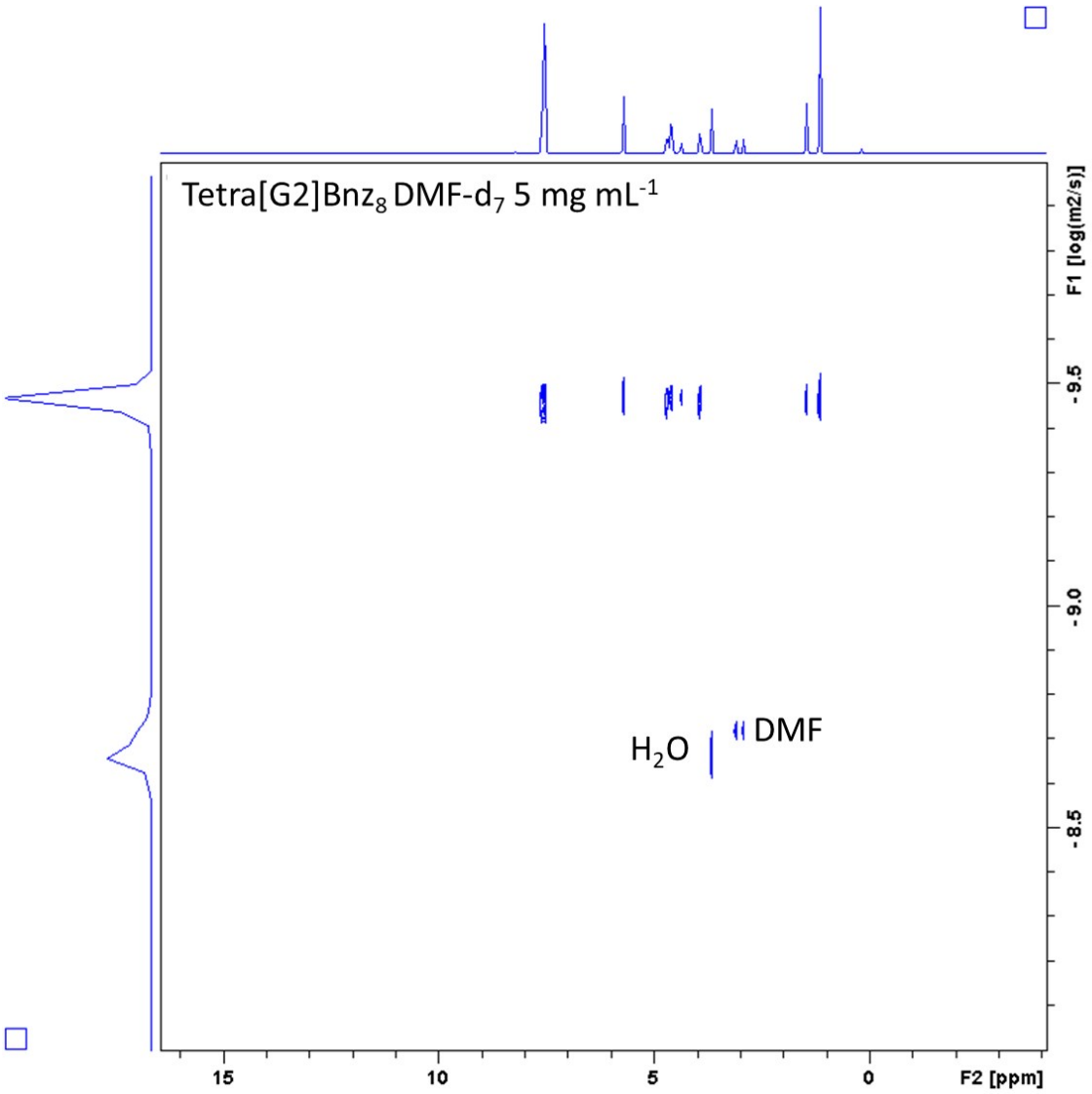

Fig. S50 DOSY-^{1}H NMR spectrum of Tetra[G2]Bnz$_8$ in DMF-d$_7$.

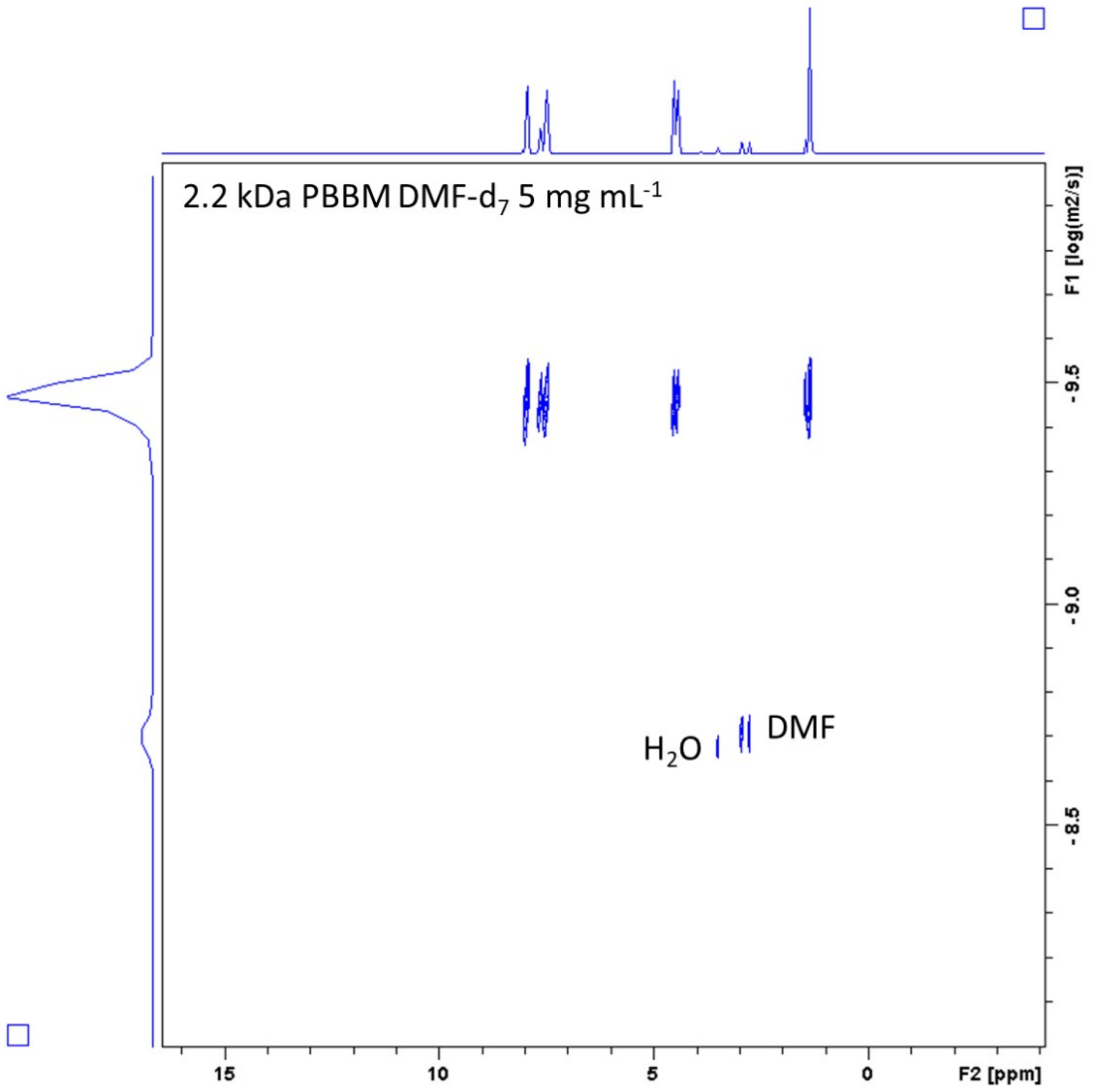

Fig. S51 DOSY-^{1}H NMR spectrum of 2.2 kDa PBBM in DMF-d_7.

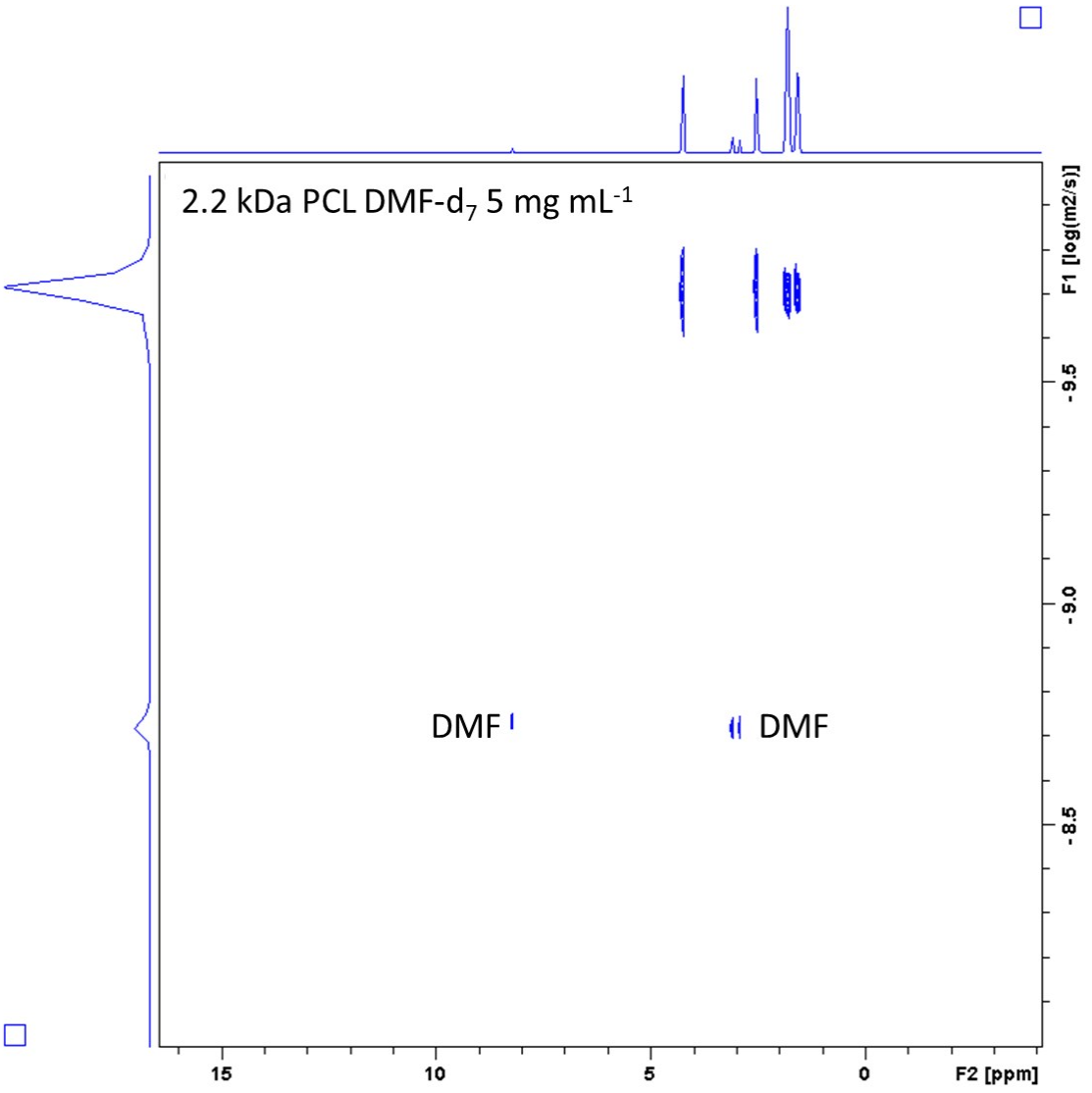

Fig. S52 DOSY-^{1}H NMR spectrum of 2.2 kDa PCL in DMF-d_7.

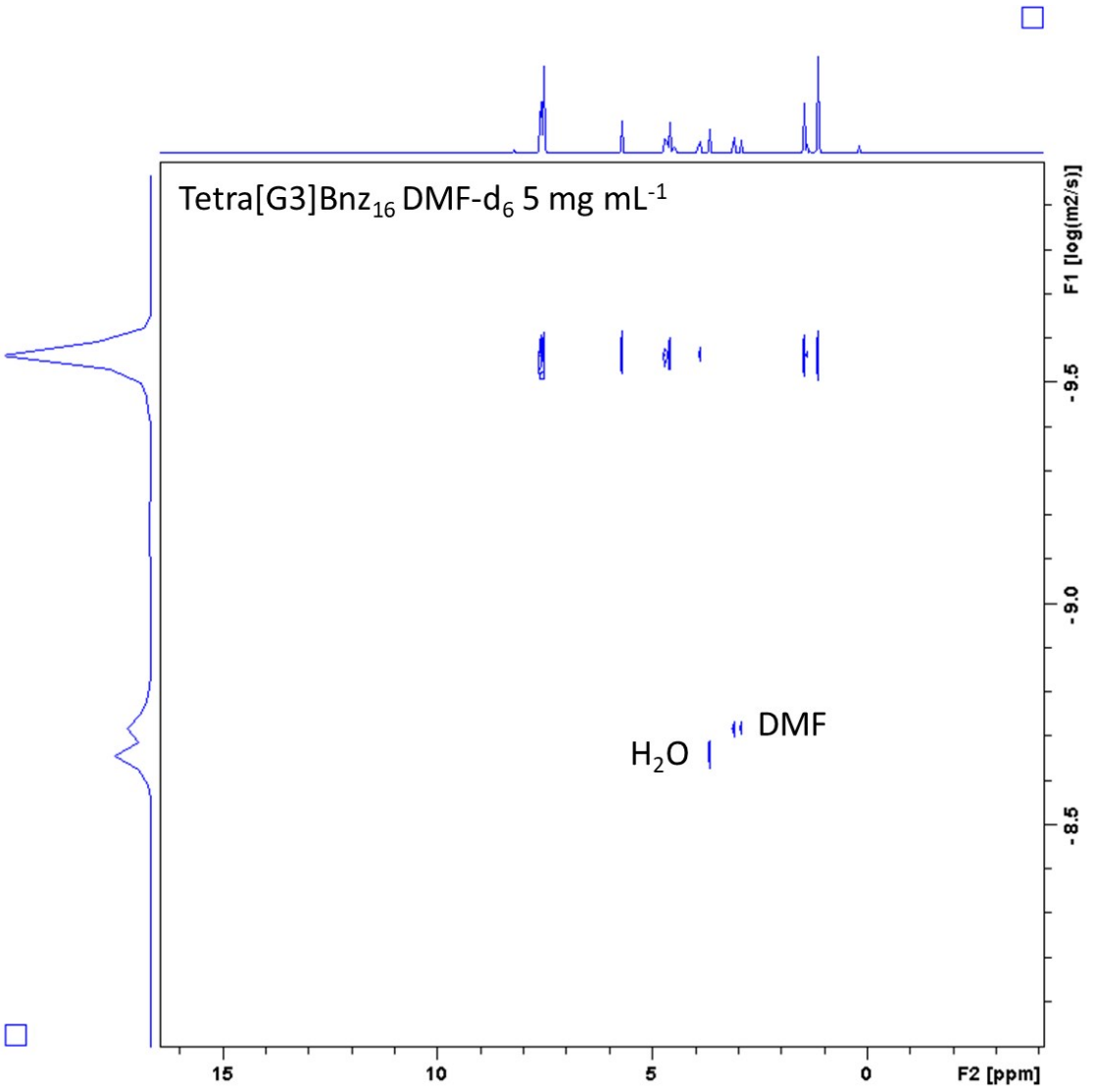

Fig. S53 DOSY-^{1}H NMR spectrum of Tetra[G3]Bnz$_{16}$ in DMF-d$_{7}$.

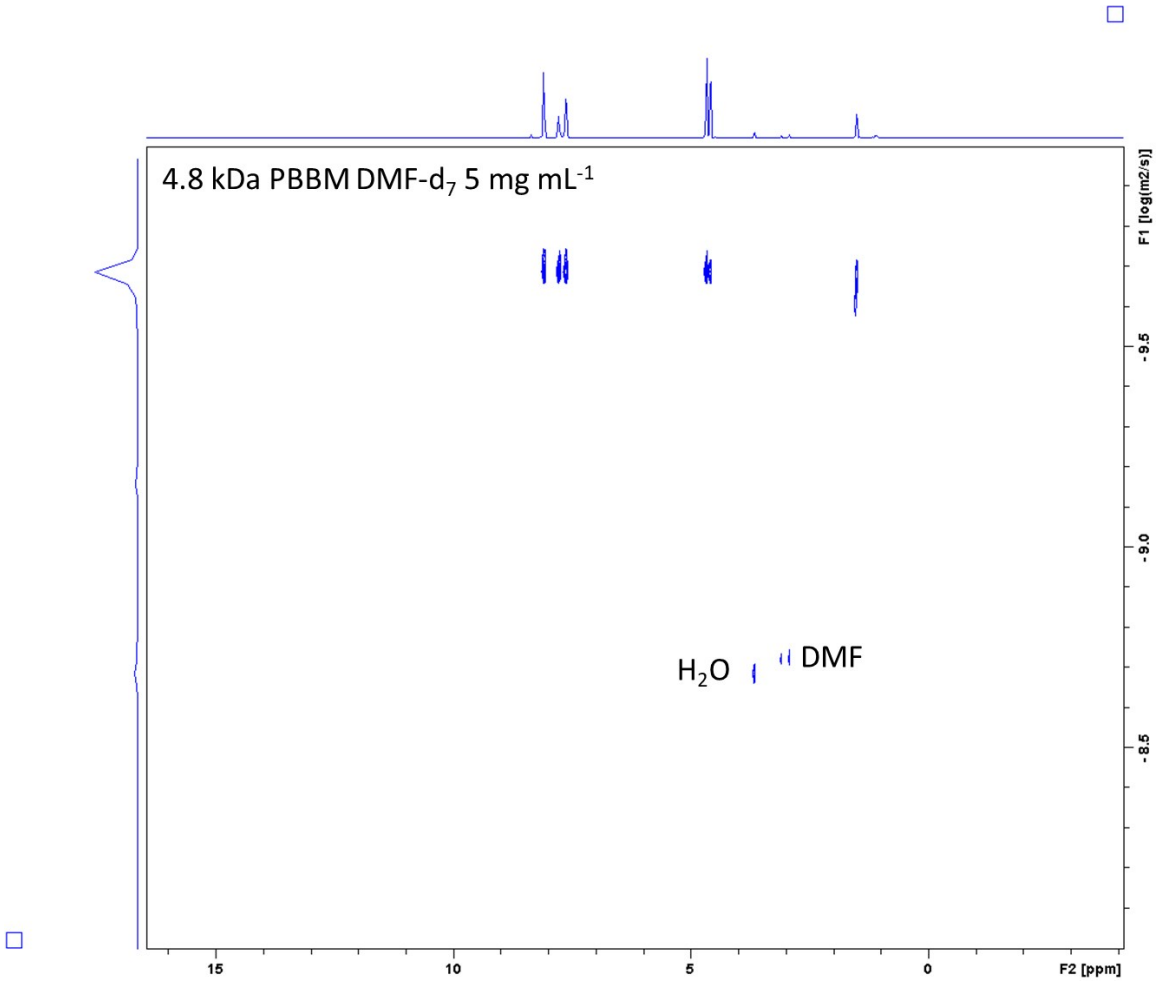

Fig. S54 DOSY-^{1}H NMR spectrum of 4.8 kDa PBBM in DMF-d_7.

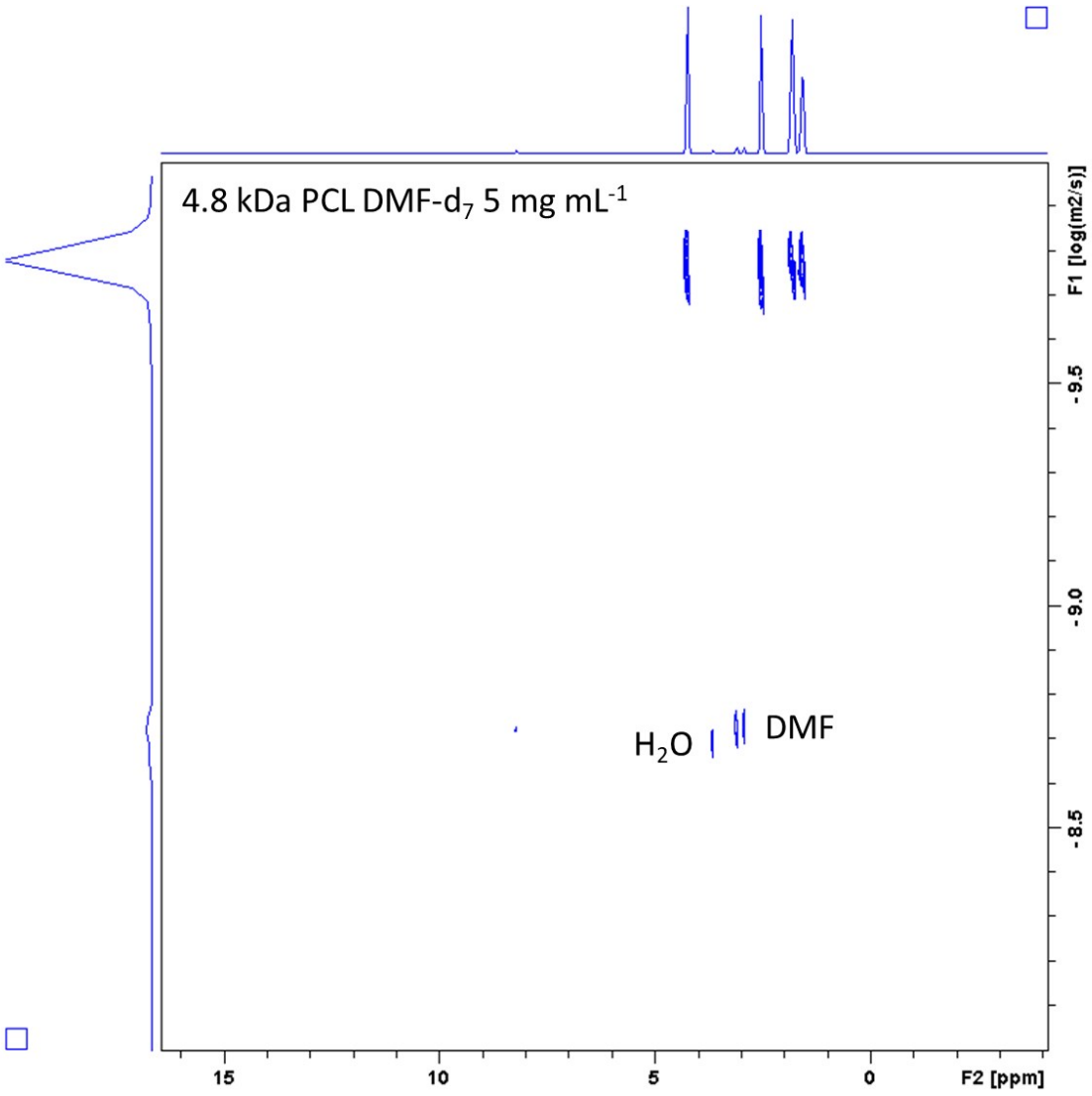

Fig. S55 DOSY-^{1}H NMR spectrum of 4.8 kDa PCL in DMF-d_7.

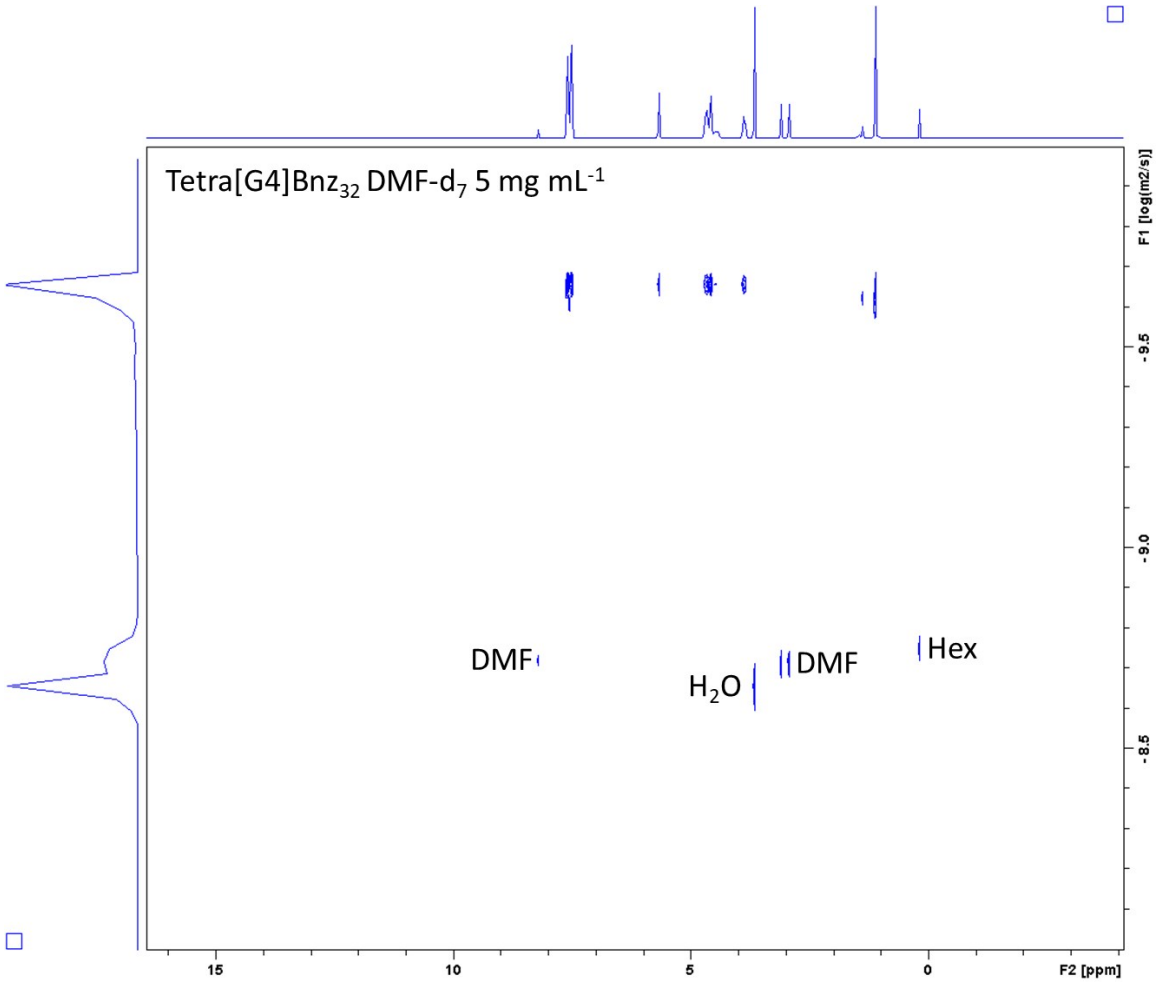

Fig. S56 DOSY-^{1}H NMR spectrum of Tetra[G4]Bnz_{32} in DMF-d_7.

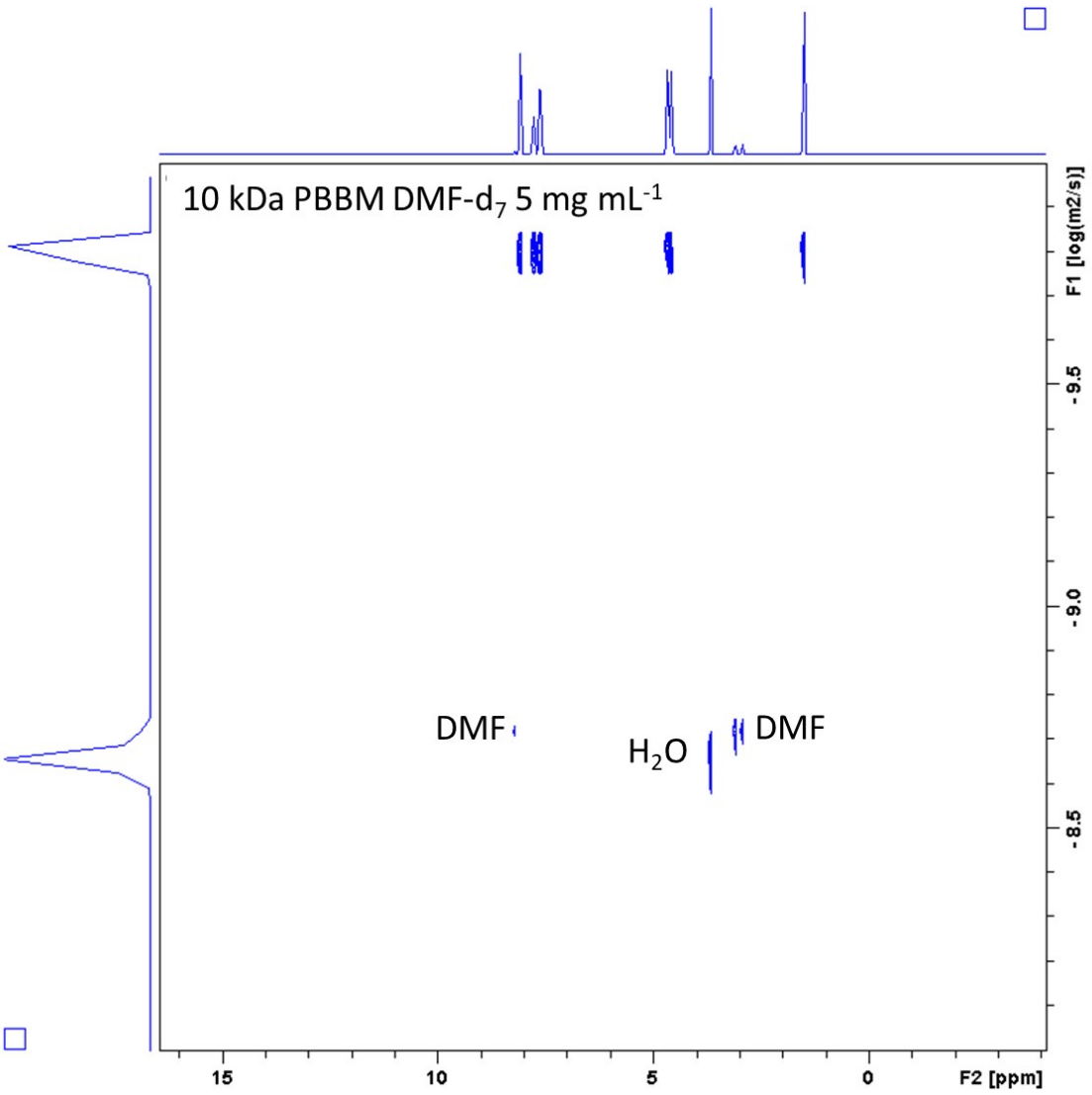

Fig. S57 DOSY-^{1}H NMR spectrum of 10 kDa PBBM in DMF-d_7.

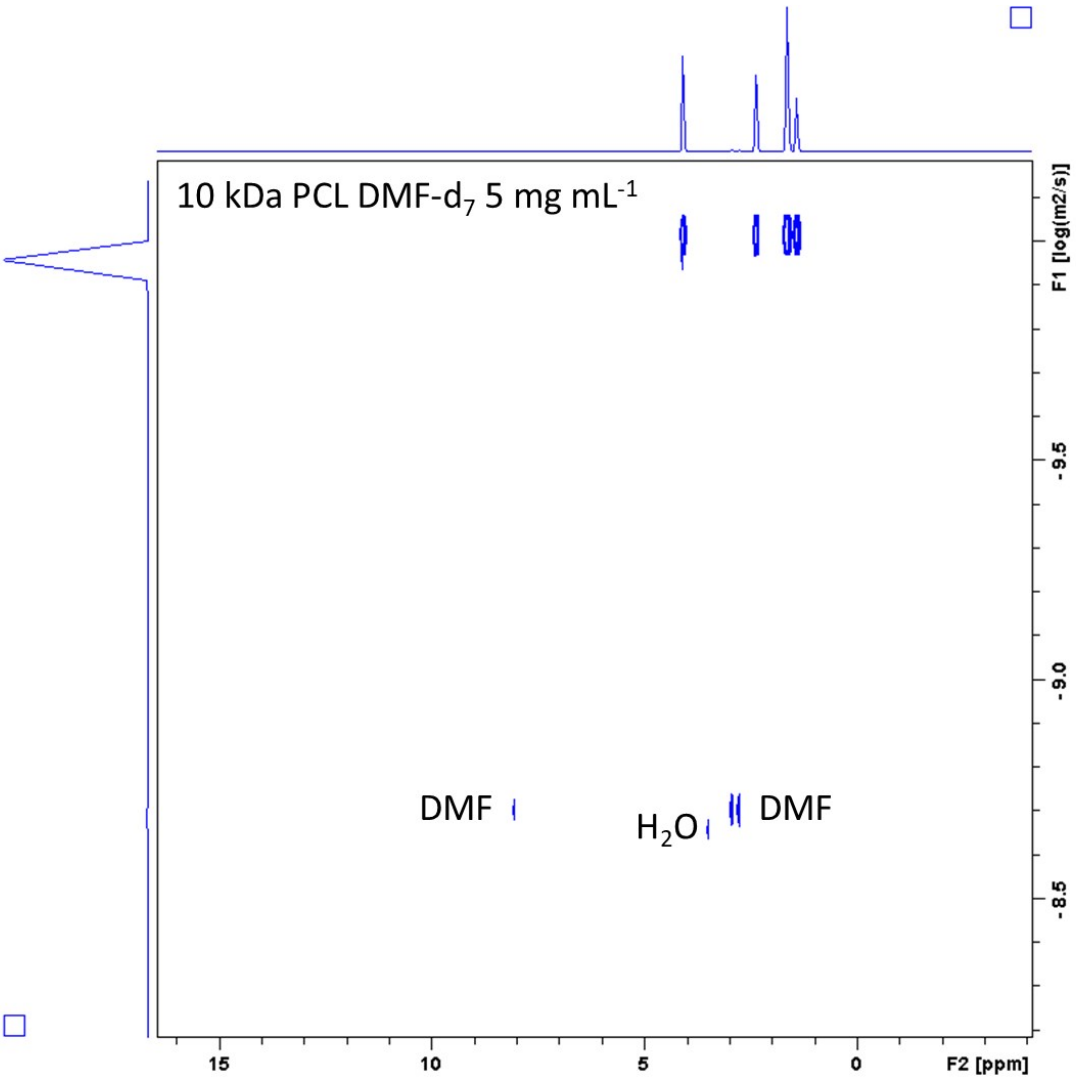

Fig. S58 DOSY-^{1}H NMR spectrum of 10 kDa PCL in DMF-d_7.

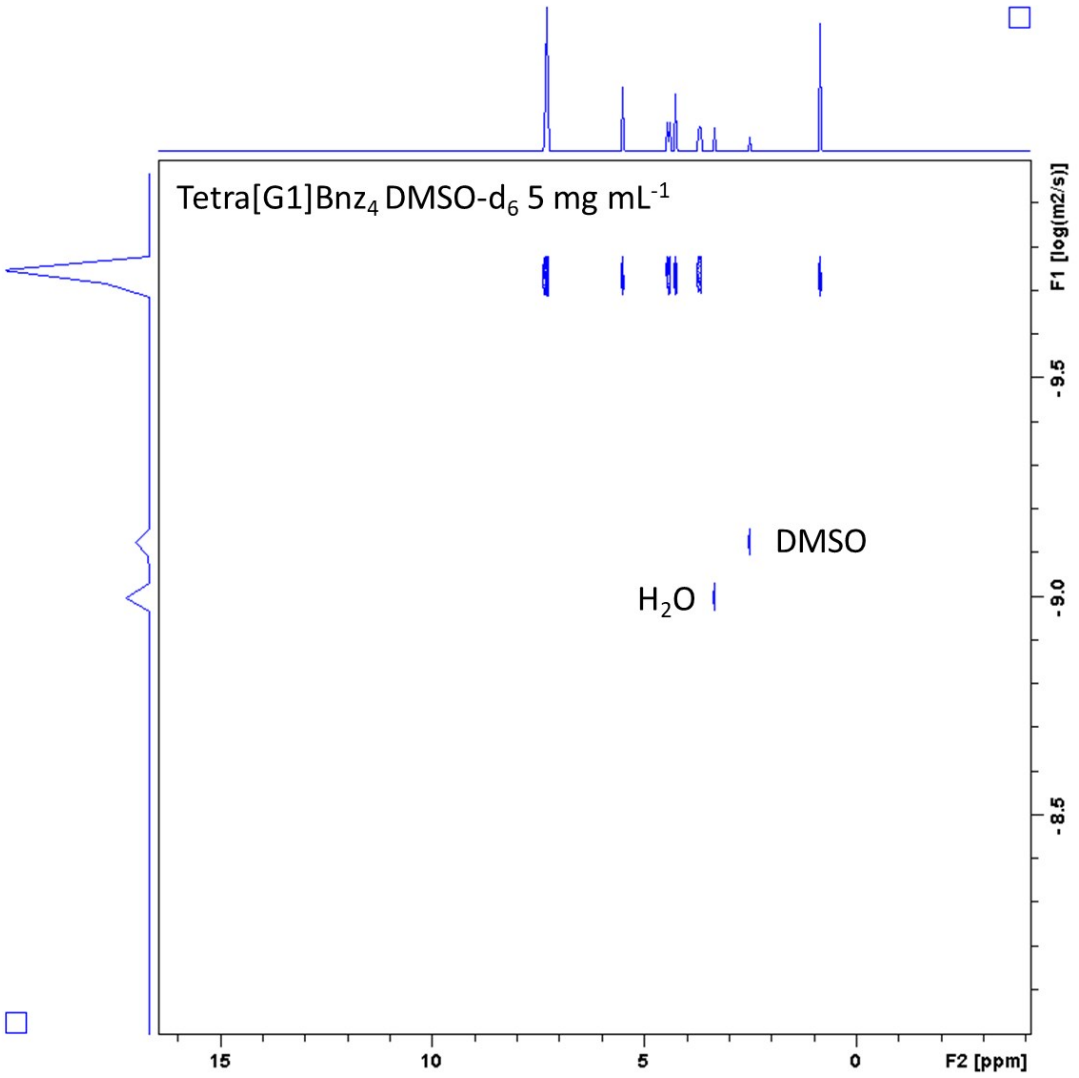

Fig. S59 DOSY-^{1}H NMR spectrum of Tetra[G1]Bnz$_4$ in DMSO-d$_6$.

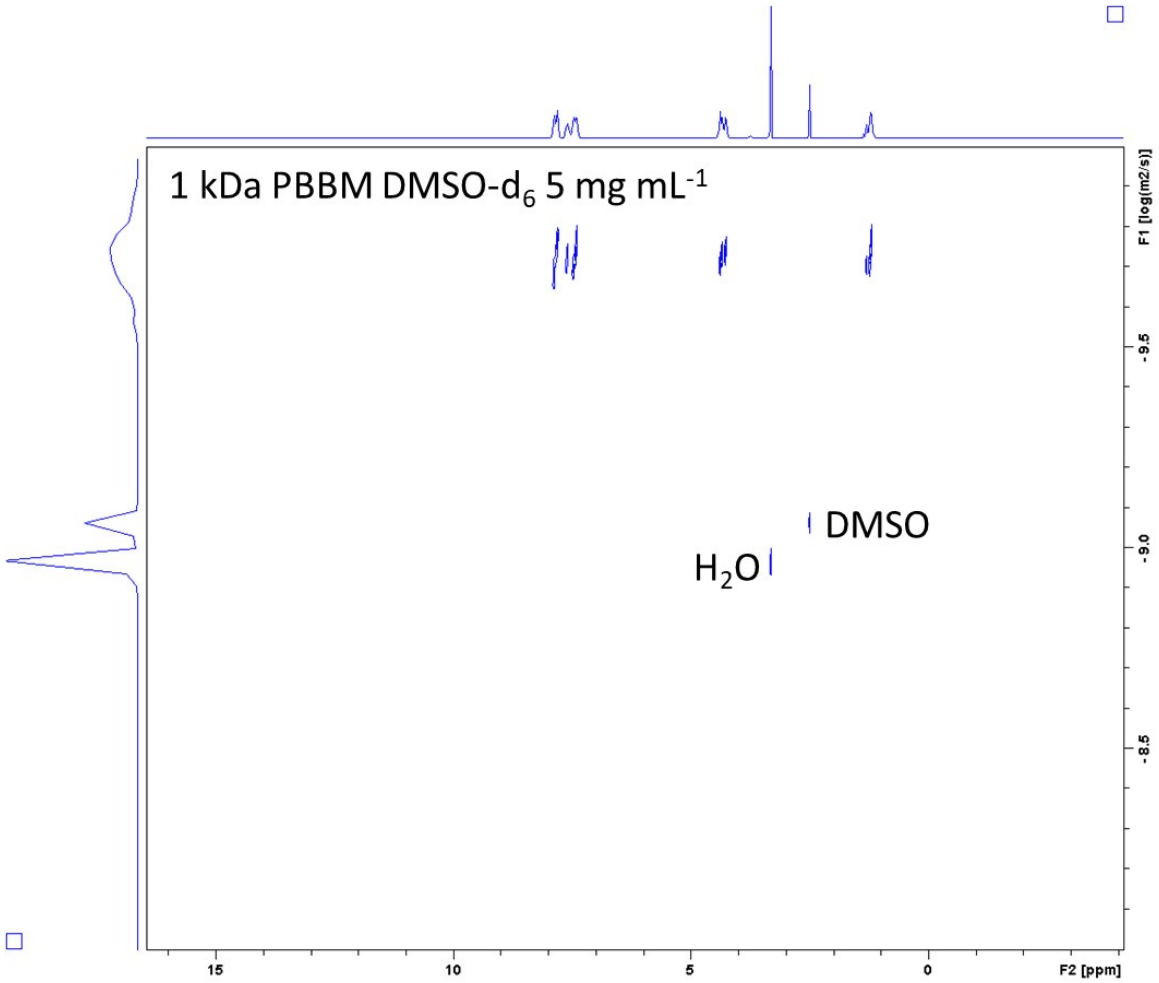

Fig. S60 DOSY-^{1}H NMR spectrum of 1 kDa PBBM in DMSO-d_6.

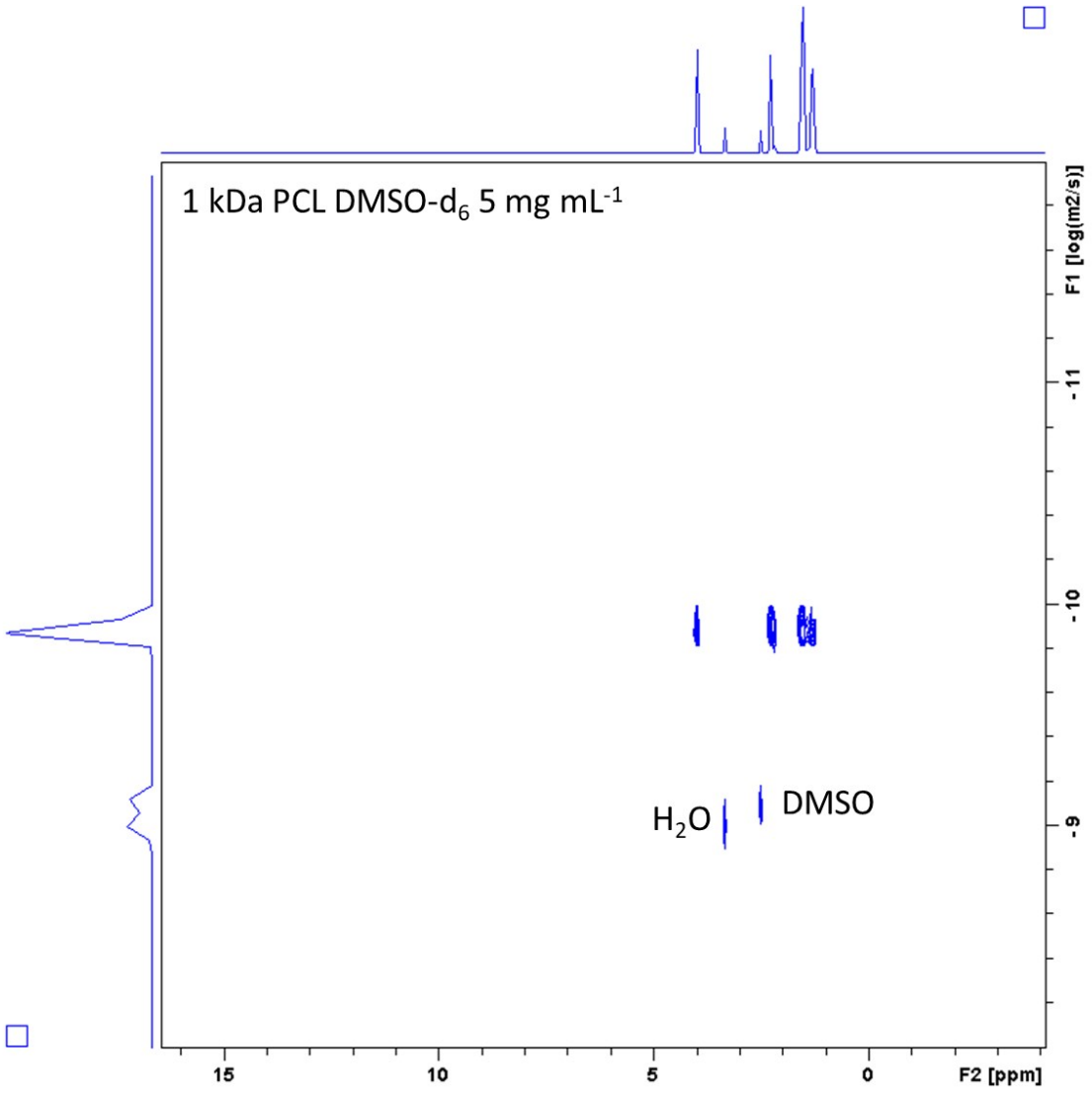

Fig. S61 DOSY-^{1}H NMR spectrum of 1 kDa PCL in DMSO-d_6.

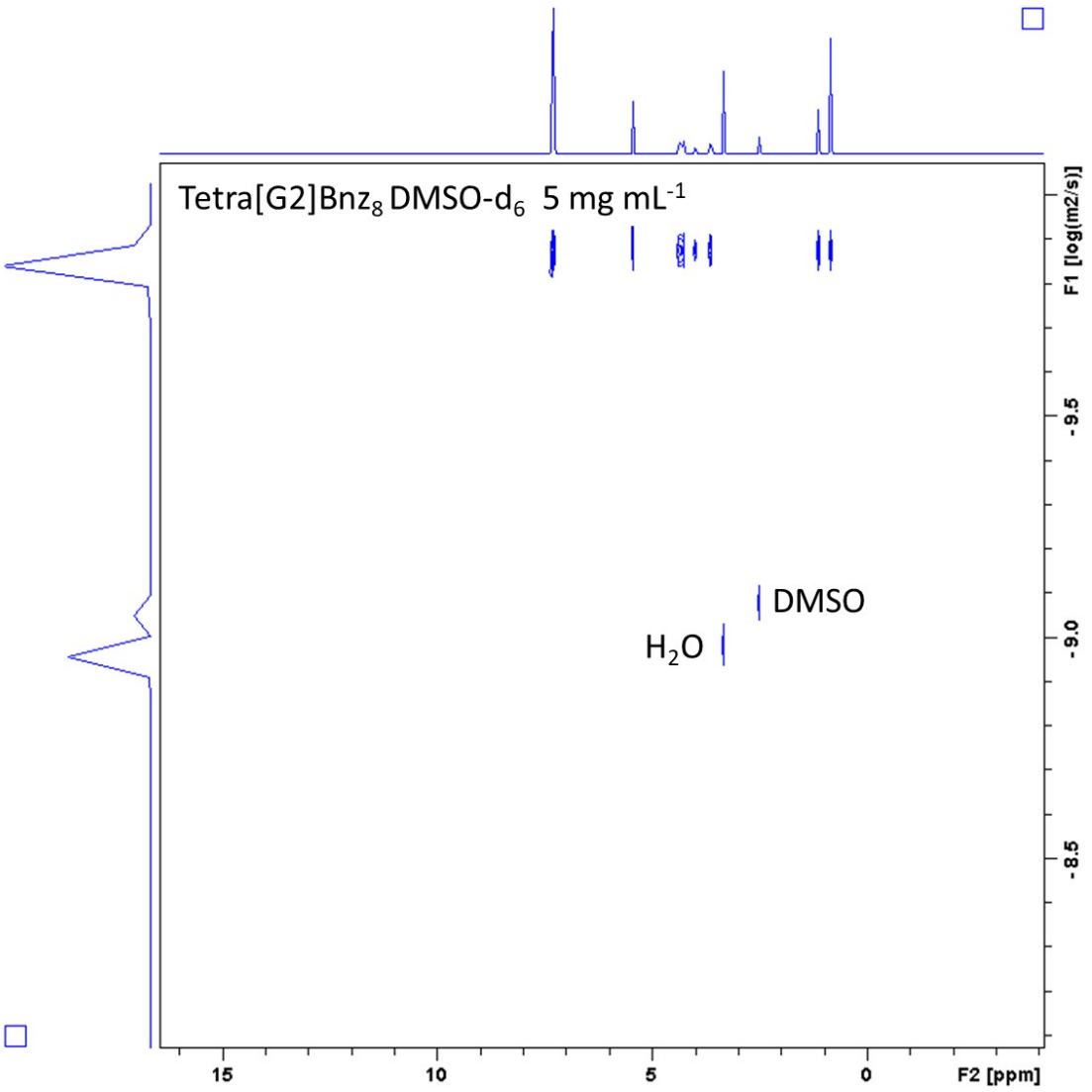

Fig. S62 DOSY-^{1}H NMR spectrum of Tetra[G2]Bnz$_8$ in DMSO-d$_6$.

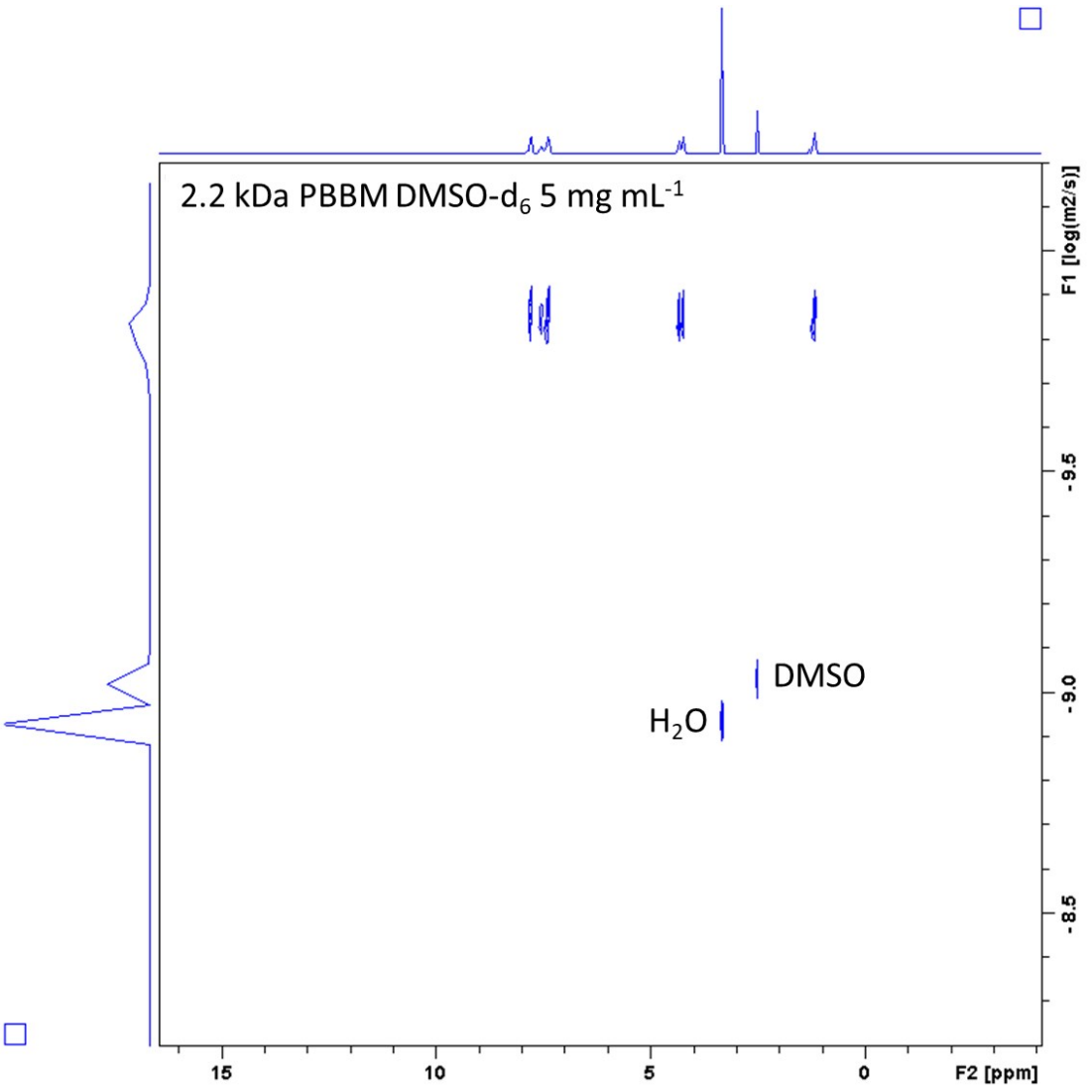

Fig. S63 DOSY-^{1}H NMR spectrum of 2.2 kDa PBBM in DMSO-d_6.

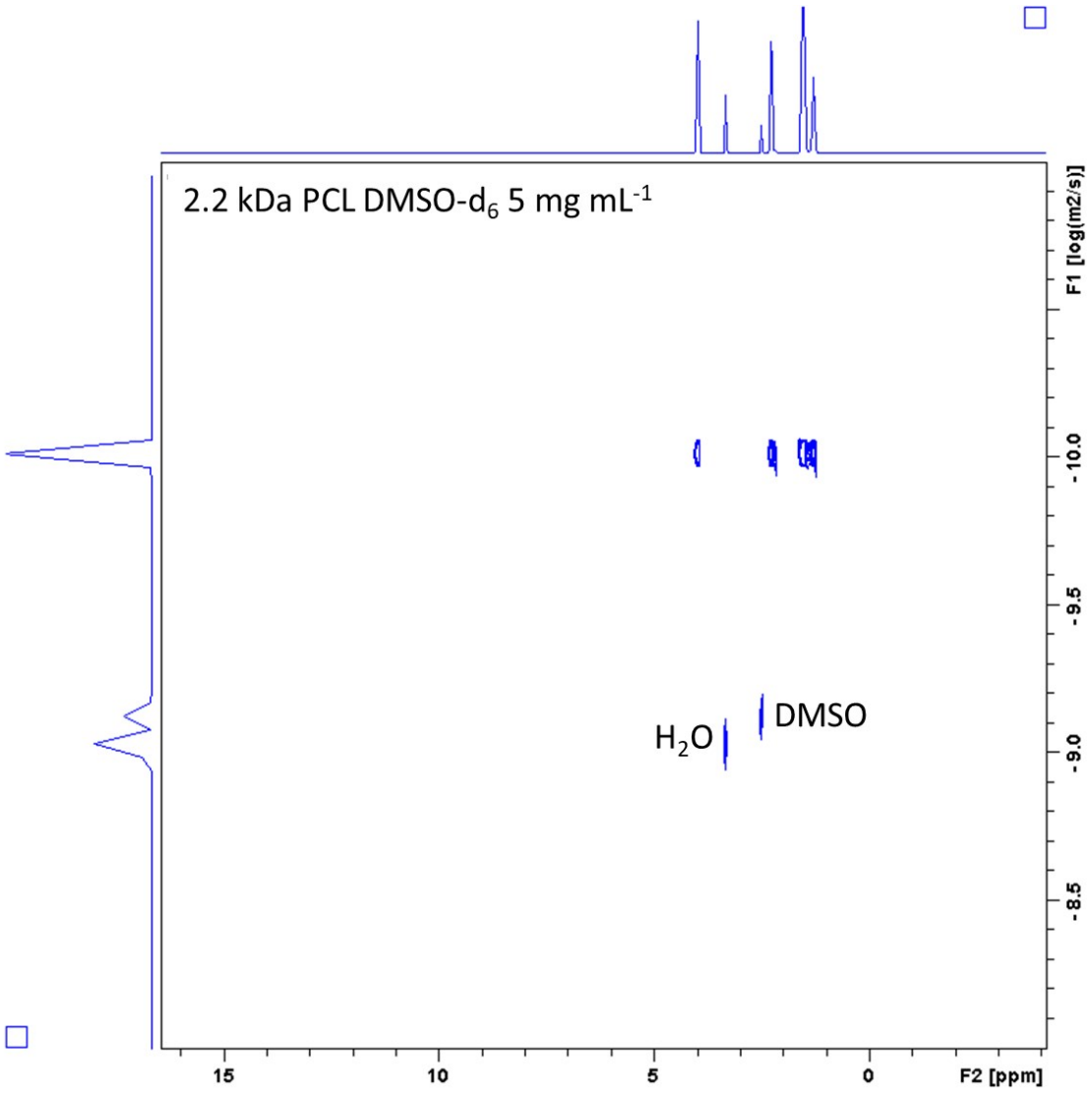

Fig. S64 DOSY-^{1}H NMR spectrum of 2.2 kDa PCL in DMSO-d_6.

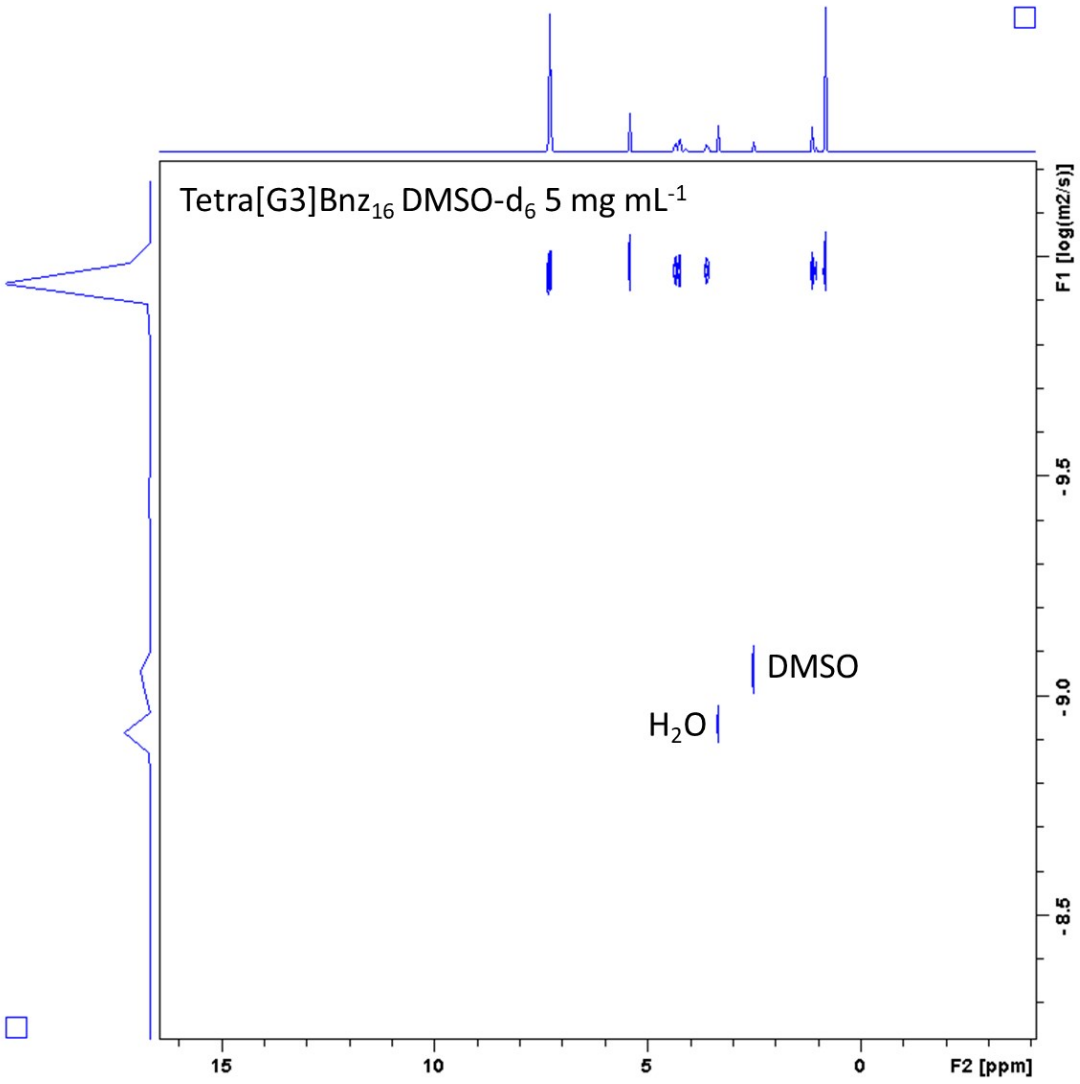

Fig. S65 DOSY-^{1}H NMR spectrum of Tetra[G3]Bnz$_{16}$ in DMSO-d$_6$.

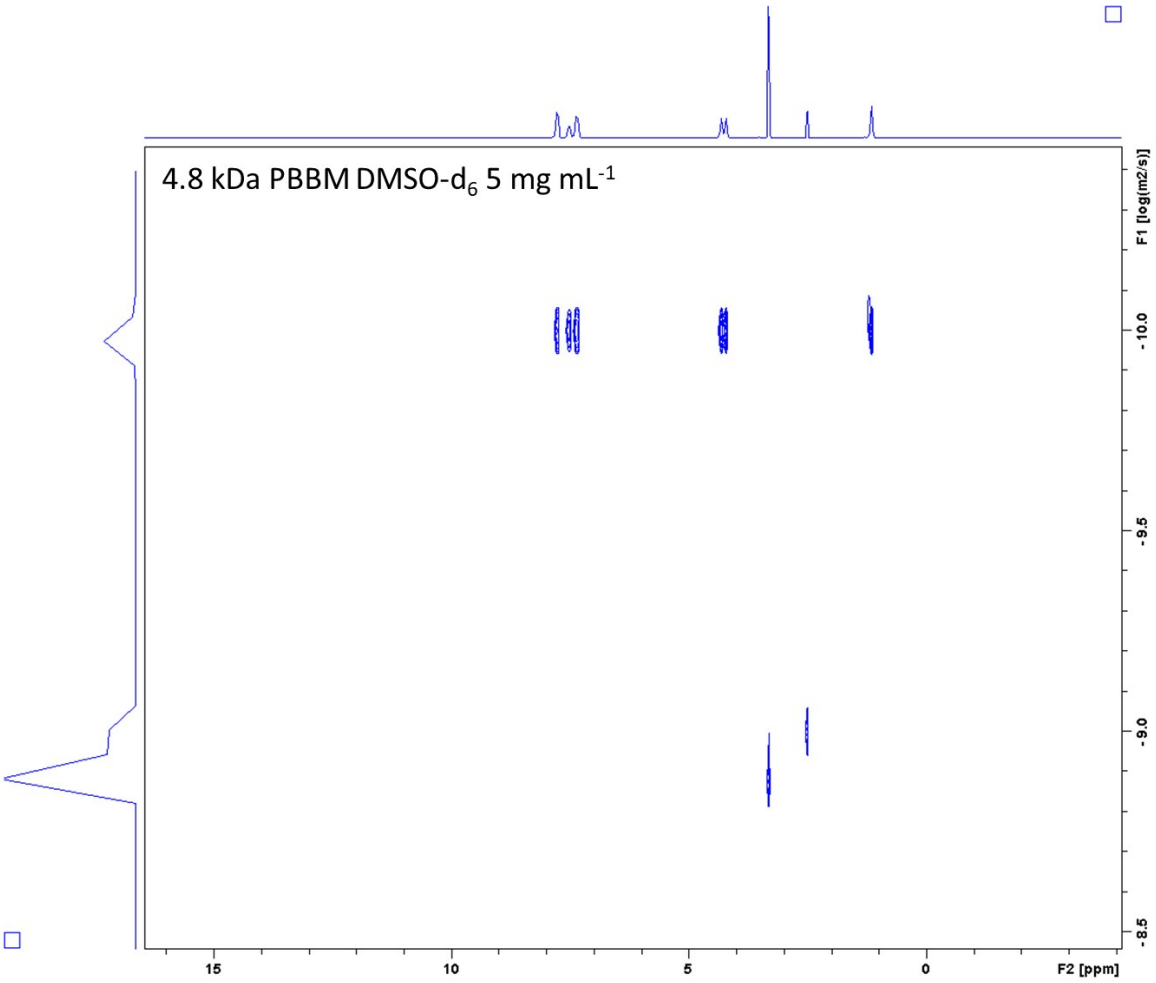

Fig. S66 DOSY-^{1}H NMR spectrum of 4.8 kDa PBBM in DMSO-d_6.

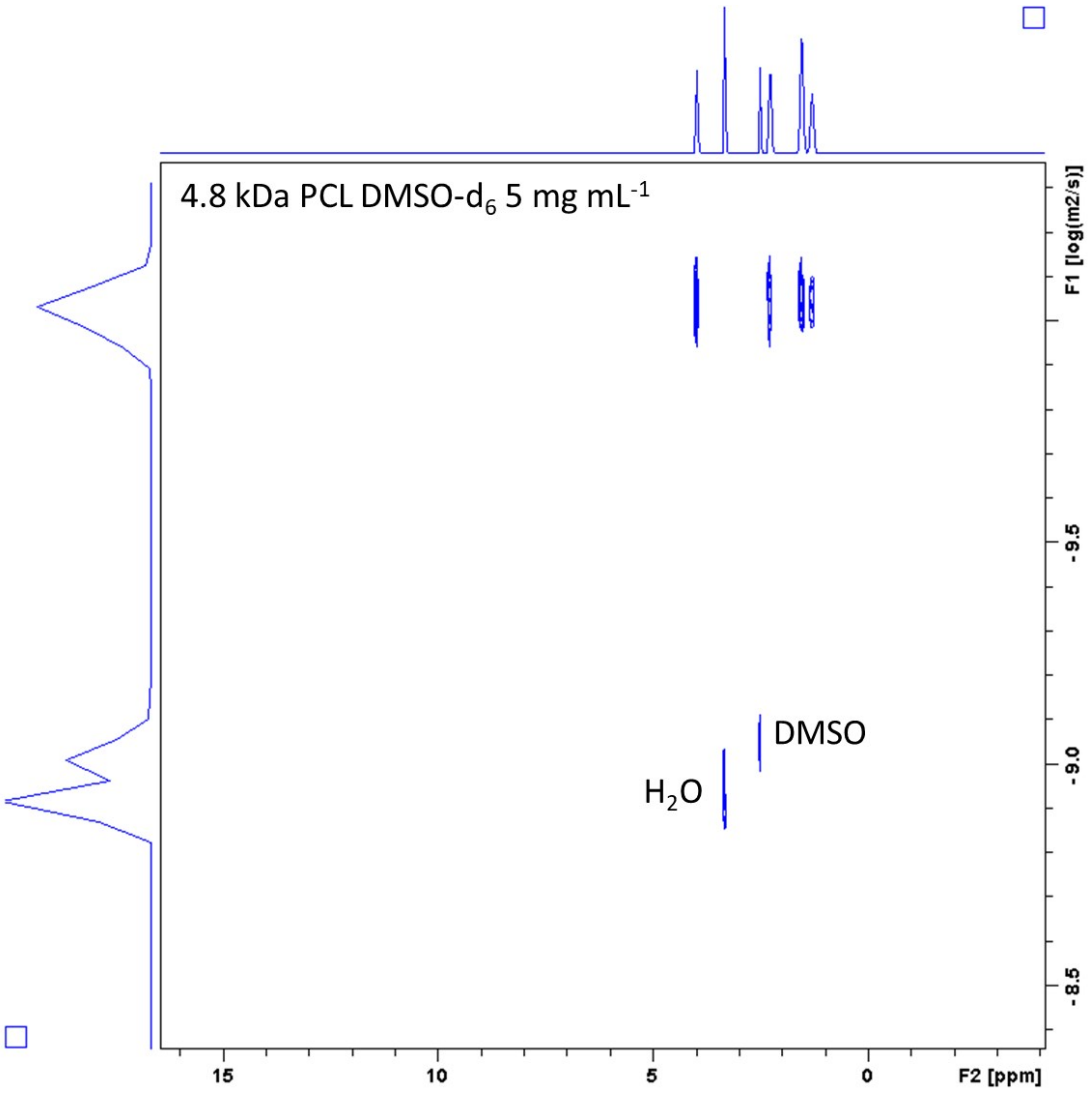

Fig. S67 DOSY-^{1}H NMR spectrum of 4.8 kDa PCL in DMSO-d_6.

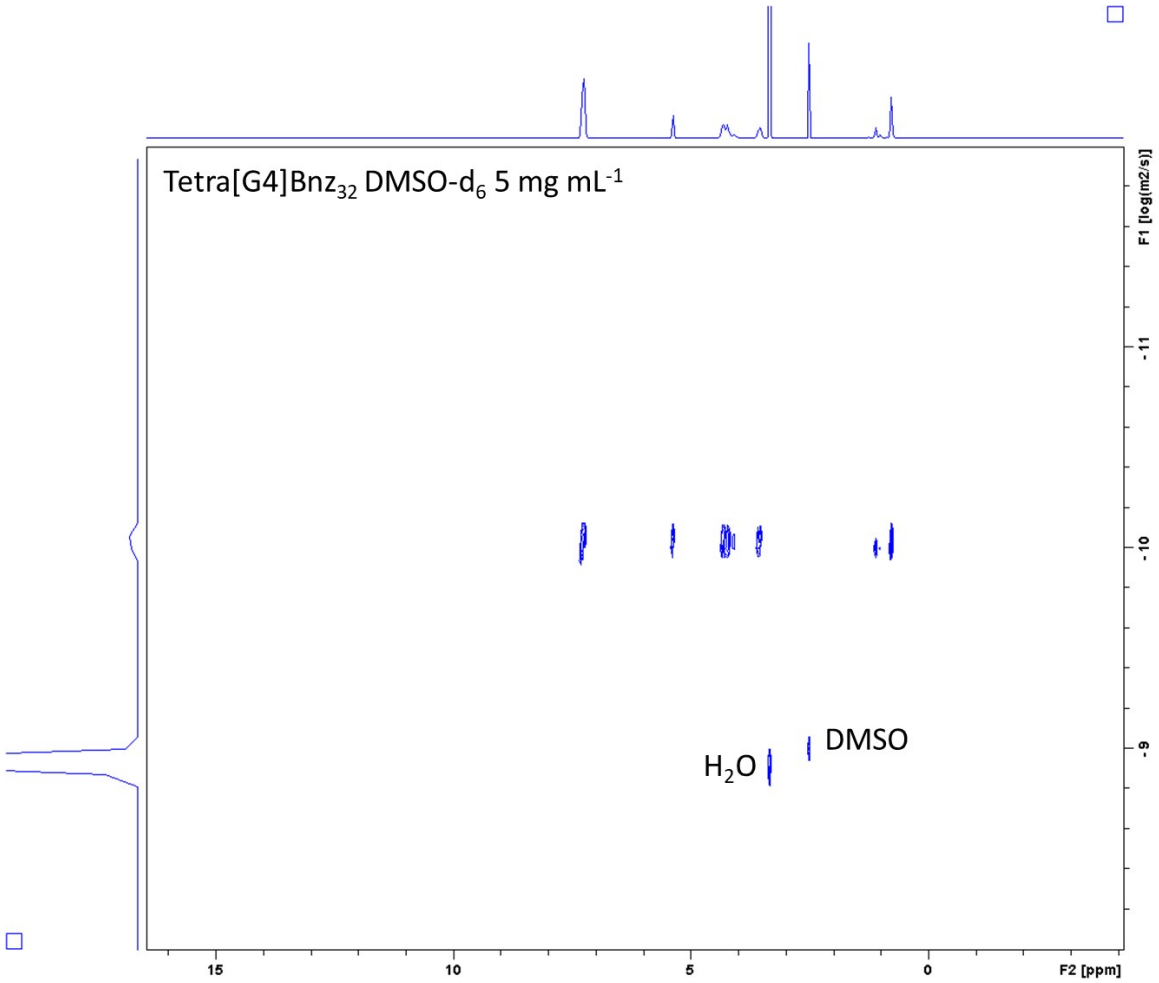

Fig. S68 DOSY-^{1}H NMR spectrum of Tetra[G4]Bnz$_{32}$ in DMSO-d$_6$.

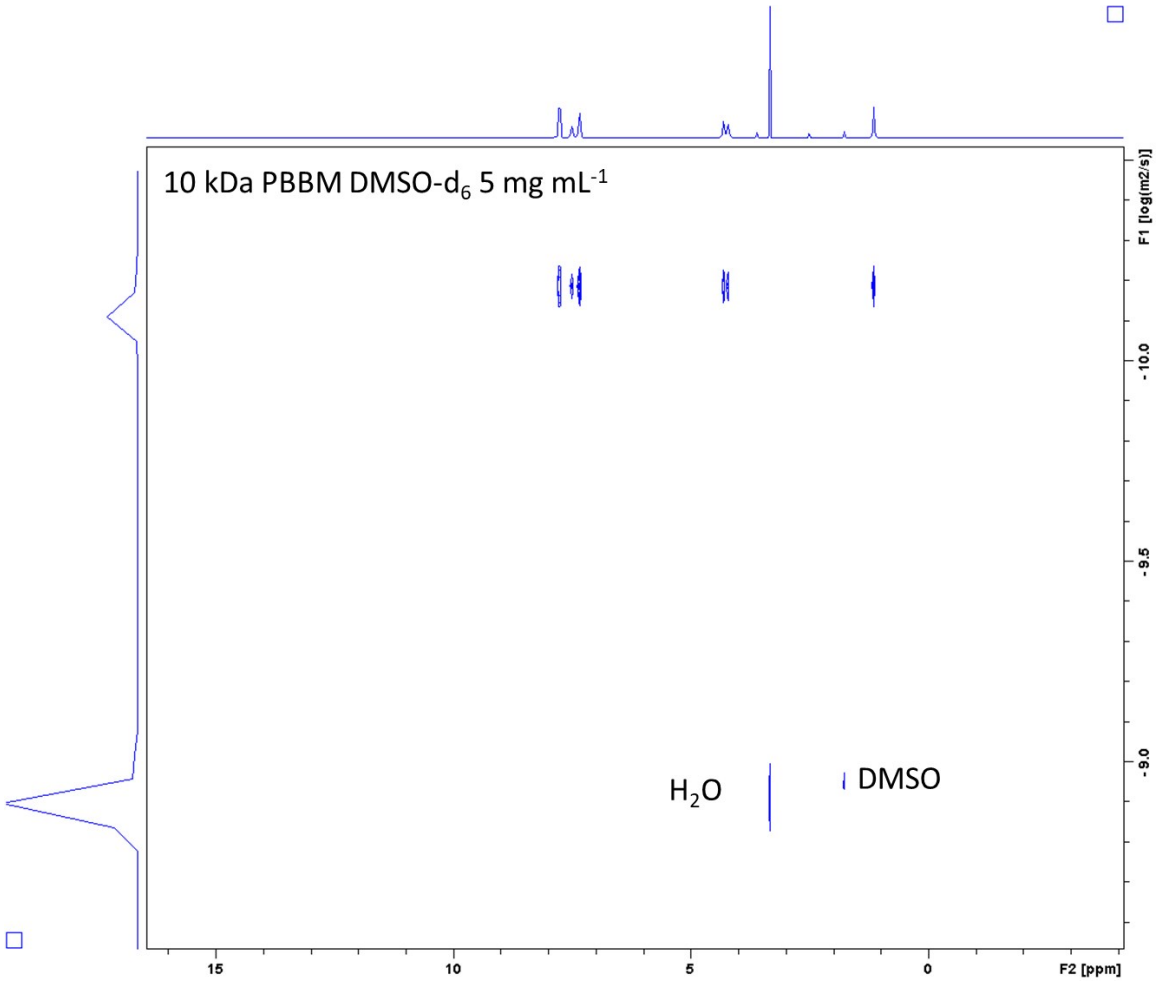

Fig. S69 DOSY-^{1}H NMR spectrum of 10 kDa PBBM in DMSO-d_6.

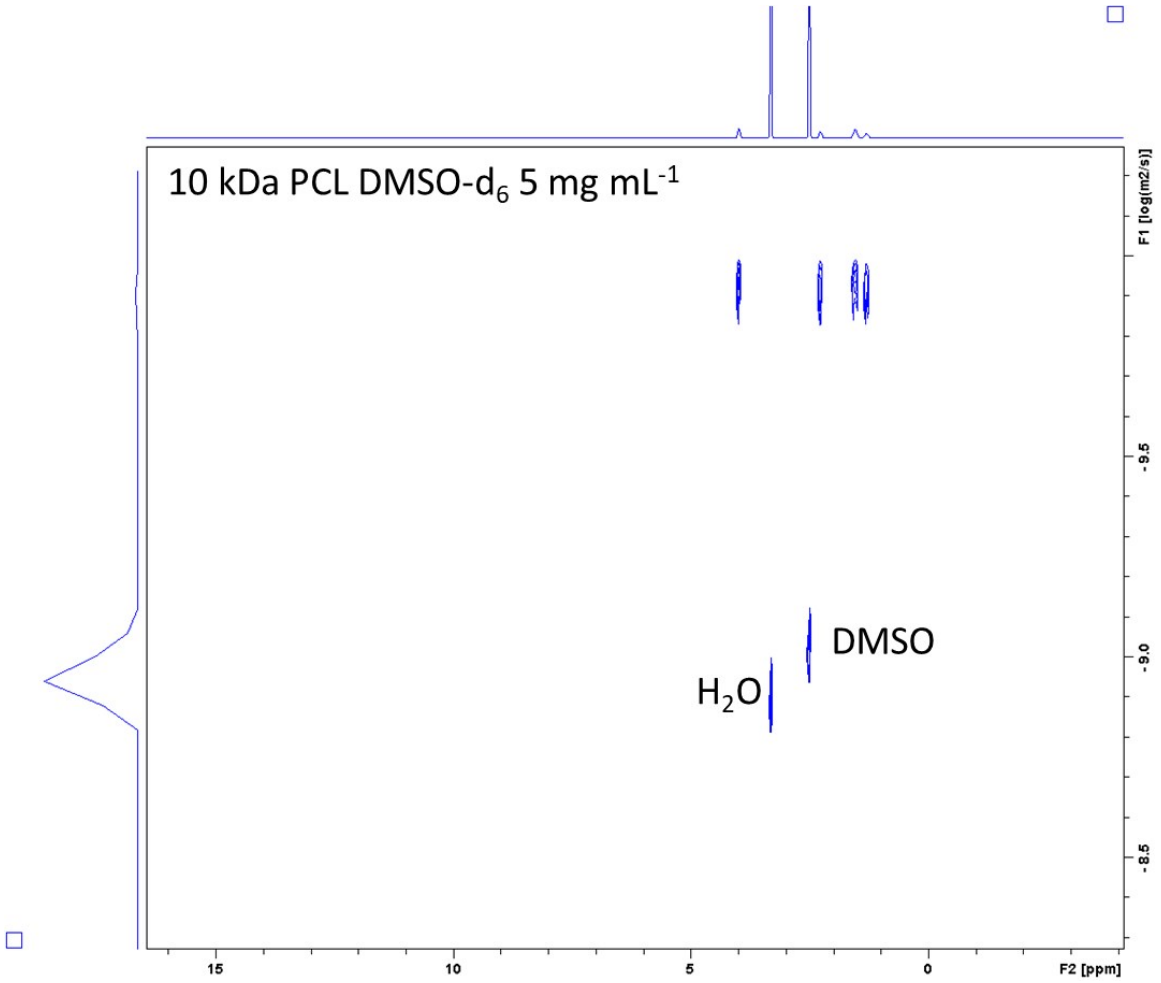

Fig. S70 DOSY-^{1}H NMR spectrum of 10 kDa PCL in DMSO-d_6.

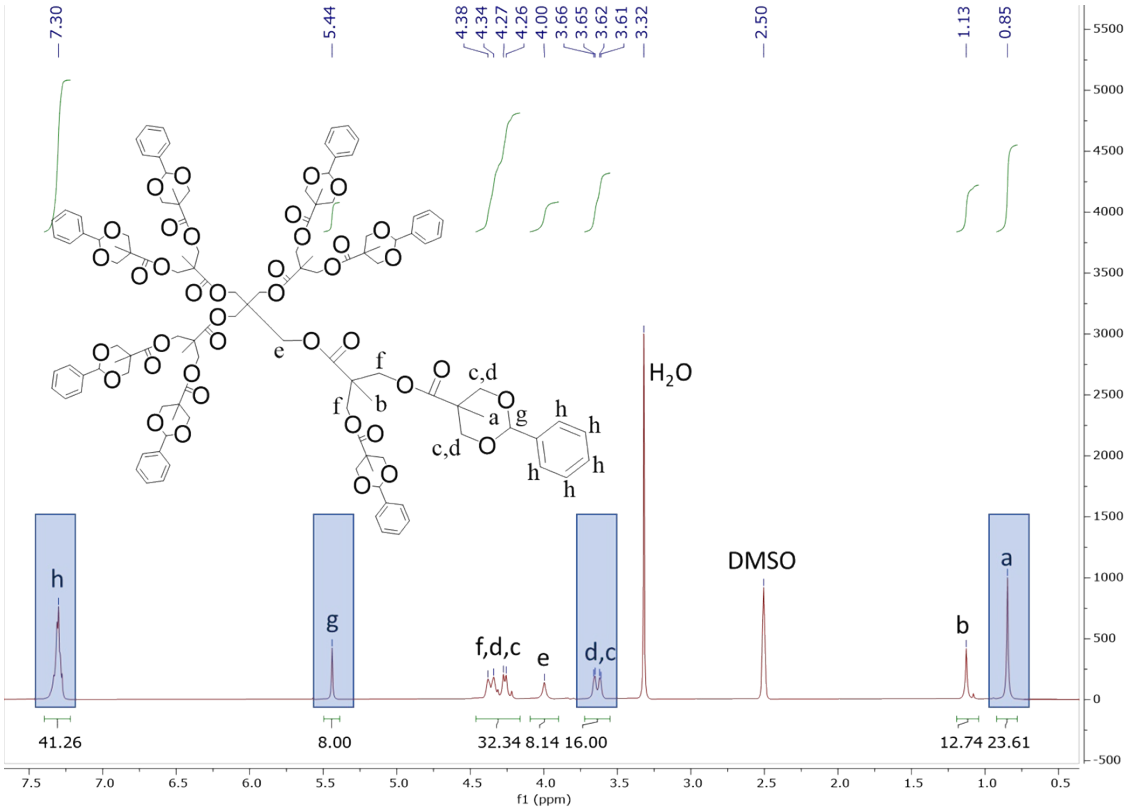

Fig. S71 Representative ^{1}H NMR of Tetra[G2]Bnz$_8$ in DMSO-d$_6$. Peaks used for DOSY-^{1}H NMR analysis are highlighted in blue.

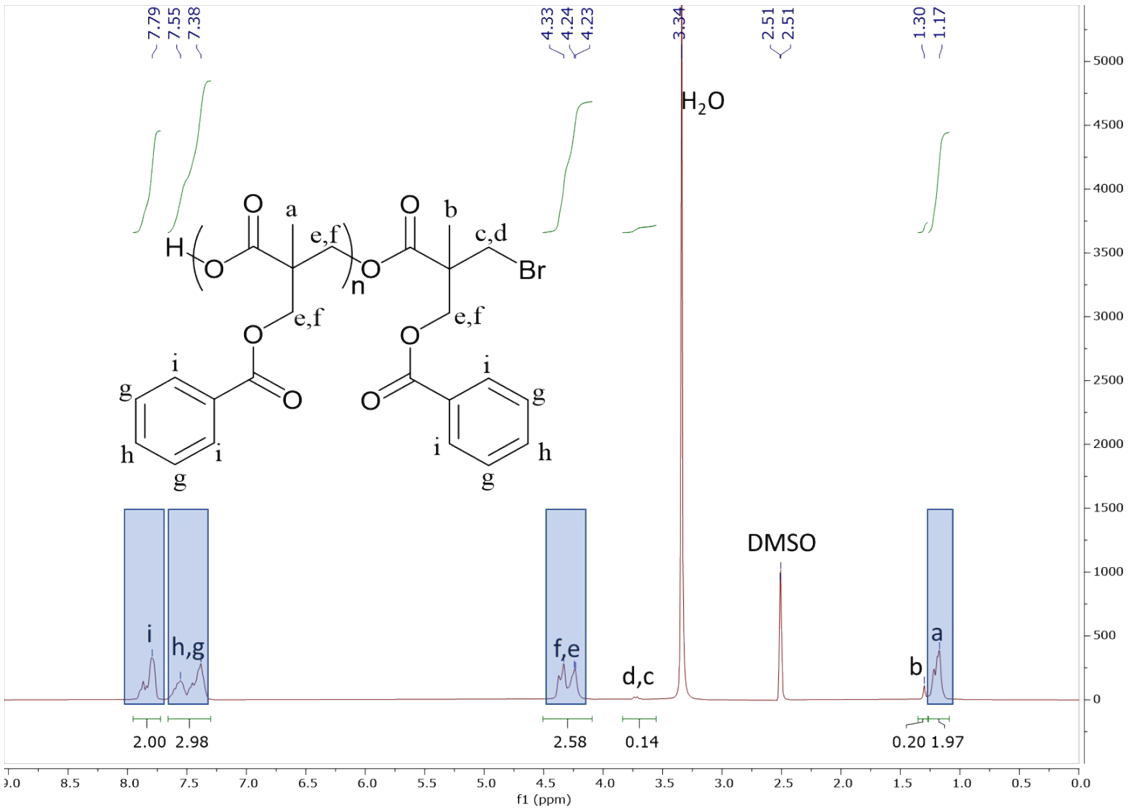

Fig. S72 Representative ^{1}H NMR of 2.2 kDa PBBM in DMSO-d_6. Peaks used for DOSY-^{1}H NMR analysis are highlighted in blue.

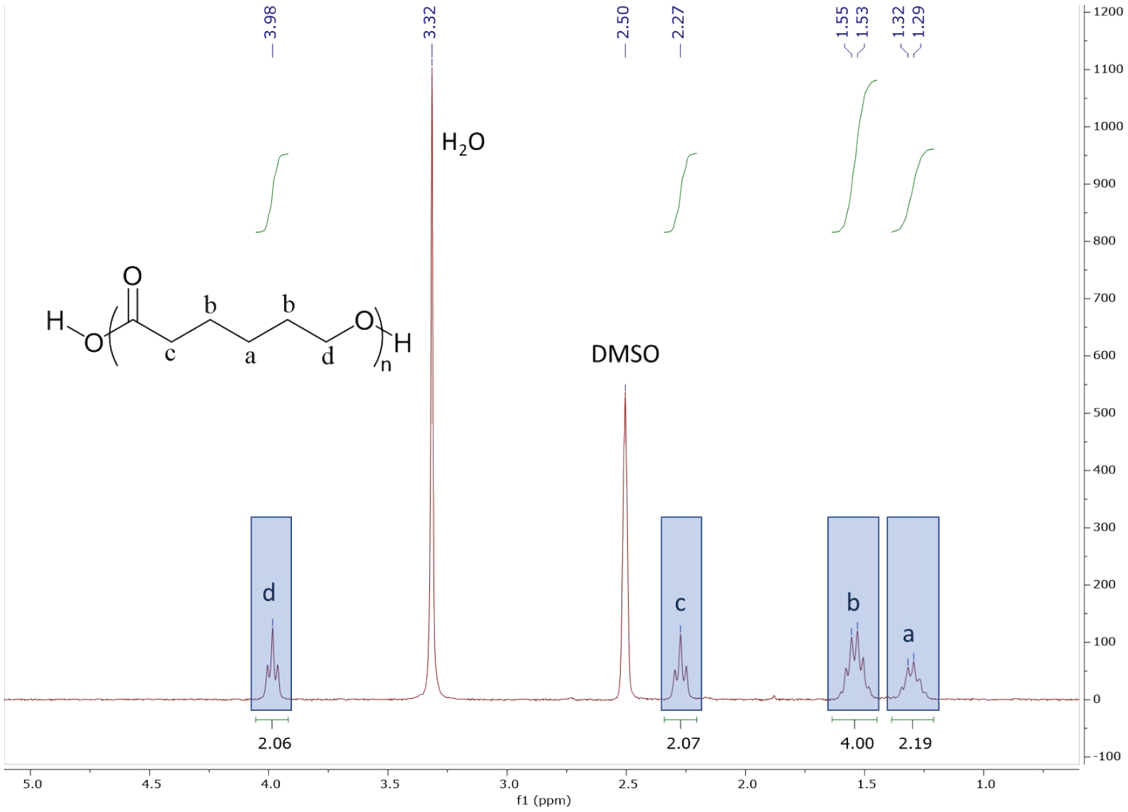

Fig. S73 Representative ^{1}H NMR of 10 kDa PCL in DMSO-d_6. Peaks used for DOSY-^{1}H NMR analysis are highlighted in blue.

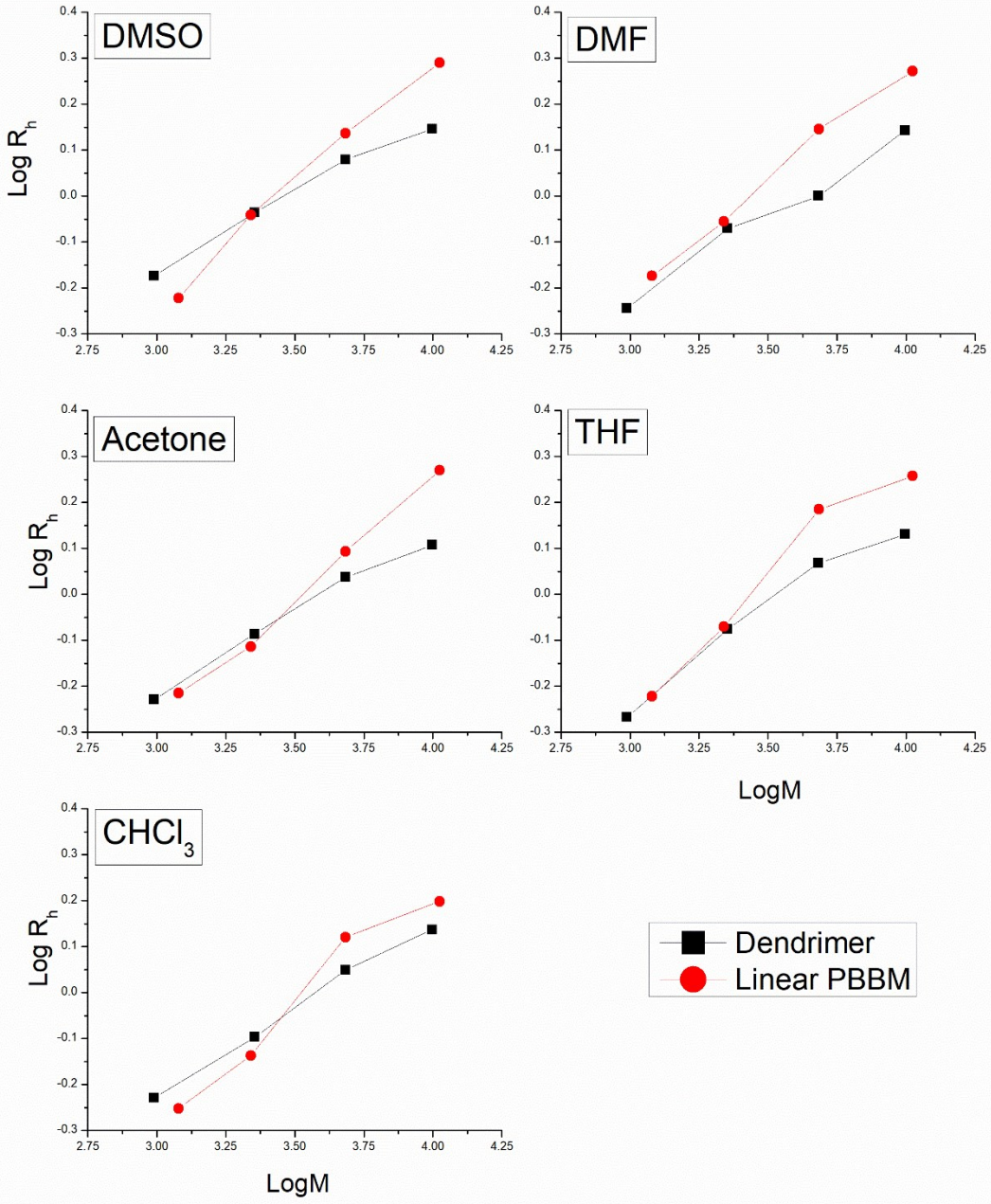

Fig. S74 Log-log plots of R_h vs. M for dendrimers and linear PBBM.

Table S1. Table of scaling parameters (a) extracted from Fig. S74 and the relation $R_h \sim M^a$.

Solvent	Tetra [G1-G4] Dendrimers	PBBM
DMSO	0.32	0.54
DMF	0.36	0.48
Ace	0.33	0.52
THF	0.40	0.53
$CHCl_3$	0.37	0.50

Table S2. Table of HSP distance ($R_{a(A-B)}$) of each solvent from the respective analog. Calculated R_h values from DOSY-^{1}H NMR experiments are included to show the similarity in trends of both $R_{a(A-B)}$ and R_h.

Tetra[G4]Bnz_{32}			45-mer PBBM			87-mer PCL		
Solvent[a]	$R_{a(A-B)}$[b]	R_h (nm)	Solvent[a]	$R_{a(A-B)}$[b]	R_h (nm)	Solvent[a]	$R_{a(A-B)}$[b]	R_h (nm)
DMSO	4.23	1.40	DMSO	3.30	1.95	THF	1.34	2.60
DMF	5.73	1.39	DMF	4.98	1.87	$CHCl_3$	1.92	2.61
THF	6.92	1.35	THF	7.24	1.81	Ace	5.44	2.56
$CHCl_3$	9.47	1.37	Ace	9.56	1.86	DMF	8.90	2.46
Ace	9.66	1.28	$CHCl_3$	9.95	1.58	DMSO	10.4	N/A

[a]The solvent column for each analog is ordered by increasing $R_{a(A-B)}$ from top to bottom.

[b]$R_{a(A-B)}$ was calculated using molecular dynamics calculations for each analog and solvent.

$R_{a(A-B)}$was also calculated using the experimental values for each solvent and those can be seen in Table S3.

Table S3. Table of experimental and literature Hansen Solubility Parameters for each solvent and polymer analog. Dispersion force and electrostatic energy is also included.

	Solubility Parameter ($MPa^{0.5}$)	δD	Coul[b]
Experimental[a]			
Tetra[G4]Bnz_{32}	25.4	18.2	17.6
45-mer PBBM	25.5	17.9	18.2
87-mer PCL	20.1	17.3	10.22
Literature[a]			
PCL	19.5	17.0	9.59
Experimental[a]			
DMSO	26.4	16.7	20.5
THF	20.3	16.9	11.3
$CHCl_3$	19.3	17.4	8.31
Acetone	18.4	14.6	11.2
DMF	23.8	15.4	18.2
Literature[a]			
DMSO	26.7	18.4	19.3
THF	19.5	16.8	9.82
$CHCl_3$	18.9	17.8	6.49
Acetone	19.9	15.5	12.5
DMF	24.9	17.4	17.8

[a]Experimental values were determined using molecular dynamics simulations. Literature values obtained from Belmares *et al.*

[b]Electrostatic energy (Coul) was used in place of δP and δH as the molecular dynamics software does not calculate polar force and H-bonding force separately. Coul was also determined for the literature values of PCL and solvents to compare to the experimentally derived values.

References

1 R. A. Ford and A. J. Gordon, *The Chemist's Companion: A Handbook of Practical Data, Techniques, and References*, Wiley-VCH VErlag GmbH & Co. KGaA, 1972.

2 S. L. Mayo, B. D. Olafson and W. A. Goddard, DREIDING: a generic force field for molecular simulations, *J. Phys. Chem.*, 1990, **94**, 8897–8909.

3 S. Plimpton, Fast Parallel Algorithms for Short-Range Molecular Dynamics, *J. Comput. Phys.*, 1995, **117**, 1–19.

4 I. Štich, R. Car, M. Parrinello and S. Baroni, Conjugate gradient minimization of the energy functional: A new method for electronic structure calculation, *Phys. Rev. B*, 1989, **39**, 4997–5004.

5 B. A. Luty and W. F. van Gunsteren, Calculating Electrostatic Interactions Using the Particle−Particle Particle−Mesh Method with Nonperiodic Long-Range Interactions, *J. Phys. Chem.*, 1996, **100**, 2581–2587.

6 D. J. Evans and B. L. Holian, The Nose–Hoover thermostat, *J. Chem. Phys.*, 1985, **83**, 4069–4074.

7 G. J. Martyna, D. J. Tobias and M. L. Klein, Constant pressure molecular dynamics algorithms, *J. Chem. Phys.*, 1994, **101**, 4177–4189.

8 C. M. Hansen, The Three Dimensional Solubility Parameter and Solvent Diffusion Coefficient. Their Importance in Surface Coating Formulation, *J. Paint Technol.*, 1967, 104.

9 Y. Luo, R. Wang, W. Wang, L. Zhang and S. Wu, Molecular Dynamics Simulation Insight Into Two-Component Solubility Parameters of Graphene and Thermodynamic Compatibility of Graphene and Styrene Butadiene Rubber, *J. Phys. Chem. C*, 2017, **121**, 10163–10173.

10 M. Belmares, M. Blanco, W. A. Goddard, R. B. Ross, G. Caldwell, S.-H. Chou, J. Pham, P. M. Olofson and C. Thomas, Hildebrand and Hansen solubility parameters from Molecular Dynamics with applications to electronic nose polymer sensors, *J. Comput. Chem.*, 2004, **25**, 1814–1826.

11 O. O. Kareem, S. P. Daymon, C. B. Keller, B. Chen, S. Nazarenko and S. M. Grayson, Synthesis and Characterization of Linear, Homopolyester, Benzoyl-Protected Bis-MPA, *Macromolecules*, 2020, **53**, 6608–6618.